

# **Design Guidance for High Temperature Concentrating Solar Power Components**

---

**Applied Materials Division**

**About Argonne National Laboratory**

Argonne is a U.S. Department of Energy laboratory managed by UChicago Argonne, LLC under contract DE-AC02-06CH11357. The Laboratory's main facility is outside Chicago, at 9700 South Cass Avenue, Argonne, Illinois 60439. For information about Argonne and its pioneering science and technology programs, see [www.anl.gov](http://www.anl.gov).

**DOCUMENT AVAILABILITY**

**Online Access:** U.S. Department of Energy (DOE) reports produced after 1991 and a growing number of pre-1991 documents are available free at OSTI.GOV (<http://www.osti.gov/>), a service of the US Dept. of Energy's Office of Scientific and Technical Information.

**Reports not in digital format may be purchased by the public from the National Technical Information Service (NTIS):**

U.S. Department of Commerce  
National Technical Information  
Service 5301 Shawnee Rd  
Alexandria, VA 22312  
**[www.ntis.gov](http://www.ntis.gov)**  
Phone: (800) 553-NTIS (6847) or (703) 605-6000  
Fax: (703) 605-6900  
Email: **[orders@ntis.gov](mailto:orders@ntis.gov)**

**Reports not in digital format are available to DOE and DOE contractors from the Office of Scientific and Technical Information (OSTI):**

U.S. Department of Energy  
Office of Scientific and Technical Information  
P.O. Box 62  
Oak Ridge, TN 37831-0062  
**[www.osti.gov](http://www.osti.gov)**  
Phone: (865) 576-8401  
Fax: (865) 576-5728  
Email: **[reports@osti.gov](mailto:reports@osti.gov)**

**Disclaimer**

This report was prepared as an account of work sponsored by an agency of the United States Government. Neither the United States Government nor any agency thereof, nor UChicago Argonne, LLC, nor any of their employees or officers, makes any warranty, express or implied, or assumes any legal liability or responsibility for the accuracy, completeness, or usefulness of any information, apparatus, product, or process disclosed, or represents that its use would not infringe privately owned rights. Reference herein to any specific commercial product, process, or service by trade name, trademark, manufacturer, or otherwise, does not necessarily constitute or imply its endorsement, recommendation, or favoring by the United States Government or any agency thereof. The views and opinions of document authors expressed herein do not necessarily state or reflect those of the United States Government or any agency thereof, Argonne National Laboratory, or UChicago Argonne, LLC.

# Design Guidance for High Temperature Concentrating Solar Power Components

---

prepared by  
Bipul Barua, Argonne National Laboratory  
Michael D. McMurtrey, Idaho National Laboratory  
Ryann E. Rupp, Idaho National Laboratory  
Mark C. Messner, Argonne National Laboratory

January 2020



## **Abstract**

This report provides guidance for the design of components for concentrating power facilities operating at high temperatures and undergoing high, secondary thermal stresses relative to the applied primary pressure stress. The design rules were developed for the design of Generation 3 CSP tubular receivers manufactured from Alloy 740H, but are generally applicable to a wide range of component types undergoing similar loads. Part 1 of the report provides procedural design rules for components to be used in conjunction with the 2019 edition of the ASME Boiler & Pressure Vessel Code. Part 2 provides corresponding design data for Alloy 740H. Part 3 of the report is a commentary describing the rationale behind the design rules and the data underlying the design material properties. Finally, Part 4 provides an extensive set of worked sample problems detailing the application of the rules to CSP components.



# Table of Contents

Abstract .....	iii
Table of Contents .....	v
Part 1: Design Rules .....	1
1-1. General criteria .....	1
1-2. Design Option A: Design by Elastic Analysis using ASME Section III, Division 5 .....	2
1-3. Design Option B: Design by Elastic Analysis using ASME Section III, Division 5 with Reduced Margin and Simplified Creep-Fatigue evaluation.....	4
1-4. Design Option C: Design by Simple Inelastic Analysis .....	6
Part 2: Design Material Data.....	8
2-1. General Criteria .....	8
2-2. Material Specification.....	8
2-3. Elastic constants .....	9
2-4. Thermal properties.....	9
2-5. Mechanical properties.....	10
2-6. Allowable Stresses.....	12
2-7. Creep, fatigue, and creep-fatigue properties .....	14
2-8. Weld strength reduction factors.....	17
2-9. Isochronous stress-strain relations.....	18
2-10. Inelastic constitutive models .....	25
2-11. Temperature limits.....	26
Part 3: Commentary.....	27
3-1. Overview .....	27
3-2. Commentary on the Design Rules .....	29
3-3. Commentary on the 740H Material Data.....	42
Part 4: Sample problems .....	58
4-1. Sample problem 1 .....	58
4-2. Sample problem 2.....	80
Acknowledgements .....	103





# Part 1: Design Rules

## 1-1. General criteria

### 1-1.1. Applicability

These design criteria apply to components in concentrating solar power facilities at temperatures above 370° C for ferritic and ferritic-martensitic steels and 425° C for austenitic stainless steels and nickel-based alloys where creep-fatigue damage in cyclic service or stress relaxation damage caused by reoccurring application of secondary load is a significant design consideration. The designer may select any of the following three design options listed in Articles 1-2, 1-3, and 1-4. A design is required to pass all the checks contained in the selected option to pass the design criteria.

The design criteria were developed for structures undergoing daily cycling. The rules below are not suited for structures that see service cycles with holds at constant load longer than 1,000 hours at temperatures greater than those listed in Part 2, Article 2-10.1.

All references to the ASME Boiler and Pressure Vessel Code (ASME B&PV Code) are to the 2019 Edition.

### 1-1.2. Design Cycle and Design Life

All three methods require the designer to use a single design composite loading cycle to represent or bound the service conditions experienced in operation. The definition of this Design Cycle consists of periodic pressure, thermal, and mechanical force boundary conditions sufficient to complete a thermal-mechanical analysis of the component along with the number of times this composite loading cycle will be repeated in service – defined as quantity  $N$ . These boundary condition histories must include times of application including all relevant hold periods at constant load. The composite cycle period is defined as  $t_p$ .

The Design Specification shall specify a Design Life denoted as  $t_{design}$ . The composite loading cycle used for design must cover the entire design life so that  $t_{design} = Nt_p$ .

### 1-1.3. Material Data

The following design criteria are to be used in conjunction with the design material data provided in Part 2.

### 1-1.4. Limitations

These criteria only cover the design of components and do not provide construction, welding, examination, or inspection criteria. These additional requirements shall be provided in the Design Specification, possibly by reference to ASME Section III, Section V, Section VIII, Section IX, or Section XI or other codes and standards documents, as appropriate.

## **1-2. Design Option A: Design by Elastic Analysis using ASME Section III, Division 5**

This option can be applied to any type of component using any material provided in Part 2 up to the maximum metal temperatures provided in the tabulated design data.

### **1-2.1. Primary Load**

Primary load analysis is to be completed using a steady-state thermal analysis of the Design Cycle and a linear elastic stress analysis using the material properties provided in Articles 0 and 2-3 of Part 2.

The component shall meet the criteria of the ASME B&PV Code Section III, Division 5, HBB-3222.1 with the following modifications:

1. The Design Loading shall be determined using Section III, Division 5, HBB-3113.1 expect references to “Service Level A Loadings” are replaced by references to the “Design Cycle” defined in Article 1-1.2.
2. The values of the allowable stress  $S_o$  are provided in Article 2-5.1 of Part 2.
3. The provisions of HBB-3222.1(c) do not apply.

### **1-2.2. Ratcheting Strain Accumulation**

The temperatures used in the ratcheting analysis are to be obtained from a transient thermal analysis of the component subject to the Design Cycle. The stresses and strains are to be obtained using a small-deformation linear elastic analysis. Material properties are provided in Articles 0 and 2-3 of Part 2.

The component shall meet the criteria of the ASME B&PV Code Section III, Division 5, HBB-T-1332 Test B-1, including the General Requirements of HBB-T-1331, with the following modifications:

1. The designer will only analyze a single cycle, the Design Cycle defined in Article 1-1.2. References to the Section III, Division 5 Service Loadings are replaced by references to the Design Cycle.
2. The values of  $S_y$  are provided in Article 2-4.1 of Part 2.
3. The temperature limit provided by Table HBB-1323 is instead provided in Article 2-10.2 in Part 2.
4. For HBB-T-1332(b) calculate the accumulated strain using a stress of  $1.0\sigma_c$ , rather than the  $1.25\sigma_c$  in the ASME Code.
5. For HBB-T-1332(b) the isochronous stress strain curves are provided in Article 0 of Part 2.
6. The strain limits in HBB-T-1332(b) are increased to 2% for base metal and 1% for weld metal.

### 1-2.3. Creep-fatigue Criteria

The temperatures used in the creep-fatigue analysis are to be obtained from a transient thermal analysis of the component subject to the Design Cycle. The stresses and strains are to be obtained using a small-deformation linear elastic analysis. Material properties are provided in Articles 0 and 2-3 of Part 2.

The component shall meet the criteria contained in the ASME B&PV Code Section III, Division 5, HBB-T-1430 with the following modifications:

1. The designer will only analyze a single cycle, the Design Cycle defined in Article 1-1.2. References to the Section III, Division 5 Service Loadings are replaced by references to the Design Cycle.
2. The design fatigue curves are provided in Article 2-6.2 of Part 2.
3. The minimum stress to rupture data are provided in Article 2-6.1 in Part 2.
4. The values of the allowable stress  $S_m$ , required for calculating the quantity  $3\bar{S}_m$ , are provided in Article 0 in Part 2.
5. The values of the relaxation strength  $S_{rL}$  and  $S_{rH}$ , required for calculating the quantity  $3\bar{S}_m$ , are provided in Article 0 in Part 2.
6. The isochronous stress-strain curves are provided in Article 0 in Part 2.
7. For HBB-T-1432 the designer shall use HBB-T-1413 for calculating the effective strain range and not any of the other options allowed in HBB-T-1432(a).
8. The creep-fatigue damage envelope is provided in Article 0 in Part 2.
9. When calculating the creep strain increment in HBB-T-1432(g) use a stress equal to  $1.0\sigma_c$ , rather than  $1.25\sigma_c$  as in Section III, Division 5.
10. When using HBB-T-1433(a) Step 5(b) to evaluate creep damage the value of  $S_{LB}$  shall be  $1.0\sigma_c$ , rather than  $1.25\sigma_c$  as in Section III, Division 5.
11. The alternate creep damage calculation procedure in HBB-T-1433(b) shall not be used. The designer must use the process defined in HBB-T-1433(a).
12. Creep damage shall be calculated from the stress history using a factor  $K' = 0.9$ .
13. The alternative criteria in HBB-T-1435 shall not be used.
14. The additional factors on weld material properties defined in HBB-T-1710 shall be applied to weldments. Applicable weld strength reduction factors are provided in Article 2-7 of Part 2.

### 1-2.4. Time Independent Buckling

For this analysis the Design Cycle loads, defined in Article 1-1.2, shall be increased by a factor of 1.5. This includes thermal stresses which can be increased by factoring the material coefficient of thermal expansion.

Additionally, the Design Cycle shall be supplemented by intermittent loads, such as wind lateral loads, that are not periodic. The method for calculating lateral loads shall be specified in the Design Specification. If this method includes load factors accounting for uncertainty in the applied loading these load factors shall be used for the lateral loads if they exceed the generic load factor of 1.5 provided in this Article. If the lateral loads specified in the Design Specification are not

factored or if the load factor is less than 1.5, the intermittent loads shall be increased by a factor of 1.5.

The factored Design Cycle plus factored intermittent loads shall be used to perform a time-independent, large deformations, incremental plastic analysis of the component using a von Mises flow theory and a temperature-dependent flow stress defined by the zero-time, hot-tensile isochronous stress strain curves given in Part 2, Article 0. If the analysis converges for one application of the combined load history, i.e. the structure does not undergo plastic collapse or buckling, the time independent buckling design criteria are satisfied.

### **1-2.5. Time Dependent Buckling**

For many CSP systems time dependent buckling will not be a significant design issue as primary stresses and steady, load-controlled lateral loads are typically small. However, if a design has high primary loads or significant steady, load controlled loadings, such as large lateral self-weight, that could cause buckling, time dependent buckling may be assessed with the following procedure. Note that such steady load controlled forces should already be included in the Design Cycle, as they are primary loads.

For this analysis the Design Cycle loads, defined in Article 1-1.2, shall be increased by a factor of 1.5. This includes thermal stresses, which can be increased by factoring the material coefficient of thermal expansion.

This factored Design Cycle shall be used to perform a time-independent, large deformations, incremental plastic analysis of the component using a von Mises flow theory and a temperature-dependent flow stress defined by isochronous curve for a time equal to the component Design Life given in Part 2, Article 0. If the analysis converges for one application of the factored Design Cycle, i.e. the structure does not undergo plastic collapse or buckling, the time dependent buckling design criteria are satisfied.

## **1-3. Design Option B: Design by Elastic Analysis using ASME Section III, Division 5 with Reduced Margin and Simplified Creep-Fatigue evaluation**

This method shall only be applied to Alloy 740H material and to components where the peak stress is minimal.

### **1-3.1. Primary Load**

The primary load provisions of Article 1-2.1 shall be used.

### **1-3.2. Ratcheting Strain Accumulation**

The ratcheting provisions of Article 1-2.2 shall be used.

### **1-3.3. Creep-fatigue Criteria**

The temperatures used in the creep-fatigue analysis are to be obtained from a transient thermal analysis of the component subject to the Design Cycle. The stresses and strains are to be obtained using a small-deformation linear elastic analysis. Material properties are provided in Articles 0 and 2-3 of Part 2.

Consider the total stress intensity (P+Q+F) from the linear elastic analysis. If at any point during the Design Cycle the total stress intensity exceeds the temperature-dependent value of  $S_y$  for the material, given in Part 2, Article 2-4.1 then Design Option B cannot be used to assess the component.

To evaluate creep-fatigue damage use the following procedure. The stresses used in these steps correspond to the maximum total stress (P+Q+F) in the linear elastic analysis.

1. Determine the maximum elastic strain range during the Design Cycle using the elastically calculated mechanical strains from the analysis and the definition of the strain range given in HBB-T-1413. Call this strain range  $\Delta\epsilon_1$ .
2. Calculate a strain range increase due to creep  $\Delta\epsilon_2$  by taking the total creep strain used to evaluate the ratcheting strain criteria in Article 1-3.2 (using HBB-T-1332 Test B-1), labeled  $\epsilon_{total}$  and dividing it by the number of repetitions of the design cycle  $N$ , i.e.  $\Delta\epsilon_2 = \epsilon_{total}/N$ . As the structure will already have passed the requirements of Article 1-3.2 the designer may alternatively conservatively use  $\Delta\epsilon_2 = 2\%/N$ .
3. Sum the two strain ranges  $\Delta\epsilon = \Delta\epsilon_1 + \Delta\epsilon_2$  and use this total strain range to determine the number of cycles to failure using the design fatigue diagrams given in Part 2, Article 2-6.2. The appropriate diagram corresponds to the maximum metal temperature in the Design Cycle. Use the design fatigue curve to determine the number of allowable cycles  $N_f$ . Calculate the fatigue damage fraction using the equation  $D_f = N/N_f$ .
4. Calculate the von Mises stress history,  $\sigma_{vm} = \sigma_{vm} = \sqrt{\left\{(\sigma_{xx} - \sigma_{yy})^2 + (\sigma_{yy} - \sigma_{zz})^2 + (\sigma_{zz} - \sigma_{xx})^2 + 6(\sigma_{xy}^2 + \sigma_{yz}^2 + \sigma_{xz}^2)\right\}}/2$  corresponding to the total stress history determined in the linear elastic analysis. Use this von Mises stress history to calculate the creep damage fraction for a single repetition of the Design Cycle using HBB-T-1411(10) with a factor  $K' = 0.9$ . That is, the scalar stress used to determine the time-to-rupture for each time increment  $\Delta t$  is the von Mises stress, not the effective stress given in HBB-T-1411 or the design by elastic analysis procedure given in HBB-T-1433. The minimum stress to rupture tables are provided in Part 2, Article 2-6.1. Call this single cycle creep damage fraction  $D_{c1}$ . The total creep damage fraction is  $D_c = ND_{c1}$ .
5. Use the creep-fatigue damage envelope provided in Part 2, Article 0 with the fatigue and creep damage fractions  $D_f$  and  $D_c$  to determine the acceptability of the component.

In this procedure the modifications to the weld material properties defined in HBB-T-1710 shall be applied to weldments. Applicable weld strength reduction factors are provided in Article 2-7 of Part 2.

### 1-3.4. Time Independent Buckling

The time independent buckling criteria of Article 1-2.4 shall be used.

### 1-3.5. Time Dependent Buckling

If applicable, the time-dependent buckling criteria of Article 1-2.5 shall be used.

## 1-4. Design Option C: Design by Simple Inelastic Analysis

This method may be applied to any material for which Part 2, Article 2-9 provides a constitutive model.

### 1-4.1. Primary Load

The primary load provisions of Article 1-2.1 shall be used.

### 1-4.2. Ratcheting Strain Accumulation

Perform a transient thermal analysis of the component under the Design Cycle using the properties in Part 2, Article 2-3. Use these temperatures to perform a small deformation inelastic stress analysis of the component under the Design Cycle loads using the inelastic constitutive model defined in Part 2, Article 2-9. For each location in the component,  $\mathbf{x}$ , this process produces a time history of stress values  $\boldsymbol{\sigma}(\mathbf{x}, t)$ , mechanical strain values  $\boldsymbol{\epsilon}(\mathbf{x}, t)$ , and temperature values  $T(\mathbf{x}, t)$ .

The analysis must repeat the Design Cycle loading until the structure achieves a steady-state response. This steady-state response is defined by the conditions, for some arbitrary time  $t$ :

1.  $\boldsymbol{\sigma}(\mathbf{x}, t) = \boldsymbol{\sigma}(\mathbf{x}, t - t_p)$
2.  $T(\mathbf{x}, t) = T(\mathbf{x}, t - t_p)$

for all times in the current repetition of the Design Cycle. Both conditions must be met. Once the analysis reaches this steady-state condition no additional repetitions of the Design Cycle are required. Extract the stress, strain, and temperature histories from the analysis corresponding to the final repetitions of the design cycle. Shift these histories in time so that the final stress, strain, and temperature histories start at time 0 and extend to time  $t_p$ . These histories,  $\boldsymbol{\sigma}(\mathbf{x}, t)$ ,  $\boldsymbol{\epsilon}(\mathbf{x}, t)$ , and  $T(\mathbf{x}, t)$ , will be used to determine the acceptability of the component.

To assess the component against the ratcheting criteria for each location in the component calculate the local ratcheting rate

$$r(\mathbf{x}) = \sqrt{\frac{2}{3} \boldsymbol{\epsilon}(\mathbf{x}, t_p) : \boldsymbol{\epsilon}(\mathbf{x}, t_p)} - \sqrt{\frac{2}{3} \boldsymbol{\epsilon}(\mathbf{x}, 0) : \boldsymbol{\epsilon}(\mathbf{x}, 0)}$$

which is the net effective strain accumulated over one cycle in the steady state condition. The ‘:’ in this equation represents tensor contraction. For each point calculate the total ratcheting strain:

$$R(\mathbf{x}) = N r(\mathbf{x})$$

This total ratcheting strain must be less than 10% for base metal and 5% for weldments at all points in the structure. If this criteria is met the structure passes the ratcheting design criteria.

### 1-4.3. Creep-fatigue Criteria

The analysis is identical to the analysis required for the ratcheting check defined in Article 1-4.2. The design analysis begins with the time-shifted histories  $\sigma(\mathbf{x}, t)$ ,  $\epsilon(\mathbf{x}, t)$ , and  $T(\mathbf{x}, t)$ .

For each point in the component:

1. Use HBB-T-1413 with  $\nu^* = 0.5$  to calculate the effective strain range  $\Delta\epsilon_{max}$  from the strain history  $\epsilon(\mathbf{x}, t)$ .
2. Use the design fatigue curves provided in Part 2, Article 2-6.2 to determine the maximum allowable number of cycles  $N_f(\mathbf{x})$ . Use the curve corresponding to the maximum metal temperature at the point under consideration.
3. Calculate the fatigue damage fraction using the equation  $D_f(\mathbf{x}) = \frac{N}{N_f(\mathbf{x})}$ .
4. Use the stress history  $\sigma(\mathbf{x}, t)$  to calculate the von Mises effective stress history at each point in the structure using the equation  $\sigma_{vm} = \sqrt{\left\{(\sigma_{xx} - \sigma_{yy})^2 + (\sigma_{yy} - \sigma_{zz})^2 + (\sigma_{zz} - \sigma_{xx})^2 + 6(\sigma_{xy}^2 + \sigma_{yz}^2 + \sigma_{xz}^2)\right\}}/2$ .
5. Use the resulting von Mises stress history  $\sigma_{vm}(\mathbf{x}, t)/K'$ , with  $K' = 0.9$ , and the local metal temperature to calculate a time history of allowable time to rupture  $T_d(\mathbf{x}, t)$  using the minimum stress to rupture provided in Part 2, Article 2-6.1.
6. Calculate the creep damage fraction using the equation  $D_c(\mathbf{x}) = N \int_0^{t_p} \frac{dt}{T_d(\mathbf{x}, t)}$ . The integral may be discretized into individual time steps.
7. Use the creep-fatigue damage envelope, provided in Part 2, Article 0, to determine whether each point in the structure passes or fails the acceptance criteria using the fatigue and creep damage fractions  $D_f(\mathbf{x})$  and  $D_c(\mathbf{x})$ .

The structure passes the creep-fatigue design provisions if each point individually passes the criteria described in 1-7 above.

### 1-4.4. Time Independent Buckling

The time independent buckling criteria of Article 1-2.4 shall be used.

### 1-4.5. Time Dependent Buckling

If applicable, the time-dependent buckling criteria of Article 1-2.5 shall be used.

## Part 2: Design Material Data

### 2-1. General Criteria

#### 2-1.1. Data tables, charts, and equations

Depending on the property, the data below is provided as tables, charts, or equations or some combination thereof. If more than one form of the data is presented the designer may use either the equations or interpolation from table or chart data. For the case where the material property depends on time or a number of cycle repetitions log-linear interpolation shall be used for that variable. Because of differences in interpolation versus the mathematical formula and because the tabulated values are rounded the three sources of data may not precisely agree.

### 2-2. Material Specification

The following table links the short material name used in this Part 2 to material specification(s) and product forms allowed for use with these design criteria.

Short material name	Nominal composition	UNS Number	Product form	Specification
Alloy 740H	Ni-25Cr-20Co	N07740	Plate, sheet, and strip	SB-435 <sup>1</sup>
		“	Bar	SB-572 <sup>1</sup>
		“	Seamless pipe and tube	SB-622 <sup>1</sup>
		“	Fittings	SB-366 <sup>1</sup>
		“	Forgings	SB-564 <sup>1</sup>

Table 2-2. Materials allowed for use with these design criteria

Notes:

<sup>1</sup> These materials shall also meet the additional requirements listed in part (a) or (b) in ASME B&PV Code Case 2702.



## Elastic constants

### 2-2.1. Young's modulus

#### 2-2.1.1. Alloy 740H

Temperature (°C)	Modulus (GPa)
20	221
100	218
200	212
300	206
400	200
500	193
600	186
700	178
800	169
900	160

Table 2-2.1.1. Design Young's modulus for Alloy 740H.

### 2-2.2. Poisson's ratio

#### 2-2.2.1. Alloy 740H

The design Poisson's ratio for Alloy 740H is 0.31 for all temperatures.

## 2-3. Thermal properties

### 2-3.1. Alloy 740H

Temperature (°C)	Mean ( $\mu\text{m}/\text{mm}/^\circ\text{C}$ )	CTE	Instantaneous ( $\mu\text{m}/\text{mm}/^\circ\text{C}$ )	CTE	Conductivity (W/(m °C))	Specific heat (J/(kg °C))
20			12.38		10.2	449
100	12.38		12.38		11.7	476
200	13.04		13.55		13.0	489
300	13.50		14.32		14.5	496
400	13.93		15.12		15.7	503
500	14.27		15.55		17.1	513
600	14.57		16.00		18.4	519
700	15.03		17.68		20.2	542
800	15.72		20.39		22.1	573
900	16.41		16.51		23.8	635

Table 2-3.1. Design thermal properties for Alloy 740H

## 2-4. Mechanical properties

### 2-4.1. Yield strength

#### 2-4.1.1. Alloy 740H

Temperature (°C)	$S_y$ (MPa)
40	621
100	594
150	577
200	562
250	548
300	538
350	531
400	529
450	529
500	529
550	529
600	529
650	529
700	529
750	508
800	463
850	418

Table 2-4.1.1. Design values of yield strength ( $S_y$ ) for Alloy 740H.

## 2-4.2. Tensile strength

### 2-4.2.1. Alloy 740H

Temperature (°C)	$S_u$ (MPa)
40	1034
100	1034
150	1034
200	1030
250	998
300	976
350	967
400	966
450	966
500	966
550	966
600	957
650	921
700	860
750	771
800	651
850	531

Table 2-4.2.1. Design values of tensile strength ( $S_u$ ) for Alloy 740H.

## 2-5. Allowable Stresses

### 2-5.1. Allowable Stress $S_o$

#### 2-5.1.1. Alloy 740

Temperature (°C)	$S_o$ (MPa)
40	295
100	295
150	295
200	279
250	276
300	276
350	276
400	276
450	276
500	276
550	276
600	274
650	226
700	146
750	84.1
800	34.5
850	21.8

Table 2-5.1.1. Allowable stress  $S_o$  in MPa for Alloy 740H.

## 2-5.2. Allowable Stress $S_m$

### 2-5.2.1. Alloy 740

Temperature (°C)	$S_m$ (MPa)
40	345
100	345
150	345
200	343
250	333
300	325
350	322
400	322
450	322
500	322
550	322
600	319
650	307
700	287
750	257
800	217
850	177

Table 2-5.2.1. Allowable stress  $S_m$  in MPa for Alloy 740H.

## 2-5.3. Relaxation Strength

### 2-5.3.1. Alloy 740

Temp. (°C)	Time (hours)							
	1	10	30	100	300	1000	3000	10000
425	483	483	483	483	483	483	483	483
450	483	483	483	483	483	483	483	483
475	483	483	483	483	483	483	483	483
500	483	483	483	483	483	483	483	483
525	483	483	483	483	483	483	483	483
550	483	483	483	483	483	483	483	483
575	481	481	481	481	481	481	481	481
600	478	478	478	478	478	476	472	459
625	469	469	469	468	466	460	445	412
650	460	460	459	456	449	428	394	345
675	445	444	441	432	412	374	328	278
700	430	425	417	395	360	310	265	221
725	406	395	377	340	296	248	208	172
750	382	358	326	280	237	195	162	132
775	348	308	270	224	186	151	124	101
800	312	256	217	176	145	116	95	76
825	272	207	171	137	111	88	71	57
850	231	164	133	105	84	66	53	42

Table 2-5.3.1. Relaxation strength as a function of time and temperature for Alloy 740H. Values are in MPa.

## 2-6. Creep, fatigue, and creep-fatigue properties

### 2-6.1. Minimum stress-to-rupture

#### 2-6.1.1. Alloy 740

The minimum stress to rupture for Alloy 740 is given by the equation

$$S_r(T, t) = \text{minimum of } \begin{cases} \text{The value of } S_u \text{ for temperature } T \text{ given in Article 5.2.1} \\ 10^{\{-1.624 \times 10^{-1}(T + 273.15)(19.284 + \log t_R) + 6.113\}} \end{cases}$$

where the temperature  $T$  is given in units of degrees Celsius, the time  $t$  is given in units of hours, and the rupture stress is provided in units of MPa.

Alternatively, the minimum stress to rupture is tabulated in Table 2-6.1.1.

		Time (hours)									
		1	10	30	100	300	1000	3000	10000	30000	100000
Temp. (°C)	425	966	966	966	966	966	966	966	966	966	966
	450	966	966	966	966	966	966	966	966	966	966
	475	966	966	966	966	966	966	966	966	966	966
	500	966	966	966	966	966	966	966	966	966	966
	525	966	966	966	966	966	966	966	966	966	923
	550	966	966	966	966	966	966	966	966	864	736
	575	962	962	962	962	962	962	950	805	692	586
	600	957	957	957	957	957	898	768	647	554	467
	625	939	939	939	939	869	729	621	521	444	372
	650	921	921	921	836	709	592	502	419	355	296
	675	891	891	824	685	578	480	405	337	284	236
	700	860	808	679	561	472	390	328	271	228	188
	725	816	668	559	460	385	316	265	218	182	150
	750	771	553	460	377	314	257	214	175	146	119
	775	677	457	379	309	256	208	173	141	117	95
	800	565	378	312	253	209	169	140	113	93	76
	825	472	313	257	207	170	137	113	91	75	60
	850	394	259	212	170	139	111	91	73	60	48

Table 2-6.1.1. Design rupture stresses ( $S_r$ ) in MPa for Alloy 740H.

## 2-6.2. Fatigue diagrams

### 2-6.2.1. Alloy 740H

The design fatigue relation for Alloy 740H is defined by the equation:

$$\Delta\varepsilon = \text{minimum of } \begin{cases} (0.0125N^{-0.08} + 0.0765N^{-0.44})/1.5 \\ 0.0125(10N)^{-0.08} + 0.0765(10N)^{-0.44} \end{cases}$$

for  $T \leq 700^\circ\text{C}$  and by

$$\Delta\varepsilon = \text{minimum of } \begin{cases} (0.03640N^{-0.19741})/1.5 \\ 0.03640(10N)^{-0.19741} \end{cases}$$

for  $700^\circ\text{C} < T \leq 850^\circ\text{C}$ .

Table 2-6.2.1 tabulates the design fatigue relation for 740H.

Cycles	Strain range $T \leq 700^{\circ}\text{C}$ (mm/mm)	Strain range $700^{\circ}\text{C} < T \leq 850^{\circ}\text{C}$ (mm/mm)
10	0.018733	0.014665
20	0.015615	0.012790
40	0.013220	0.011154
100	0.010855	0.009308
200	0.009504	0.008118
400	0.008427	0.007080
1000	0.007236	0.005908
2000	0.006336	0.005153
4000	0.005618	0.004494
10000	0.004875	0.003750
20000	0.004427	0.003271
40000	0.004051	0.002852
100000	0.003639	0.002380

Table 2-7.2.1. Design fatigue relation for Alloy 740H.

Figure 2-6.2.1 plots the design fatigue relation for 740H.

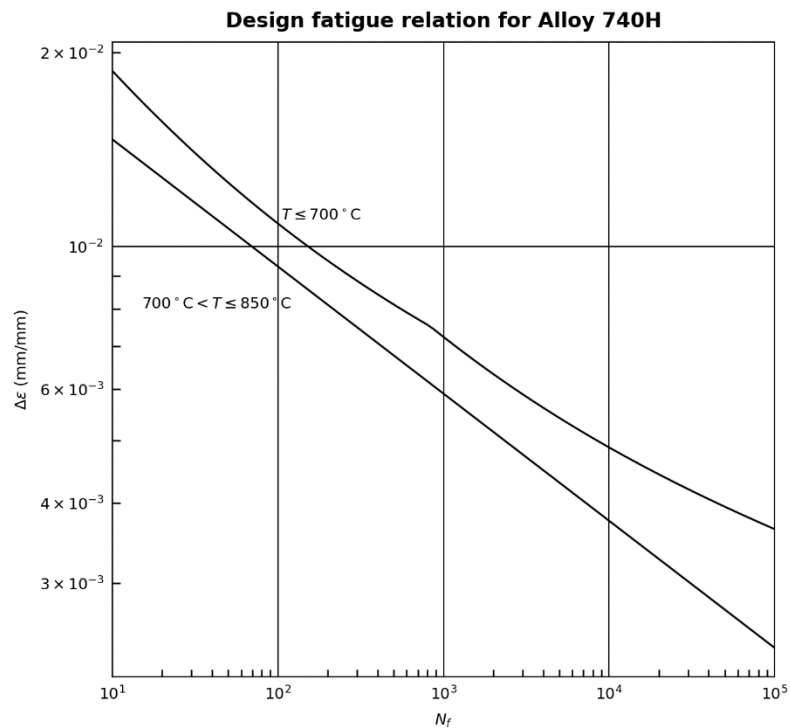


Figure 2-6.2.1. Design fatigue relation for Alloy 740H.



## 2-6.3. Creep-fatigue damage envelopes

### 2-6.3.1. Alloy 740H

Figure 2-6.3.1 provides the creep-fatigue damage envelope for Alloy 740H. Regions below the curve are acceptable.

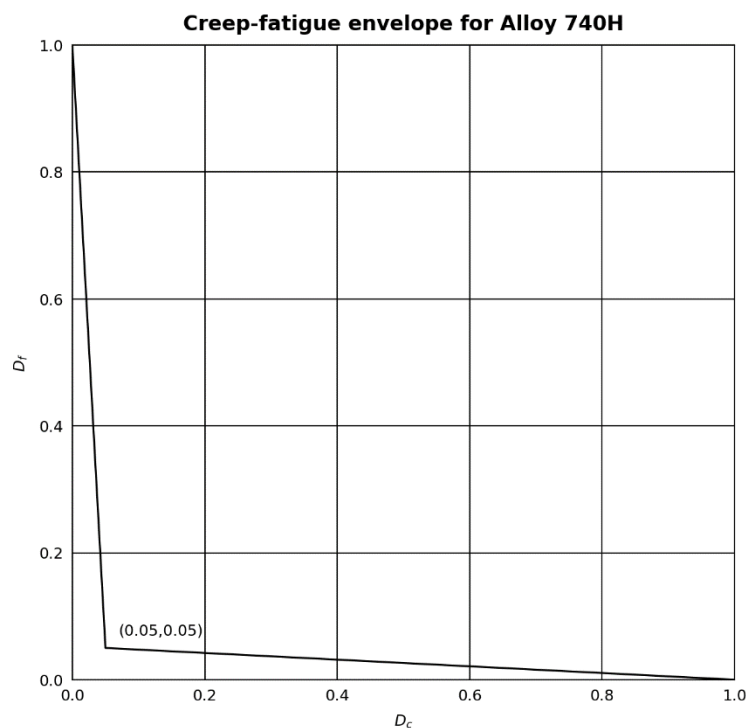


Figure 2-6.3.1. Creep-fatigue damage envelope for Alloy 740H.

## 2-7. Weld strength reduction factors

### 2-7.1. Alloy 740H

Table 2-7.1 lists weld strength reduction factor corresponding to each allowable Alloy 740H weld type:

Weld type	Temperature	Stress rupture factor
GTAW or GMAW, matching filler <sup>1</sup>	$T > 425^{\circ}\text{C}$	0.7

Table 2-7.1. Weld stress rupture factors for Alloy 740H

Notes:

<sup>1</sup> Welds shall be post-weld heat treated according to the criteria described in ASME B&PV Code Case 2702 (e).

## 2-8. Isochronous stress-strain relations

### 2-8.1. Alloy 740H

The isochronous stress-strain relations for Alloy 740H are described by the following equations where  $\varepsilon$  is the total strain,  $\sigma$  the stress,  $T$  temperature, and  $t$  time:

$$\begin{aligned}\varepsilon &= \varepsilon_e + \varepsilon_p + \varepsilon_c \\ \varepsilon_e &= \frac{\sigma}{E} \\ \varepsilon_p &= \begin{cases} \begin{cases} 0 & \sigma \leq \sigma_0 \\ K \left( \frac{\sigma - \sigma_0}{\sigma_0} \right)^n & \sigma > \sigma_0 \end{cases} & 600^\circ\text{C} \leq T \leq 800^\circ\text{C} \\ \begin{cases} 0 & \sigma \leq \sigma_1 \\ -\frac{1}{\delta} \ln \left( 1 - \frac{\sigma - \sigma_1}{\sigma_p - \sigma_1} \right) & \sigma > \sigma_1 \end{cases} & T > 800^\circ\text{C} \end{cases} \\ \varepsilon_c &= \dot{\varepsilon}_o e^{\frac{B\mu b^3}{AkT}} \left( \frac{\sigma}{\mu} \right)^{\frac{-\mu b^3}{AkT}} t\end{aligned}$$

Article 2-2.1.1 provides the Young's modulus,  $E$ . Tables 2-8.1.1 and 2-8.1.2 lists the parameters for the equations. For Table 2-8.1.1 parameters shall be interpolated linearly between temperatures in the table. The units for temperature are  $^\circ\text{C}$ , stress is in MPa, time in hours, and strains in mm/mm. The relations shall not be used for temperatures outside those provided in Table 2-8.1.1, i.e. the relations are only valid for  $600^\circ\text{C} \leq T \leq 850^\circ\text{C}$ . In these equations the shear modulus  $\mu$  shall be calculated with the formula

$$\mu = \frac{E}{2(1 + \nu)}$$

with  $E$  the Young's modulus defined in Article 2-2.1.1 and  $\nu$  the Poisson's ratio defined in Article 2-2.2.1.

Temperatures	Ramberg-Osgood model parameters			Voce hardening model parameters		
	$\sigma_0$ (MPa)	K	n	$\sigma_p$ (MPa)	$\sigma_1$ (MPa)	$\delta$
600°C - 700°C	400.24	0.0704	6.6480			
725°C	374.20	0.0357	7.1315			
750°C	348.16	0.0181	7.6150			
775°C	312.255	0.0055	10.971			
800°C	276.35	0.0017	14.327	574.991	455.850	908.324
825°C				521.631	319.315	2212.205
850°C				468.271	182.780	3516.087

Table 2-8.1.1. Parameters for the  $\varepsilon_p$  contribution to the Alloy 740H isochronous stress-strain relation.

Parameter	Value
$\dot{\varepsilon}_o$	$1.19 \times 10^{10} \text{ hr}^{-1}$
k	$1.38064 \times 10^{-20} \text{ mJ/K}$
b	$2.53 \times 10^{-07} \text{ mm}$
A	-10.98557
B	-0.53098

Table 2-8.1.2. Parameters for the  $\varepsilon_c$  contribution to the Alloy 740H isochronous stress-strain relation.

Figures 2-8.1.1 to 2-8.1.11 plot the isochronous stress-strain relations for Alloy 740H.

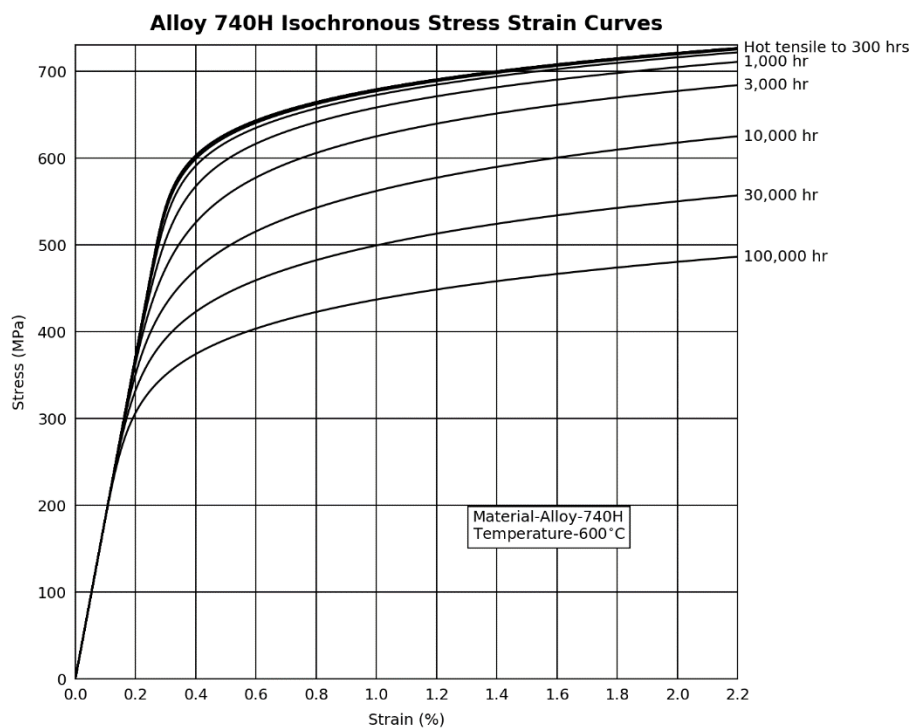


Figure 2-8.1.1. Design isochronous stress-strain curve for Alloy 740H at 600° C.

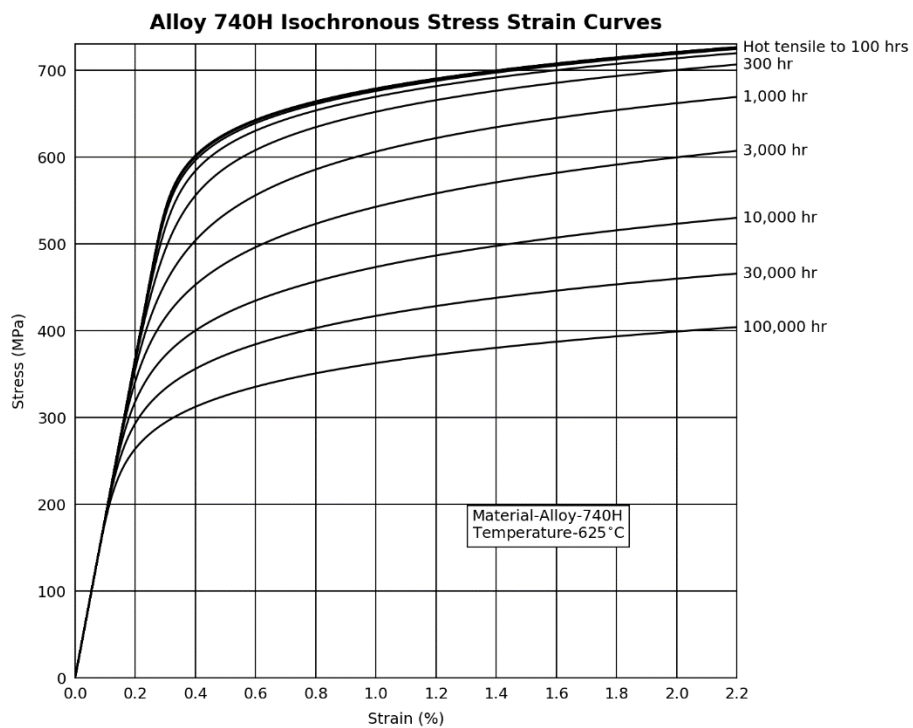


Figure 2-8.1.2. Design isochronous stress-strain curve for Alloy 740H at 625° C.

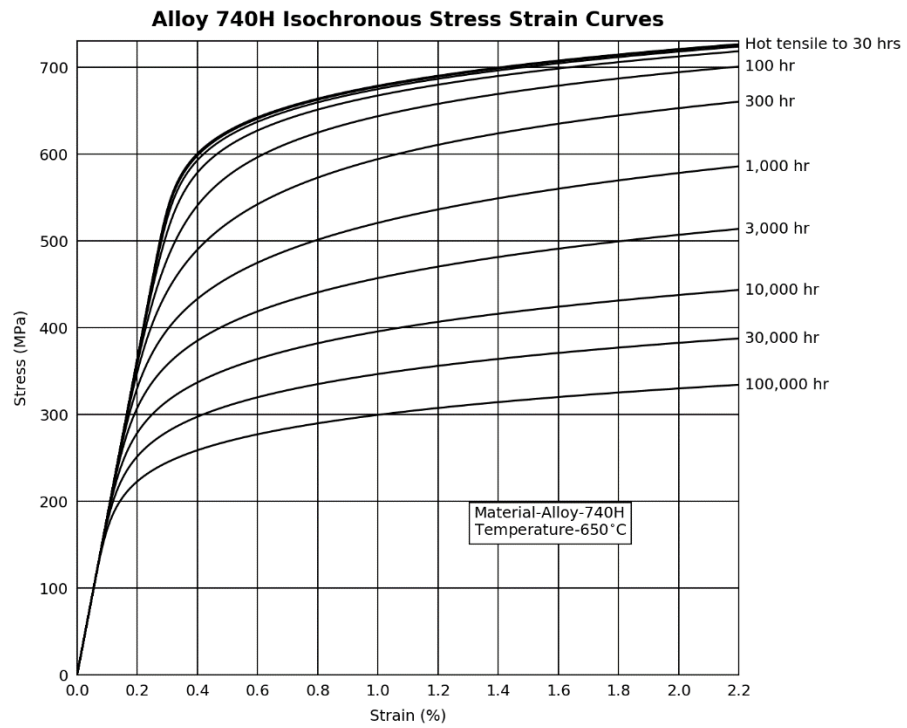


Figure 2-8.1.3. Design isochronous stress-strain curve for Alloy 740H at 650° C.

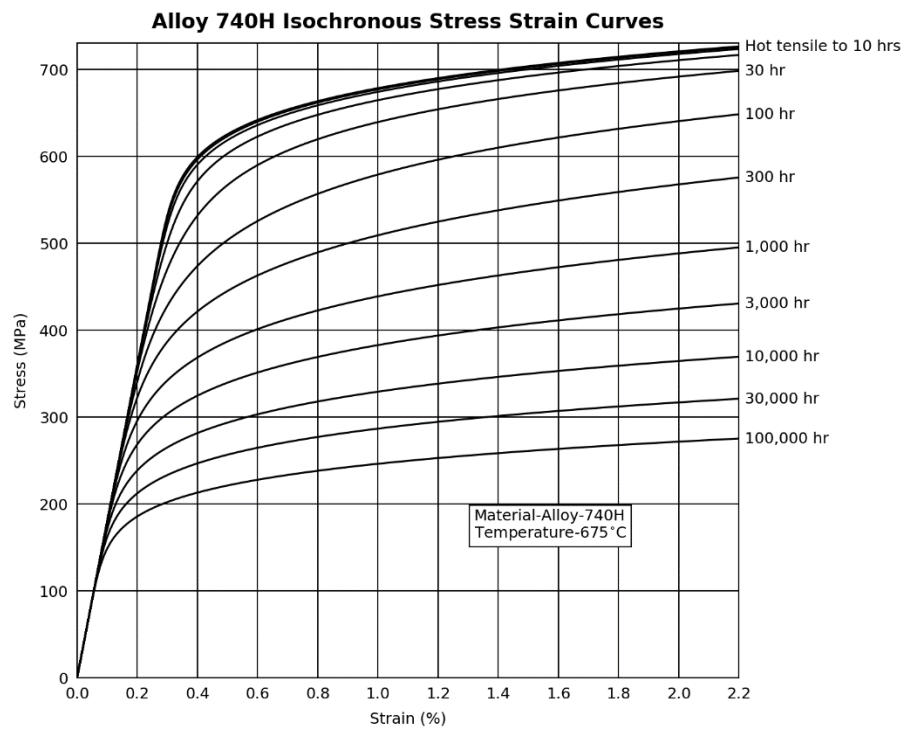


Figure 2-8.1.4. Design isochronous stress-strain curve for Alloy 740H at 675° C.

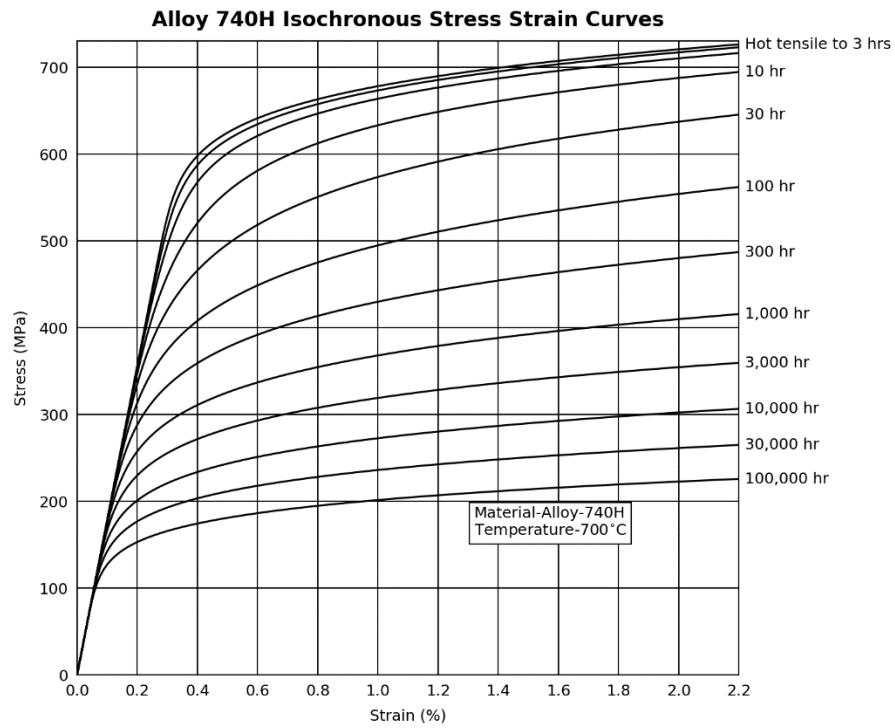


Figure 2-8.1.5. Design isochronous stress-strain curve for Alloy 740H at 700° C.

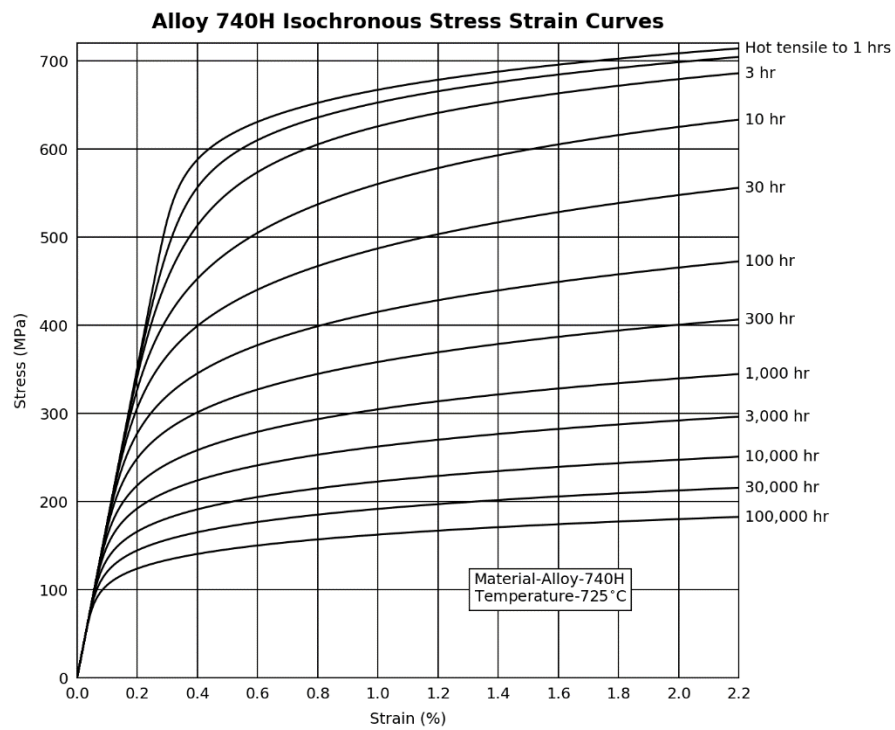


Figure 2-8.1.6. Design isochronous stress-strain curve for Alloy 740H at 725° C.

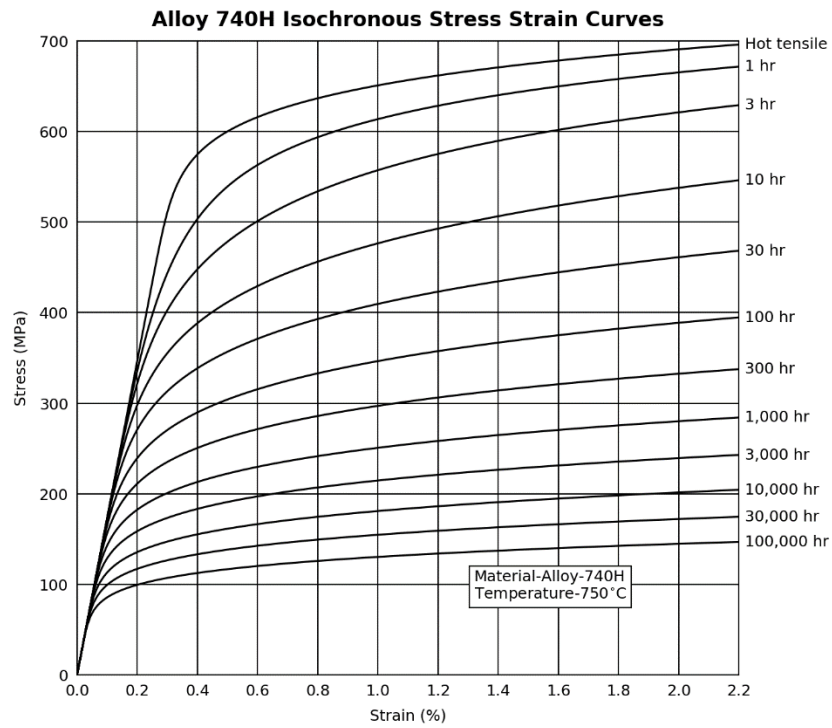


Figure 2-8.1.7. Design isochronous stress-strain curve for Alloy 740H at 750° C.

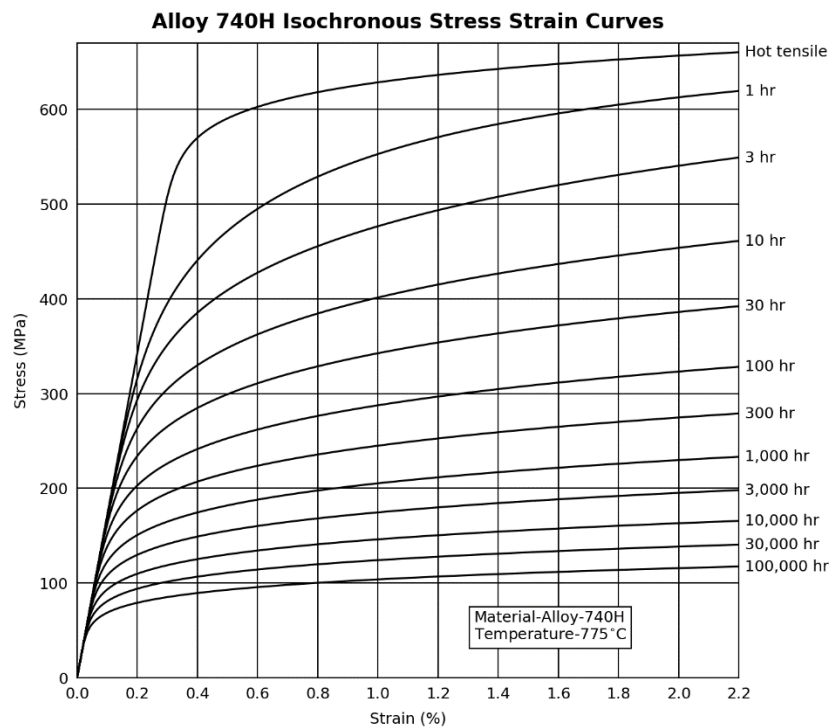


Figure 2-8.1.8. Design isochronous stress-strain curve for Alloy 740H at 775° C.

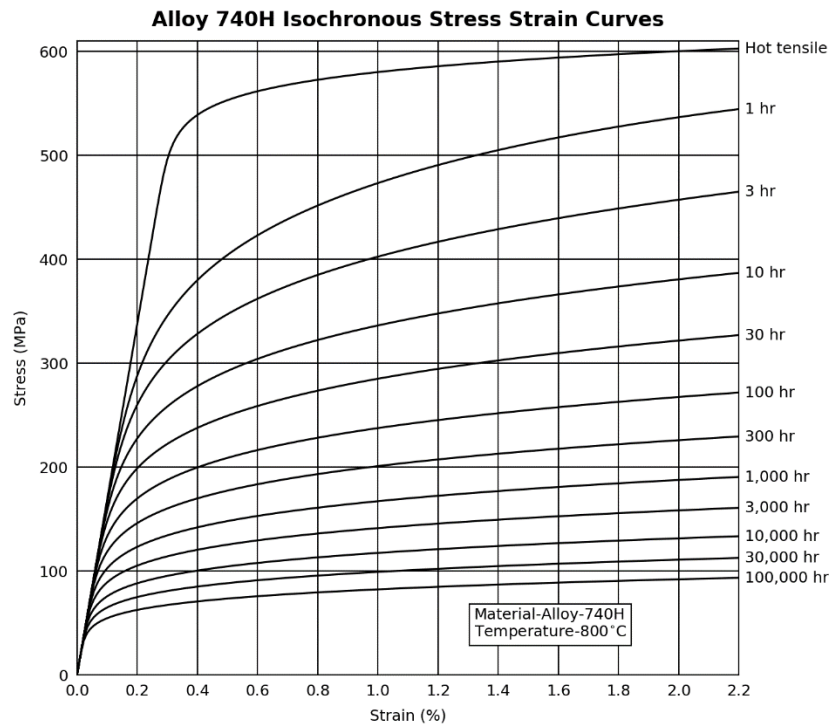


Figure 2-8.1.9. Design isochronous stress-strain curve for Alloy 740H at 800° C.

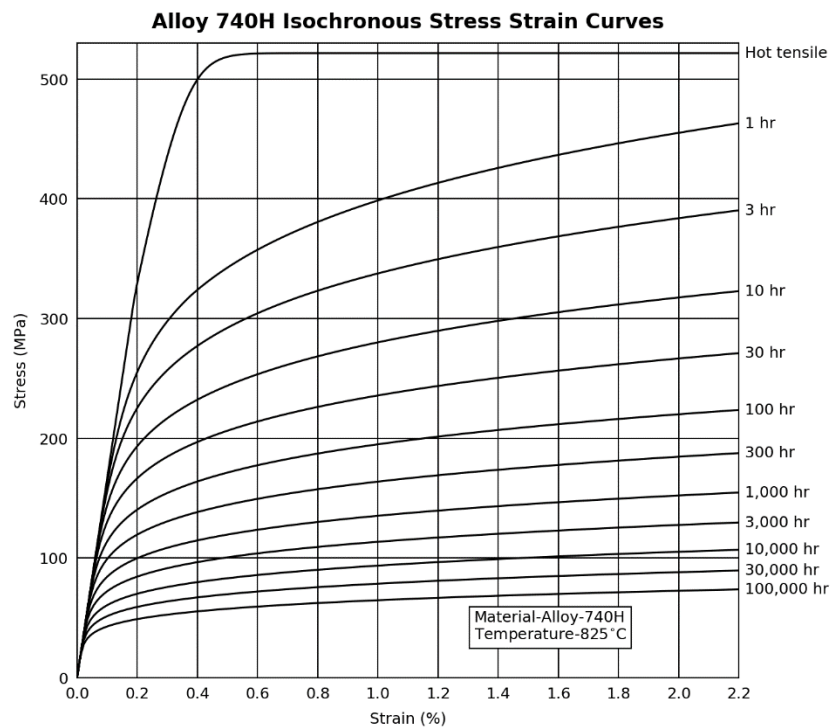


Figure 2-8.1.10. Design isochronous stress-strain curve for Alloy 740H at 825° C.



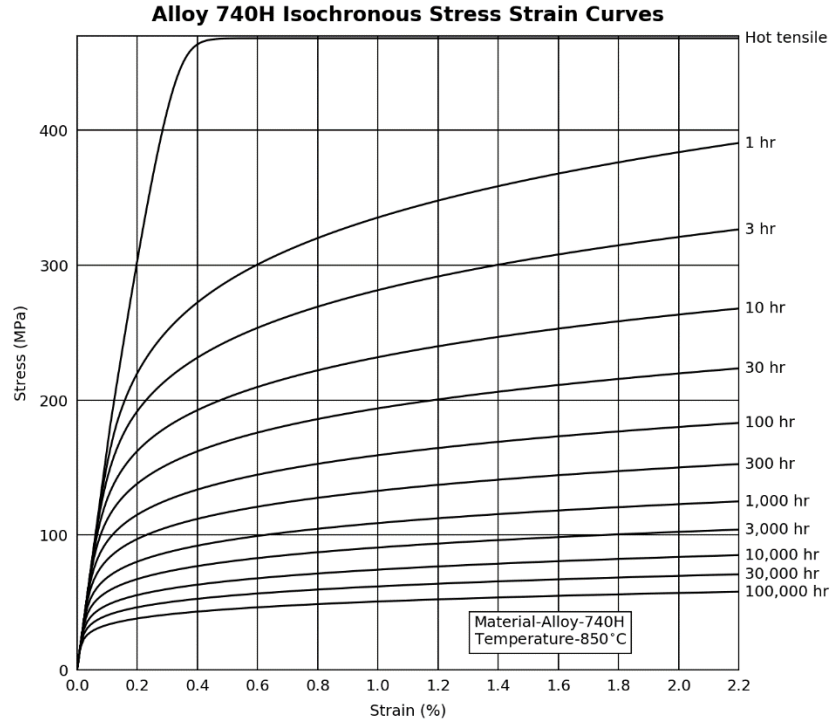


Figure 2-8.1.11. Design isochronous stress-strain curve for Alloy 740H at 850° C.

## 2-9. Inelastic constitutive models

### 2-9.1. Alloy 740H

The follow inelastic constitutive model may be used for Alloy 740H for  $600^{\circ}\text{C} \leq T \leq 850^{\circ}\text{C}$ :

$$\dot{\sigma} = C: (\dot{\epsilon} - \dot{\epsilon}_t - \dot{\epsilon}_c)$$

with  $\dot{\sigma}$  the rate of the Cauchy stress tensor,  $C$  the isotropic elasticity tensor constructed using the temperature-dependent Young's modulus provided in Article 2-2.1.1 and Poisson's ratio provided in Article 2-2.2.1,  $\dot{\epsilon}$  is the total strain rate,  $\dot{\epsilon}_t$  is the thermal strain rate provided by the equation

$$\dot{\epsilon}_t = \alpha \dot{T} \mathbf{I}$$

with  $\alpha$  the instantaneous coefficient of thermal expansion provided in Article 2-3.1,  $\dot{T}$  the temperature rate, and  $\mathbf{I}$  the identity tensor, and  $\dot{\epsilon}_c$  is the creep strain rate provided by the equation

$$\dot{\epsilon}_c = \dot{\epsilon}_o e^{\frac{B\mu b^3}{AkT}} \left( \frac{\sigma_v}{\mu} \right)^{\frac{-\mu b^3}{AkT}} \frac{\mathbf{s}}{\sigma_v}$$

where Article 2-8.1 defines the parameters in this equation,  $\sigma_v = \sqrt{\frac{3}{2} \mathbf{s} : \mathbf{s}}$ , and  $\mathbf{s}$  is the deviatoric stress tensor.

## **2-10. Temperature limits**

### **2-10.1. Minimal creep threshold**

#### **2-10.1.1. Alloy 740H**

The temperature at which Alloy 740H accumulates 0.1% strain at a stress of  $S_o$  over 100,000 hours life is 595° C.

### **2-10.2. Limit on O'Donnell-Porowski method**

#### **2-10.2.1. Alloy 740H**

The cutoff temperature for the B-1 and B-2 tests in ASME Section III, Division 5, HBB-T-1332 is 600° C for Alloy 740.

## Part 3: Commentary

### 3-1. Overview

The purpose of the design methods and material data contained in this report is to enable the design of components for solar receivers that operate in conditions where secondary stresses can cause significant creep or creep-fatigue damage. In the context of solar systems, secondary stresses are typically thermal stresses and primary stresses are typically caused by pressure. Therefore, these design criteria are shaped towards structures that see low pressures but high thermal gradients, operate at high temperatures in the creep regime, and see daily load cycling. These conditions point towards eventual component failure via creep or creep-fatigue damage accumulated during daily application and relaxation of the thermal stress, rather than creep failure caused by long times at constant pressure loads.

Commercial practice, for example Sections I and VIII of the ASME Boiler and Pressure Vessel Code, guards against creep failure under primary loads by including creep rupture properties in the high temperature allowable stresses. This approach is reasonable for components that see long periods of hold time at fixed conditions and limited numbers of load cycles. It is less reasonable for components which see large numbers of load cycles, like CSP systems, as it does not account for the damaging effect of secondary load. Figure 3-1.1 illustrates the differences between steady state load conditions, traditional high temperature nuclear systems assuming a moderate amount of load cycling interspersed with relatively long hold periods, and CSP systems by illustrating representative stress/time histories

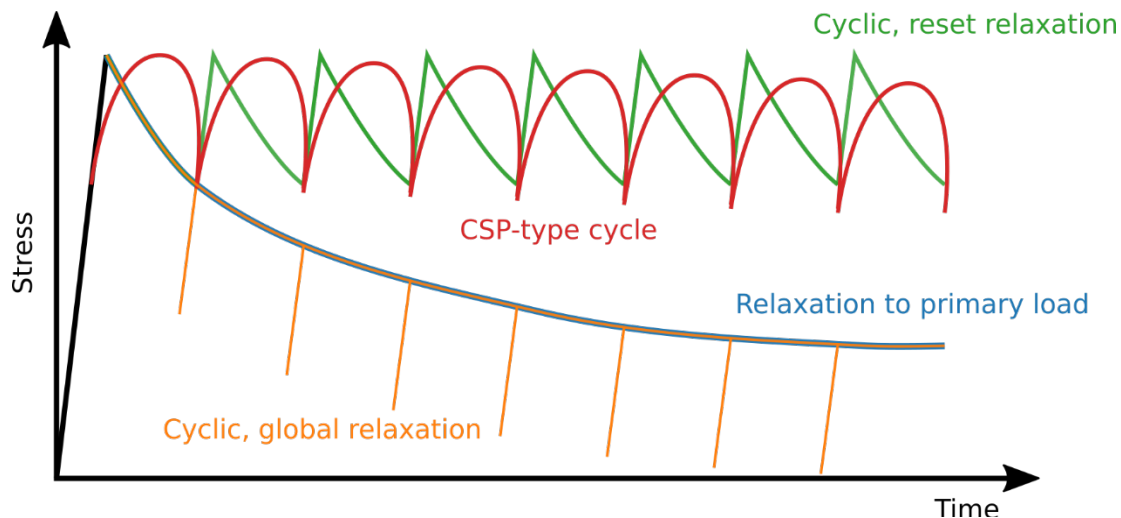


Figure 3-1.1. Illustration of four different types of loading histories: (1) Steady-state, non-cyclic loading where the component stresses relax to the primary load. (2) Cyclic load where the secondary stresses do not cause the component to reset to the initial value of load. (3) Cyclic load where the secondary stresses cause the component to reset to the initial, high level of stress each cycle. (4) A prototypical CSP load cycle where the loads increase and decrease gradually throughout the cycle period. Conventional Section I and Section VIII design assumes a load of type (1), Section III, Division 5 high temperature nuclear design assumes either (2) or (3) with criteria to determine if the global relaxation mode occurs. This report provides design rules suitable for load type (4).

The key challenge to address in developing an adequate high temperature CSP design method is to guard against creep and creep-fatigue damage caused by cyclic secondary stresses. In the context of a tubular receiver these stresses would be the daily application of the thermal stress caused by both the through-wall and circumferential thermal gradients. However, the design criteria also provide:

1. allowable stress criteria for steady-state primary loads to maintain compatibility with current commercial practice and to provide a minimum section thickness;
2. ratcheting design criteria to prevent service failures caused by excess deformation;
3. buckling criteria, to prevent both time-independent elastic-plastic buckling and time-dependent buckling caused by creep deformation.

However, for the sample designs considered in Part IV it is creep damage caused by the daily application of secondary thermal stresses that dictates the maximum design life of the component. The design rules below lump this damage mechanism in with creep-fatigue design. Indeed, as Figure 3-1.2 illustrates, creep-relaxation damage caused by secondary loads is one end of the spectrum of loadings encompassed by the creep-fatigue design procedures. On the other end of the spectrum is pure fatigue damage and in between lies creep-fatigue interaction. If the components sampled in Part IV operated at somewhat lower metal temperatures then creep-fatigue interaction would control the component life. If they operated at much lower temperatures then pure fatigue damage would control the life. The creep-fatigue interaction diagram therefore encompasses the full range of failure mechanism for low pressure, high thermal stress components.

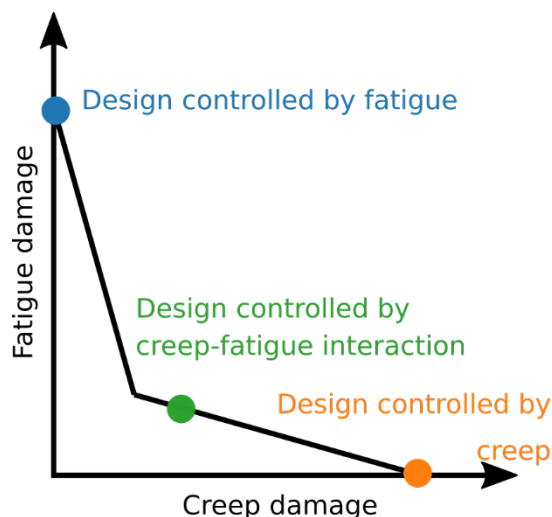


Figure 3-1.2. Illustration of how the creep-fatigue checks used here encompass failure by pure fatigue, failure by pure creep, and failure by creep-fatigue interaction. The region of the design envelope an efficient component occupies depends on the relative severity of the primary and secondary load, the type of load cycle, and the average metal temperature.

The design rules in Part I are given procedurally and the component must pass all the required design checks to be considered adequate. However, for the types of CSP components envisioned when creating these design processes a more practical process would be to first find the minimum component thickness using the primary load, allowable stress design procedures. If the primary stress is low, as for the sample problems in Part IV, this minimum thickness might be too thin to

feasibly manufacture. If so, this minimum thickness should be increased to the thinnest manufacturable section.

Once this thinnest section has been determined the designer should evaluate creep-fatigue damage using one of the options presented in Part I. If the component passes the creep-fatigue criteria using the minimum section thickness determined above then the designer can proceed to evaluating the remaining criteria (ratcheting and buckling). These will only rarely constrain the design – most often the design thickness will be determined by the tradeoff between the primary load allowable stresses and the secondary creep-fatigue checks.

Figure 3-1.3 illustrates this tradeoff and demonstrates that if the design does not pass the creep-fatigue check for the minimum section thickness determined by the primary load design then the component will need to be reconfigured – increasing the section thickness will only increase the secondary load on the component and make it more difficult to pass the creep-fatigue criteria. At high metal temperatures CSP components will be constrained by the minimum section thickness provided by the primary load design criteria and the maximum section thickness provided by the creep-fatigue design criteria.

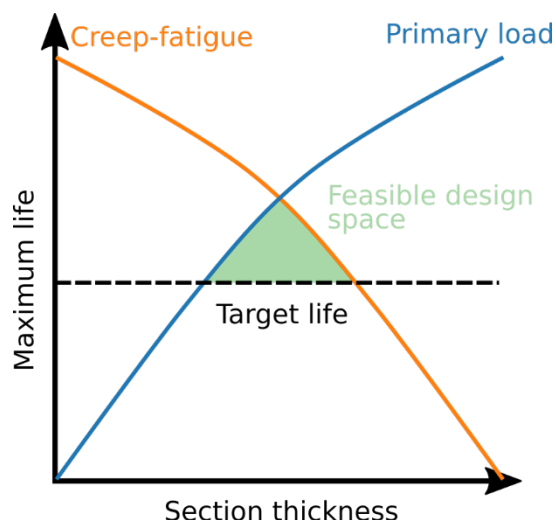


Figure 3-1.3. Illustration of the tradeoff between primary load criteria setting a minimum section thickness and creep-fatigue criteria setting a maximum section thickness. The green shaded region is that feasible design space – the thicknesses that meet or exceed the target design life. Note that the minimum primary load section thickness provides the most economic design, hence the design strategy suggested here.

The ratcheting and buckling criteria represent important potential failure modes but rarely constrain the design of CSP components. The design should check these criteria only after they achieve a feasible design considering the primary load and creep-fatigue design provisions.

## 3-2. Commentary on the Design Rules

### 3-2.1. General Criteria

The high temperature/low temperature cutoff is standard ASME practice – 370° C for ferritic and ferritic-martensitic steels and 425° C for austenitic stainless steels and nickel-based alloys. CSP

components are likely to spend most or all of their service life in the creep regime and so these rules focus exclusively on high temperature applications.

The design provisions here are focused on CSP structures undergoing daily cycling. They may not be adequate for structures with long hold times. The threshold temperature was based on the temperature at which the material accumulates 0.1% strain at the allowable stress  $S_o$  over 100,000 hours. This is essentially a negligible creep criteria.

Several of the Design Options are modifications of the Section III, Division 5 ASME Boiler and Pressure Vessel Code rules covering the design of high temperature nuclear reactor components. These modifications were developed starting from the 2019 edition of the ASME Code.

To simplify the design process these rules work with a single, representative Design Cycle. This is a collection of periodic structural and thermal boundary conditions that adequately represent the operating cycle of the component. For a CSP system this would likely be a daily cycle that reasonably represents the standard operation of the facility. An example for a solar receiver could be the service conditions on the solar equinox. Section III, Division 5 of the ASME Code contains rules for evaluating several different types of loading cycles with different expected frequencies. The current rules could be extended to cover multiple cycle types at the expense of a more complicated design process.

The design methods here use a similar database of material properties to the ASME rules, but alter the design margin encoded in the ASME data to reflect the relative consequences of failure between CSP and nuclear systems. As such, the design rules should be used with the provided material data, not the information in Section III of the ASME Code.

The rules here only cover component design. A complete design and construction code would require rules for construction, welding, examination, and inspection. The Design Specification could provide these criteria by reference to the ASME Code. Structures passing these design rules should also pass the Section VIII, Division 2 design by analysis criteria. These provisions could then be used to supplement the design of a Code-stamped component to ensure the component will perform well under cyclic conditions at high temperatures – conditions not currently considered in detail by either Section I or Section VIII.

### **3-2.2. Design Option A**

This design option is based on the Section III, Division 5 ASME Boiler and Pressure Vessel Code covering the design and construction of high temperature nuclear reactors. The design methods contained in Section III, Division 5 are well documented<sup>1,2</sup> and so this commentary only provides a general overview of the approach. The focus of the commentary is on the modifications made to the base ASME method to account for the unconventional operating cycles and temperatures of

---

<sup>1</sup> R. I. Jetter, “Subsection NH—Class 1 Components in Elevated Temperature Service” in *Companion Guide to the ASME Boiler and Pressure Vessel Code*, Volume 1, K. R. Rao ed. ASME Press, New York, NY, 2009.

<sup>2</sup> M. H. Jawad, and R. I. Jetter, *Design & Analysis of ASME Boiler and Pressure Vessel Components in the Creep Range*. ASME Press, New York, NY, 2009.

CSP systems as well as modifications made to account for the lower consequences of failure when comparing nuclear reactors to CSP facilities.

The Section III, Division 5 checks mirror those used in these design rules. The Code mandates a primary load check against allowable stresses plus checks for ratcheting, creep-fatigue, and buckling. The methods used in Design Option A are those from the ASME Code simplified, modified, and with reduced design margin.

### **3-2.2.1. Primary load**

Section III, Division 5 actually contains two primary load design checks: one mirroring the Section I / Section VIII allowable stress checks where the primary stress is compared to some temperature-dependent but time-independent allowable stress  $S_o$ . This check uses a design temperature and pressure that bound the standard, non-faulted service conditions. The Code also has second primary stress check against a time- and temperature-dependent allowable stress  $S_{mt}$ . This check uses the Service Loads provided by the Owner's Design Specification. The nuclear code accounts for different expected frequencies and severities of loading by providing A, B, C, and D Service Load categories. The time-dependent primary load check uses different margins depending on the load category. Finally, Section III, Division 5 requires not only that each individual Service Load pass the allowable stress check but also that the time-fraction of all the service loadings combined remains less than one.

As discussed above, these rules for CSP components operate only with a single Design Cycle. This is a compromise between Section I and VIII practice, which only typically use Design Conditions and do not account explicitly for cyclic service, and the Section III, Division 5 practice of evaluating the component against all expected transients, classifying each particular transient based on its severity and expected frequency.

The rules retain a check against a time-independent allowable stress using the primary stress from a set of Design Conditions, now determined as the bounding temperature, pressure, and nozzle loads from the Design Cycle. This is analogous to current Section I and VIII commercial practice. The design rules omit the Section III, Division 5 check against time-dependent allowable stress and the use-fraction check for several reasons:

1. This retains the direct connection to current commercial practice and does not add the complication of an additional time-dependent allowable stress check.
2. As discussed above, the primary load check for CSP systems is unlikely to be the controlling factor. The main point of the primary load check in high temperature CSP systems is to provide a reasonable minimum section thickness, which can be done without invoking time-dependent allowables.
3. The allowable stress  $S_o$  is based on 100,000 hour extrapolated creep properties. This is not far removed from 10-30 year design lives for actual components.

The determination of the  $S_o$  allowable stress values is discussed below in 3-3.7. This process is essentially consistent across Section III, Division 5 and Section I/Section VIII, Division 2 and so a reasonable modification of the design rules could be to use Section I or Section VIII rules to first

design the component and then apply the ratcheting, creep-fatigue, and buckling checks provided in these rules. This would be consistent with the complete approach described above and yet also ensure the component passes the Section I or Section VIII criteria.

The Section III, Division 5 allowable stress  $S_{mt}$  has two parts: a time-independent allowable stress  $S_m$  and a time-dependent allowable stress  $S_t$ .  $S_{mt}$  is simply the lesser of the two for a given time and temperature. While the design rules use neither stress as an allowable stress, the Section III, Division 5 ratcheting and creep-fatigue rules use the values of  $S_m$  to bound the time-independent initial stresses experienced by a component. As such, Design Option A requires values of  $S_m$  to complete the ratcheting and creep-fatigue design checks. Section 3-3.8 describes how these values are obtained.

HBB-3222.1(c) requires a buckling check per the Section III, Division 5 rules. The present design rules provide an alternative method for assessing buckling failure.

### **3-2.2.2. Ratcheting Strain Accumulation**

The design rules use a simplified version of the B-1 test from Section III, Division 5, Subsection HB, Subpart B, Nonmandatory Appendix T. The B-1 test is an implementation of the O'Donnell-Porowski<sup>3</sup> approach. This approach in turn builds on the classical work of Bree<sup>4</sup> and so the ratcheting test is most accurate for cylindrical thin-walled pressure vessels. However, it can be conservatively used for other types of structures where the peak stress is negligible. If the structure has significant peak stress Design Option C can be used.

Essentially, the design rules retain the Section III, Division 5 approach and simply remove additional margin included in the nuclear code. The ASME implementation of the method increases the core stress calculated by O'Donnell-Porowski by 25%. The design rules here do not increase the core stress. As such, this method uses a best-estimate of the accumulated strain, rather than the bounding values used in Section III, Division 5. Additionally, the design rules increase the allowable accumulated strains from 1% for base metal and ½ % for welds to 2% for base metal and 1% for welds. This reflects the reduced consequences of failure for CSP components and is in line with previous CSP design guidance.

The O'Donnell-Porowski method uses isochronous stress-strain curves to convert stress, temperature, and time into accumulated strain. Isochronous stress strain curves are a way to graphically depict a monotonic deformation relation for a material (see 3-3.14). They are constructed from a database of monotonic tension and creep tests and provide a simple way to link stress to deformation for materials at high temperature.

### **3-2.2.3. Creep-fatigue criteria**

---

<sup>3</sup> W. O'Donnell, and J. Porowski, "Upper bounds for accumulated strains due to creep ratcheting" *Journal of Pressure Vessel Technology*, 96(3), pp. 150-154, 1974.

<sup>4</sup> J. Bree, "Elastic-plastic behavior of thin tubes subjected to internal pressure and intermittent high-heat fluxes with application to fast-nuclear-reactor fuel elements" *Journal of Strain Analysis for Engineering Design*, 2(3), pp. 226-238, 1967.



Creep-fatigue interaction describes extensive experimental data showing that the combination of cyclic strain controlled deformation interspersed with holds at constant strain is more damaging than either holding at constant strain or cycling with the same strain range but no hold periods. A variety of microstructural mechanisms have been posited to explain the interaction<sup>5,6,7</sup>, but for the purposes of developing design rules it is sufficient to note the empirical phenomenon.

Creep-fatigue interaction can be quantified using a creep-fatigue interaction diagram. This requires first selecting definitions for fatigue and creep damage individually. All modern high temperature design methods define fatigue damage using Miner's rules using strain-based, temperature-dependent fatigue diagrams. These diagrams are constructed from experimental data and show the number of cycles to failure for a given combination of temperature, strain range, and R ratio (see Section 3-3.11). Often fully-reversed loading ( $R = -1$ ) is most damaging and used to construct design fatigue curves. Fatigue damage is then defined as  $D_f = N/N_f$  where  $N$  is the actual number of cycles at fixed strain range and temperature and  $N_f$  is the number of cycles to failure from the fatigue diagram.

The process of going from a full 3D strain state to a scalar strain range requires the definition of an effective strain range. These rules adopt the ASME definition.

There is an ongoing disagreement as to how to quantify creep damage at constant stress or constant strain. Several methods have been proposed and are in use in current design and fitness for service standards. These techniques include time fraction, used in the ASME Boiler and Pressure Vessel Code, ductility exhaustion<sup>8</sup>, used in the RCC-MRx and R5 Codes, and the Omega method<sup>9</sup> used in API-579/ASME FFS-1. These different methods will all lead to somewhat different predictions for rupture given the same stress/strain/time history. However, studies have shown overall they are all about equally accurate<sup>10,11</sup>. These design rules adopt the ASME time-fraction approach.

Time fraction is a very straightforward method for calculating a creep damage fraction. It needs a scalar effective stress measure – a map from a 3D state of stress to a scalar stress – and a database of the material rupture stress as a function of time and temperature. The rupture stress information

---

<sup>5</sup> S. W. Nam, S. C. Lee, and J. M. Lee, "The effect of creep cavitation on the fatigue life under creep-fatigue interaction" *Nuclear Engineering and Design*, 153(2–3), pp. 213–221, 1995.

<sup>6</sup> J. Wareing, "Creep-fatigue interaction in austenitic stainless steels" *Metallurgical Transactions A*, 8(5), pp. 711–721, 1977

<sup>7</sup> M. Sauzay, M. Mottot, L. Allais, M. Noblecourt, I. Monnet, and J. Périnet, "Creep-fatigue behaviour of an AISI stainless steel at 550°C" *Nuclear Engineering and Design*, 232(3), pp. 219–236, 2004.

<sup>8</sup> R. M. Goldhoff, "Uniaxial Creep-Rupture Behavior of Low-Alloy Steel Under Variable Loading Conditions" *Journal of Basic Engineering*, 87(2), pp. 374–378, 1965.

<sup>9</sup> M. Prager, "Development of the MPC Omega Method for Life Assessment in the Creep Range" *Journal of Pressure Vessel Technology*, 117(2), pp. 95–103, 1995.

<sup>10</sup> S.-L. Mannan, F.-Z. Xuan, X.-C. Zhang, Y.-C. Lin, S.-T. Tu, and X.-L. Yan, "Review of creep–fatigue endurance and life prediction of 316 stainless steels" *International Journal of Pressure Vessels and Piping*, 126–127, pp. 17–28, 2014.

<sup>11</sup> S. Zhang, and Y. Takahashi, "Evaluation of high temperature strength of a Ni-base alloy 740H for advanced ultra-supercritical power plant" in *Proceedings from the Seventh International Conference on Advances in Materials Technology for Fossil Power Plants*, 2013.

can be derived from creep test results (see 3-3.10). Given this information creep damage is defined as  $D_c = t/t_R$  where  $t$  is the time at fixed stress and temperature and  $t_R$  is the time-to-rupture for that stress and temperature.

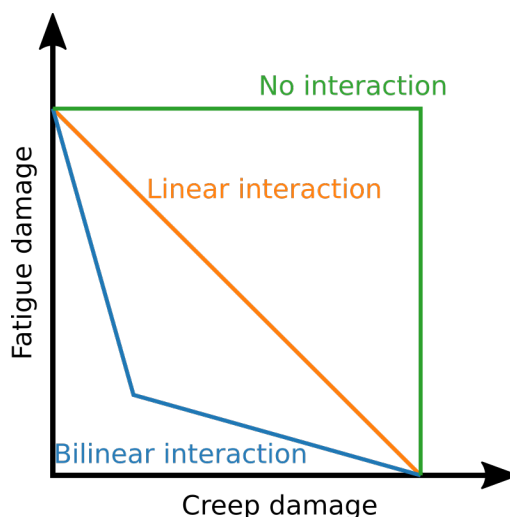


Figure 3-2.2.3.1. Various interaction types demonstrated on a creep-fatigue interaction diagram.

Given a definition of fatigue and creep damage a creep-fatigue interaction diagram can be constructed from a database of creep-fatigue test results. Creep fatigue tests, sometimes called dwell-fatigue tests, are strain-controlled cyclic tests with hold periods at constant strain on either or both of the maximum tension or maximum compression side of the cycle. Often these tests use fully reversed loading cycles, thought to be the most damaging. The full stress/strain/time hysteresis information is recorded during the test and this history used to calculate creep and fatigue damage using the corresponding definitions. Plotting the results of a number of creep-fatigue tests at different conditions produces a design envelope of the type sketched in Figure 3-2.2.3.1 (see Section 3-3.12). Note the definition of creep and fatigue damage affects the shape of the diagram – the same experimental data could produce different interaction diagrams using different definitions of damage. Therefore it is critical to use an interaction diagram calculated using consistent definitions of damage.

This process describe the generic creep-fatigue model used to calculate damage in the ASME Code and in all three design options described here. Design Option A uses the ASME Section III, Division 5, Subsection HB, Subpart B design by elastic analysis rules to determine the strains, stresses, temperatures, and times required to calculate damage and check conditions against the design envelope. While the elastic method is venerable, it has been well-validated by past experience and has the important advantage over other methods in that it requires only a linear elastic stress analysis of a single cycle repetition. This means that while the design rules are somewhat complicated the design analysis is straightforward and easily accomplished.

For full details of the development of the design by elastic analysis method see the reference material on the Section III, Division 5 rules, cited above. This following provides a brief overview. This process must be repeated at each point in a component to find the limiting location.

1. Perform a linear elastic stress analysis of a loading cycle and extract the elastic strain range, using the ASME definition of effective strain range. The Section III, Division 5 rules provide methods for combining the effects of multiple types of load cycles. These rules are not relevant here, as the current design criteria work with a single Design Cycle.
2. Modify the elastically calculated strain range to account for plasticity and creep using bounding formula provided in the ASME Code.
3. Calculate the fatigue damage using the modified strain range.
4. Use one of the following two methods to construct a stress relaxation history:
  - a. Use the method of isochronous curves to calculate a stress relaxation history starting from the modified strain range determined above. The method of isochronous curves assumes that stress relaxation will follow the monotonic stress/strain/time relation described by the isochronous curves. This is a conservative bounding assumption – the real stress relaxation history will generally be less severe.
  - b. Use a differential description of the material's creep deformation to integrate a stress relaxation history starting from the strain range determined above. This approach is more accurate than the method of isochronous curves but requires solving an ordinary differential equation.
5. Use the stress relaxation history, divided by a design factor, to calculate creep damage.
6. Consult the creep-fatigue interaction diagram to determine whether the point passes the design criteria.

The modified rules for CSP structures given here follow this general process with several modifications from the ASME rules.

First, the design margin is modified to account for the relative consequences of failure between CSP and nuclear structures. The fatigue damage in the ASME nuclear code uses fatigue diagrams with factors of 20 on the number of cycles to failure and 2 on the strain range. These rules, as described in Section 3-3, adopt factors of 10 and 1.5. These rules divide the stress relaxation history by a factor 0.9, retaining the ASME design by elastic analysis factor for creep damage. Additionally, as with the ASME approach, these rules use a statistical minimum stress to rupture to calculate creep damage, rather than the average property. The O'Donnell Porowski core stress and a material dependent relaxation strength are used to bound the amount of stress relaxation calculated with the method of isochronous curves. The ASME rules apply a factor of 1.25 on both quantities, here the rules do not increase these lower relaxation limits by any factor, instead using the average material property. Note the current rules provide values of the relaxation strength (see 3-3.9), whereas the current ASME rules require the designer to determine this from material test data or a separate relaxation analysis.

Second, the ASME method is simplified by disallowing the use of several alternate methods for calculating strain ranges and relaxation histories. This is done solely to simplify the design process.

Finally, as noted in Figure 3-1.1 there are two types of cyclic stress relaxation for classical high temperature structures modeled with elastic, perfectly-plastic, power-law creep material under cycles consisting of instantaneous loading, hold at constant load, and instantaneous unloading:

resetting relaxation where each cycle starts out at the same, high value of stress and global relaxation where the structure follows a global, constant-load relaxation curve with small elastic transients during the load/unload periods. The global relaxation mode is highly desirable from a design point of view as these sorts of structures spend more time at lower levels of stress and hence accumulate less creep damage. The ASME Section III, Division 5 rules contain a test to determine which mode will occur for a given component, based on the classical condition of reverse plasticity causing load resets. If the structure falls into the global relaxation mode the ASME rules allow an alternate, less damaging calculation of creep damage based on a global relaxation history.

The current rules do not allow this alternate method, essentially forcing the designer to treat CSP components as if they follow a resetting relaxation history. As described in more detail below, Alloy 740H and other high strength nickel alloys suitable for service at the high metal temperatures envisioned in future CSP concepts are unlikely to plastically yield during service. This might suggest that CSP structures will follow a global relaxation mode.

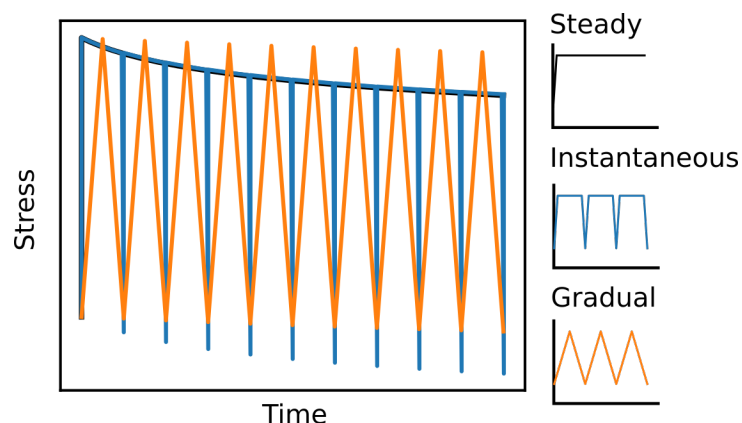


Figure 3-2.2.3.2. Stress relaxation histories for various cycles with the same total strain range but different loading cycle types.

However, Figure 3-2.2.3.2 demonstrates a problem with the classical division of structures into global and resetting relaxation. The past work establishing these categories was predominantly aimed at nuclear applications where the components are loaded and unloaded quickly compared to long hold periods at fixed conditions. CSP facilities do not operate in this mode, as they generally load follow the incident solar radiation which increases and decreases continually through the daily operation cycle. The figure shows three relaxation histories for an elastic-power law creep material, all starting from the same initial strain: steady relaxation at fixed strain, cyclic relaxation through a fixed strain range where the strains are applied instantaneously, held fixed, and instantaneously reversed, and cyclic relaxation through the same range where the strains are gradually applied and removed in a triangle wave pattern (see inset). Both cyclic histories undergo the same total strain range and have the same total period, the only difference is in how the strains are applied and removed.

The instantaneous and gradual cycles produce very different relaxation histories. The instantaneous cycle validates the classical global relaxation mode where the cyclic relaxation history follows the steady relaxation curve with short elastic transients. In contrast, the gradual cycle produces very little global relaxation over the 10 cycles shown the diagram, more closely resembling a resetting relaxation history.

Power law creep materials relax faster at high values of strain. This behavior explains the difference between the instantaneous and global cycles. The instantaneous cycle always relaxes at the highest value of strain and therefore relaxes comparatively quickly. The gradual cycle, on average, relaxes at lower values of strain and hence much more slowly. This simple example demonstrates that creep resistance is not always a good thing – materials that creep faster also shed load faster. This example also justifies the restriction in the design rules disallowing the use of the alternate, global relaxation calculation even if the structure would qualify for the alternate using the ASME rules. CSP cycles are much more akin to the gradual load cycle in the example, as opposed to nuclear structures which operate more like the instantaneous cycle.

The component is slowly globally relaxing in Figure 3-2.2.3.2 as reverse plasticity is not causing a full cycle reset. Design Options A and B conservatively neglect this slow relaxation. Option C accounts for it using inelastic analysis.

### **3-2.2.4. Buckling criteria**

Part 4 provides some perspective on the relative importance of time-independent buckling, time-dependent buckling, and the other design criteria. The fundamental conclusion is that time-independent buckling under lateral wind loading may be a significant design concern whereas time-dependent creep buckling is unlikely to constrain designs due to the low steady primary loads envisioned in future CSP systems. However, the design criteria provide methods for both time independent and creep buckling to provide guidance for systems that may have non-standard high, steady primary loads, for example systems with substantial self-weight. Additionally, the creep buckling rules come at little conceptual cost as they share a similar analysis method to the time independent buckling method.

For time independent buckling the rules require a direct stability assessment of the structure using the constitutive response given by the time-independent (hot tensile) isochronous curves. As described in 3-3.14 these represent a best-estimate, average properties description of the monotonic tension response of the material. It is therefore reasonable to use this response to represent the deformation of a structure under time-independent loading conditions, using standard  $J_2$  flow theory to extend the uniaxial tensile response to 3D stress states. The design criteria requires a large-deformation inelastic analysis of the component and so directly accounts for elastic and elastic-plastic buckling mechanisms. As described in Part 1 the Design Cycle must be supplemented in this analysis with any transient, non-cyclic lateral loads – for example wind loading.

The time-dependent buckling provisions use the method of isochronous curves. This approach has been successfully used to evaluate buckling in high temperature structures<sup>12</sup> and forms the basis of the buckling exemption charts in ASME Section III, Division 5. The idea of the method is to replace a time-dependent creep analysis with a time-independent elastic-plastic analysis using the

---

<sup>12</sup> D. S. Griffin, “Design Limits for Elevated-Temperature Buckling” In *Welding Research Council Bulletin 443 External Pressure: Effect of Initial Imperfections and Temperature Limits*, pp. 11-26, 1999.

appropriate isochronous curve to represent the stress redistribution caused by creep over the design life. This concept is empirical, but has been validated by past work<sup>13</sup>.

The analysis for the time-dependent buckling check is then fundamentally the same as for the time-dependent check: a large-deformation, inelastic analysis of the component under steady-state loading. The only differences are that for the time-dependent check the designer uses the appropriate isochronous curve to represent the material's constitutive response and the loading for time-dependent buckling should only include the steady and periodic loads given in the Design Cycle and not any additional, transient lateral loads. The rationale here is the evaluation should only include the loads causing significant creep deformation – brief transients like wind loading will not cause creep deformation.

The load factors used in the buckling analysis are 1.5. This provides a 50% safety factor accounting for uncertainties in the applied loads, the deformation properties of the actual material (keeping in mind that the isochronous curves represent an average, not a lower-bound, response), and any geometric imperfections in the fabricated component that might contribute to lower the buckling load. The factor of 1.5 was extracted from the ASME Boiler & Pressure Vessel Code Section III, Division 5 for Service Level D (most severe/least frequent) Loads. This means the current rules adopt the most aggressive/least conservative ASME factor, reflecting the lower consequences of failure in CSP versus nuclear systems.

### **3-2.3. Design Option B**

High temperature nickel superalloys like 740H are designed to have high strength at elevated temperatures. Newer alloys like Alloy 617, Alloy 740H, and Alloy 282 are so strong that they are unlikely to deform plastically in service – note the yield strength for Alloy 740H exceeds 400 MPa even above 800° C. This does not mean that these materials will remain linear elastic – creep deformation can and does occur even below the time-independent yield point. However, assuming the material does not undergo time-independent plastic deformation greatly simplifies the design process. Options B and C take advantage of this assumption.

CSP components undergo daily cycling and will typically descend to temperatures below the creep range during the inactive night periods. This means during each daily cycle they have only a relatively short period of time to undergo stress relaxation. Additionally, high temperature nickel alloys like 740H are creep-resistant, meaning they undergo relatively little creep deformation under typical operating conditions.

Design Option B takes advantage of these material characteristics. Using Design Option B requires that the component remain linear elastic. This criteria is checked by analyzing the Design Cycle with a linear elastic stress analysis and comparing the resulting stress intensities to the temperature dependent material yield strength. As the design values of  $S_y$  typically lower-bound the actual material properties such an analysis adequately demonstrates that the component will not yield, even accounting for uncertainty in material properties.

---

<sup>13</sup> *ibid.*

Design Option B uses the same primary load, ratcheting, and buckling methods as Method A. Simplifications to the O'Donnell-Porowski approach for strong materials would be possible, but the simplified process is not significantly easier to execute than the base approach required in Method A.

The simplifications in Design Option B are in the creep-fatigue analysis. The method applies two basic simplifications to the ASME Section III, Division 5, Subsection HB, Subpart B, Nonmandatory Appendix T design by elastic analysis method:

1. The elastically-calculated effective strain range used to calculate fatigue damage only needs to be modified for creep deformation, not plasticity.
2. The elastically-calculated stresses corresponding to the Design Cycle loading can be used to calculate creep damage.

The first simplification is justified as the material does not undergo time independent plastic deformation. Figure 3-1.1 describes the second simplification (compare the reset-relaxation to the CSP-type cycle). It relies on two observations made above:

1. A resetting cyclic stress relaxation history reasonably bounds the response of CSP components operating at high temperatures. High strength materials like Alloy 740H will not yield in service and so the elastically-calculated stresses are a reasonable starting point for a relaxation damage calculation.
2. High strength materials like Alloy 740H will not undergo significant stress relaxation during the relatively short cycle period typical for CSP components. As such, the elastic stress history without any additional relaxation caused by creep is reasonably representative.

Both assumptions do involve some conservative approximation. As discussed above, CSP components will gradually undergo global relaxation, albeit at a much slower rate than a steady-state relaxation analysis would predict. However, it is conservative to ignore this slow global relaxation. Similarly, high strength materials will undergo some amount of stress relaxation caused by creep. Again, this small amount of relaxation can be conservatively neglected. Designers can use Option C if they want to gain the additional design life provided by a more accurate global and in-cycle relaxation analysis.

### **3-2.4. Design Option C**

Like Option B this design option takes advantage of the assumption that high strength materials like Alloy 740H will not yield in service. As with Option B this requires a preliminary linear-elastic analysis to confirm the Design Cycle loads do not cause yielding.

Design by inelastic analysis has long been considered the gold standard for high temperature design<sup>14</sup> – likely to produce the most accurate, least-over conservative design analysis and the

---

<sup>14</sup> A. K. Dhalla, *Recommended practices in elevated temperature design: a compendium of breeder reactor experiences (1970-1987): Volume III – Inelastic analysis*. Welding Research Council Bulletin, 1991.

most efficient final designs. However, there are two practical problems in implementing design by inelastic analysis in engineering practice:

1. Accurate constitutive models for high temperature cyclic deformation are difficult to develop. There is comparatively little high temperature deformation data available to calibrate models and developing a mathematical description of high temperature cyclic plasticity is notably challenging.
2. A complete inelastic analysis requires the analysis to simulate the full service history of a component. For CSP components this might be 10,000 daily cycles, each requiring multiple time steps to capture the details of the daily loading cycle. This results in analysis with on the order of millions of time steps. These cannot be parallelized using current methods meaning that the calculation time becomes infeasibly long even for very small finite element models.

Design Option C attempts to retain some of the advantages of a design by inelastic method while overcoming these two disadvantages. This option retains the primary load and buckling criteria from Design Option A. It alters the approach for the ratcheting strain and creep-fatigue checks.

Design by inelastic analysis requires generating a full time/strain/stress history for each point of the component. Once this history has been generated the accumulated strain over the component's service life can be directly calculated and compared to appropriate service limits. Similarly, the strain/time history can be used to calculate a fatigue damage fraction, the stress/time history used to calculate a creep damage fraction, and these used in conjunction with the creep-fatigue damage envelope to assess the component against the creep-fatigue limits.

This design method retains the ASME effective strain range formula for converting a 3D strain history to a scalar effective strain. The Section III, Division 5 rules use the Huddleston model<sup>15</sup> for generating an effective stress from a 3D stress relaxation history for calculating creep damage. This model is more accurate than simply using the von Mises effective stress, as in the current design rules, but requires multiaxial creep rupture data to calibrate. This data is not available for Alloy 740H and so the current rules recommend using the von Mises stress based on experience with Alloy 617. This material is similar to 740H in that both are  $\gamma'$  strengthened Ni-alloys and multiaxial creep testing on Alloy 617 demonstrates that using the von Mises stress adequately captures multiaxial rupture in that material. The design rules use the von Mises strain as a metric for assessing strain limits. This choice is somewhat arbitrary, but reasonable given the use of the von Mises stress in the creep damage calculation.

For ratcheting strain the design method here doubles the pointwise ASME strain limits from 5% for base metal and 2.5% for welds to 10% for base metal and 5% for welds. Additionally, the creep damage calculation uses a safety factor of 0.9, instead of the 0.7 recommended by ASME. Both changes reflect the lower consequences of failure for CSP systems versus nuclear components.

---

<sup>15</sup> R. L. Huddleston, "An Improved Multiaxial Creep-Rupture Strength Criterion" *Journal of Pressure Vessel Technology*, 107(November), pp. 421–429, 1985.



The key challenge is calculating a representative time/strain/stress history corresponding to many repetitions of the design cycle. The design method takes advantage of the material strength by neglecting plastic deformation. This greatly simplifies the task of constructing a material model, as an elastic-creep is sufficient to describe the material deformation.

The final constitutive model described in 3-3.15 is deliberately further simplified to a temperature and stress-dependent power law description of creep that does not use any internal variables to track material state. This greatly abstracts the representation of creep deformation – the model does not capture primary or tertiary creep – but also allows the designer to use a steady cyclic analysis of the component to describe deformation and stress relaxation over an arbitrary large number of load cycles. This means a relatively short cyclic analysis of a few repetitions of the design cycle can be used to calculate deformation and damage over the full service life of the component.

A history-independent material model of the type used here will, under repeated applications of a cyclic load history, eventually reach a cyclic steady state where the stresses and strain rates become periodic<sup>16</sup>. Design Option C takes advantage of this concept by requesting the designer first determine this steady, periodic response and then calculate deformation and damage over the whole cyclic history of the component as if this steady response was repeated for the entire service life.

The clear advantage of this approach is that the designer does not need to simulate the full cyclic history of the component. The steady response can generally be identified by repeating the Design Cycle for tens of applications, not thousands.

There are however several disadvantages. First, as noted above, the history-independent description of creep cannot capture real, observed material behavior like primary and tertiary creep. Tertiary creep can safely be neglected as the creep damage calculation will screen structures that enter this deformation regime. Neglecting primary creep is conservative for calculating stress relaxation damage as faster creep rates are actually helpful in relaxing stress, but not necessarily for calculating ratcheting strain accumulation. However, as creep-fatigue is likely to be the controlling design criteria for future CSP structures this approximation can be accepted.

Second, applying the steady-cyclic response to the full service history neglects the cyclic-transient part of the deformation history. Depending on the material response this might mean approximating the damage and strain accumulated over the first few hundred cycles. However, as CSP systems are typically designed for thousands of cycles this approximation is reasonable. Additionally, this design method does not completely neglect damage and strain accumulated during this period, but rather approximates the response of the component in this regime with the steady-cyclic response. This approximation is generally reasonable, even if it is inexact.

---

<sup>16</sup> C. O. Frederick, and P.J. Armstrong, “Convergent internal stresses and steady cyclic states of stress” *Journal of Strain Analysis for Engineering Design*, 1(2), pp. 154–159, 1966.

### **3-3. Commentary on the 740H Material Data**

#### **3-3.1. General Criteria**

Currently, data in Section III, Division 5 of the ASME Code is provided in either graphs or tables. A more modern design code would provide equations so that the various material property correlations could be easily digitized. This set of data endeavors to provide equations, where possible. However, some of the data is still provided in tables to be compatible with current Section II properties (for example  $S_y$ ).

#### **3-3.2. Material Specification**

The intent of this set of design rules is to allow the use of Alloy 740H in any non-cast product form. Currently welded tube and pipe is not included in ASME Code Case 2702, adding Alloy 740H for Section I use. If the Code Case is amended in the future to include welded tube these design data could be relatively easily updated with conforming allowable stress values. The weld reduction factors in 2-8 would provide a way to design seam welded material against the creep-fatigue and ratcheting limits.

Code Case 2702 includes additional requirements on the material heat treatment, providing two options (a and b) to satisfy the additional requirements. These design rules retain those additional restrictions.

#### **3-3.3. Elastic constants**

This information comes from the Alloy 740H material data sheet.

#### **3-3.4. Thermal properties**

This information comes from the Alloy 740H material data sheet. The instantaneous coefficients of thermal expansion were calculated from the provided mean coefficients.

#### **3-3.5. Yield strength**

This data comes from ASME Code Case 2702. The values above 800° C are extrapolated.

#### **3-3.6. Tensile strength**

This data comes from ASME Code Case 2702. The values above 800° C are extrapolated.

#### **3-3.7. Allowable stress $S_o$**

ASME Code Case 2702 provides the Section I allowable stresses for Alloy 740H up to 800° C. This allowable stress is defined by the lesser of (at each temperature);

1. The minimum specified tensile strength of the material divided by 3.5.

2. The minimum specified yield strength of the material multiplied by a factor of 0.67 or 0.9 depending on the material ductility (this criteria does not control for Alloy 740H).
3. The minimum specified tensile strength of the material multiplied by the ratio of the average temperature-dependent tensile strength to the room temperature tensile strength multiplied by a factor of 1.1/3.5.
4. The minimum specified yield strength of the material multiplied by the ratio of the average temperature-dependent yield strength to the room temperature yield strength multiplied by a factor of 0.67 or 0.9, depending on the material.
5. The average creep rupture strength of the material at 100,000 hours multiplied by a factor less than 0.67.
6. The minimum creep rupture strength of the material at 100,000 hours multiplied by factor of 0.8.
7. The full stress to cause a strain of 1% in 100,000 hours.

Full details of this calculation are provided in ASME Section II, Mandatory Appendix 1.

Section III, Division 5 uses a similar allowable stress  $S_o$  adopted for use here. The definition of this allowable stress is identical, except where the value of the time-dependent allowable stress  $S_{mt}$  at 300,000 hours exceeds the value defined above. This extra provision is ignored here, as these design rules do not use  $S_{mt}$ .

These rules adopt the values provided in ASME Code Case 2702 up to 800° C. The remaining value at 850 ° C is in the regime controlled by creep properties and values were calculated using the rupture and creep deformation models described below.

### **3-3.8. Allowable stress $S_m$**

This is a time-independent allowable stress used in Section III, Division 5. This quantity is not used as an allowable stress in the design criteria presented here. However, it is used in the creep-fatigue and ratcheting rules to determine a typical initial cyclic relaxation stress using the  $3\bar{S}_m$  criteria. As such the designer needs these values to complete a design analysis.

The definition of  $S_m$  is provided in Section II but it is analogous to the time-independent criteria 1-4 above. The values of  $S_m$  were then calculated from the values of  $S_y$  and  $S_u$  described previously and tabulated in the design document.

### **3-3.9. Relaxation strength**

As described in Part 2, the design by elastic analysis creep-fatigue and ratcheting criteria construct a relaxation analysis based on a starting strain value. Notionally, for a power-law creep material stress relaxation would continue until the stress in the component reaches the primary stress. However, in practice material effects, quantified by backstresses in cyclic plasticity models, tend to provide a material relaxation strength – a stress below which relaxation ceases – that can be

higher than the component primary stress. The design by elastic analysis process then includes rules preventing the stress from falling below the relaxation strength.

The material data in Section III, Division 5 and related ASME Code documents are nearly complete – a designer can complete a design without recourse to additional, outside information. However, the relaxation strength is an exception – it is not tabulated in the current Code. However, HBB-T-1324 does allow the designer to use a uniaxial relaxation analysis starting from a stress of  $1.5S_m$  to determine the relaxation strength. Relaxation models for the HBB Class A materials are not currently provided. For these design rules the tabulated relaxation strengths are based on the inelastic material model described in 3-3.15.

### 3-3.10. Minimum stress-to-rupture

#### 3-3.10.1. Experimental database

The minimum stress to rupture describes the stress that will cause rupture in a given time at a given temperature with reasonable lower-bound material response. The direct experimental measurement of this value is a creep rupture test. In these tests uniaxial specimens are loaded in temperature-controlled furnaces with a dead-load stress and left to deform until they rupture. The minimal experimental measurements are the controlled dead-load stress and temperature and the corresponding rupture time. More sophisticated tests might measure the deformation as a function of time, typically using a combination of extensometers and linear variable differential transformers (LVDTs) to measure deformation directly from the specimen.

However, it is essentially impossible to run sufficient creep tests to fully interpolate between the two experimental conditions (stress and temperature) for all values needed in a design calculation. Moreover, for some applications very long-term rupture stresses are required (30+ years), whereas the test time for the available creep test database is often much shorter, on the order of years at the most. Therefore, a predictive model for the rupture stress as a function of rupture time and temperature is first calibrated to the experimental data and then this model is used to generate design rupture stresses.

For this purpose 54 creep rupture tests on Alloy 740H were identified and collated. Table 3-3.10.1.1 shows the raw experimental data used to develop the rupture correlation below. The vast majority of these tests were extracted from the DOE report summarizing the fossil energy development program for Alloy 740H<sup>17</sup>, however a few confirmatory tests were completed at INL (marked with an asterisk in the table).

Temperature (°C)	Rupture Stress (MPa)	Rupture time (hours)
700	480	308.8
700	320	3795.3
700	480	392.6
700	420	1082.2

---

<sup>17</sup> R. Purgert et al. *Boiler materials for ultra supercritical coal power plants*. DOE technical report, 2015.

Temperature (°C)	Rupture Stress (MPa)	Rupture time (hours)
700	340	5227.4
700	480	512.5
700	300	14871.3
700	480	517.4
700	320	9745.1
700	265	30956.7
700	420	1082
700	340	5688
750	370	142.8
750	320	358.3
750	265	1275.4
750	180	8034
750	180	9787.9
750	370	275.4
750	300	984.6
750	220	7201.6
750	180	22896
750	370	311.9
750	320	658.5
750	300	1020.2
750	265	2185.4
750	220	7355.2
750	180	20789.4
750	370	296.7
750	320	484.8
750	300	914.6
750	220	7382.8
750	180	24061
750	300	723
750	265	2345
750	370	229.7
750	370	242
750	320	553
750	180	18756
800	250	173
800	250	279
800	180	1491
800	130	6883
800	180	1634
800	120	9855
800	110	15864
800	250	259
800	180	1497
800	150	3609
800	250	199

Temperature (°C)	Rupture Stress (MPa)	Rupture time (hours)
800	100	17674
750*	265	3168
750*	320	861
800*	200	1535
850*	100	3053

Table 3-3.10.1.1. Creep rupture database collated to define minimum stress to rupture design data. Tests marked with an asterisk were conducted at INL as part of the project sponsoring the development of these design rules.

### 3-3.10.2. Larson-Miller correlation

A Larson-Miller<sup>18</sup> correlation is used to interpolate and extrapolate the rupture test data to determine design values of minimum stress-to-rupture. The Larson-Miller parameter

$$LMP = T(\log t_r + C),$$

with  $T$  being the absolute temperature,  $t_r$  the rupture time, and  $C$  a parameter, generally correlates to the logarithm of the stress to rupture. This correlation can be used to fill in values of rupture stress for various conditions and extrapolate the short-term data to longer rupture times.

Larson-Miller correlations can be generated by finding the optimal value of the parameter  $C$  and the corresponding polynomial relation between the Larson-Miller parameter and the log of the rupture stress that best fit the experimental data. Figure 3-3.10.2.1 illustrates the process used to develop the log-linear Larson-Miller relation used here to establish values of the minimum rupture stress. Current ASME practice is to develop a 95% confidence lower bound prediction interval on the data and use that lower bound to determine the minimum stress to rupture. That process was followed here. The figure shows both the mean-property Larson-Miller model (used as the average stress to rupture in generating  $S_o$  and the creep-fatigue interaction diagram) and the 95% confidence model, used here to generate the minimum stress to rupture table. The figure also shows the best-fit value of the parameter  $C$  and the Pearson correlation coefficient of the log-linear relation.

<sup>18</sup> F. R. Larson, J. Miller, "A time-temperature relationship for rupture and creep stresses" *Transactions of the ASME*, 74, pp. 765–771, 1952.

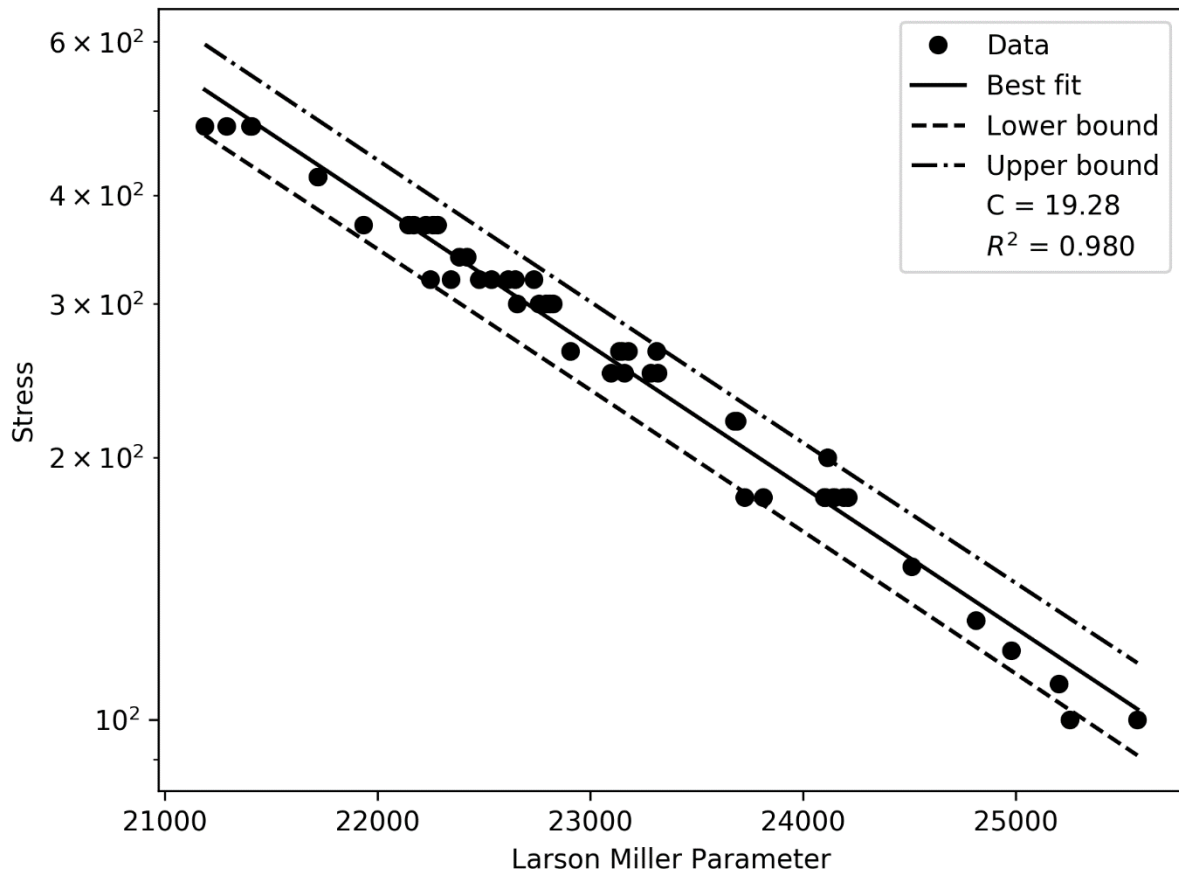


Figure 3-3.10.2.1. Larson-Miller correlation used to generate the average and minimum stress to rupture for Alloy 740H.

### 3-3.11. Fatigue diagrams

#### 3-3.11.1. Experimental database

A high temperature fatigue curve is a relation between a fixed cyclic strain range and temperature and the resulting number of cycles to failure. Typically these diagrams are generated using fully-reversed, strain-controlled fatigue tests at fixed temperature. These tests uniaxially cycle a sample over a fully-reversed strain range, holding temperature constant using a temperature-controlled furnace or induction heater. The test cycle is repeated until the sample fails. To protect equipment and specimens, failure may be defined by a set percentage drop in the maximum stress due to the presence of a crack. Design fatigue curves interpolate these test results, typically using strain range/cycles to failure relations for fixed temperatures.

Table 3-3.11.1.1 lists the fatigue test data used to generate the design correlations. All these tests are for fully-reversed strain cycling at a fixed temperature and strain rate. The table lists the temperature, strain range, number of cycles to failure, and the source of the data. Test results were collected from the literature and dedicated experiments run at INL as part of this project.

Temperature (°C)	Strain range (%)	Cycles to failure	Source
700	1.49	293	Zhang and Takahashi <sup>19</sup>
700	1.19	467	Zhang and Takahashi
700	0.97	1931	Zhang and Takahashi
700	0.69	12046	Zhang and Takahashi
700	0.66	15104	Zhang and Takahashi
700	0.53	287843	Zhang and Takahashi
750	0.60	14987	INL
750	0.6	19023	INL
750	0.60	7950	INL
750	1.00	1767	INL
750	1.00	1095	INL
760	1.40	147	Jena <sup>20</sup>
760	1.20	383	Jena
760	1.01	671	Jena
760	0.80	1457	Jena
760	0.60	6566	INL
800	1.00	653	INL
850	0.40	19969	INL
850	0.40	47048	INL
850	1.00	409	INL
850	1.00	402	INL

Table 3-3.11.1.1. Fatigue test data collated to generate the design fatigue relations.

### 3-3.11.2. Design fatigue curves

Typically, strain-based fatigue curves show decreasing cycles to failure as the temperature increases at a fixed strain range. ASME procedure is to provide a set of temperature dependent curves. The designer uses the curve corresponding to the highest metal temperature at the point of interest.

The data from 3-3.11.1.1 was grouped into two sets: 700° C and below and 700° C to 850° C. Because this is, to our knowledge, the total fatigue dataset for Alloy 740H the design rules use the curve based on the 700° C for all temperatures less than 700° C. This is almost certainly conservative. An optimized set of design data would include fatigue tests at lower temperatures, allowing a less restrictive design fatigue correlation.

Once grouped, two inverse power law curves were fit to the data using least squares regression. These two curves, corresponding to the two temperature groups, provide the mean property fatigue correlation.

<sup>19</sup> S. Zhang, and Y. Takahashi, “Creep and Creep-Fatigue Deformation and Life Assessment of Ni-Based Alloy 740H and Alloy 617” In *ASME 2018 Pressure Vessels and Piping Conference*, pp. V06AT06A060-V06AT06A060. American Society of Mechanical Engineers, 2018.

<sup>20</sup> P. S. Jena et al. “Low cycle fatigue behavior of nickel base superalloy IN 740H at 760° C: Influence of fireside corrosion atmosphere” *International Journal of Fatigue*, 116, pp. 623-633, 2018.



Design fatigue charts include factors of safety. The ASME nuclear code uses a factor of 2 on the strain range and 20 on the cycles to failure. Based on the lower consequences of failure for CSP systems, the design fatigue curves here use a factor of 1.5 on strain range and 10 on cycles to failure. Figure 3-3.11.2.1 shows that these factors bound the uncertainty in the fatigue data and provide a healthy design margin guarding against detrimental environmental/fatigue interactions, initial defects, and other uncertainty.

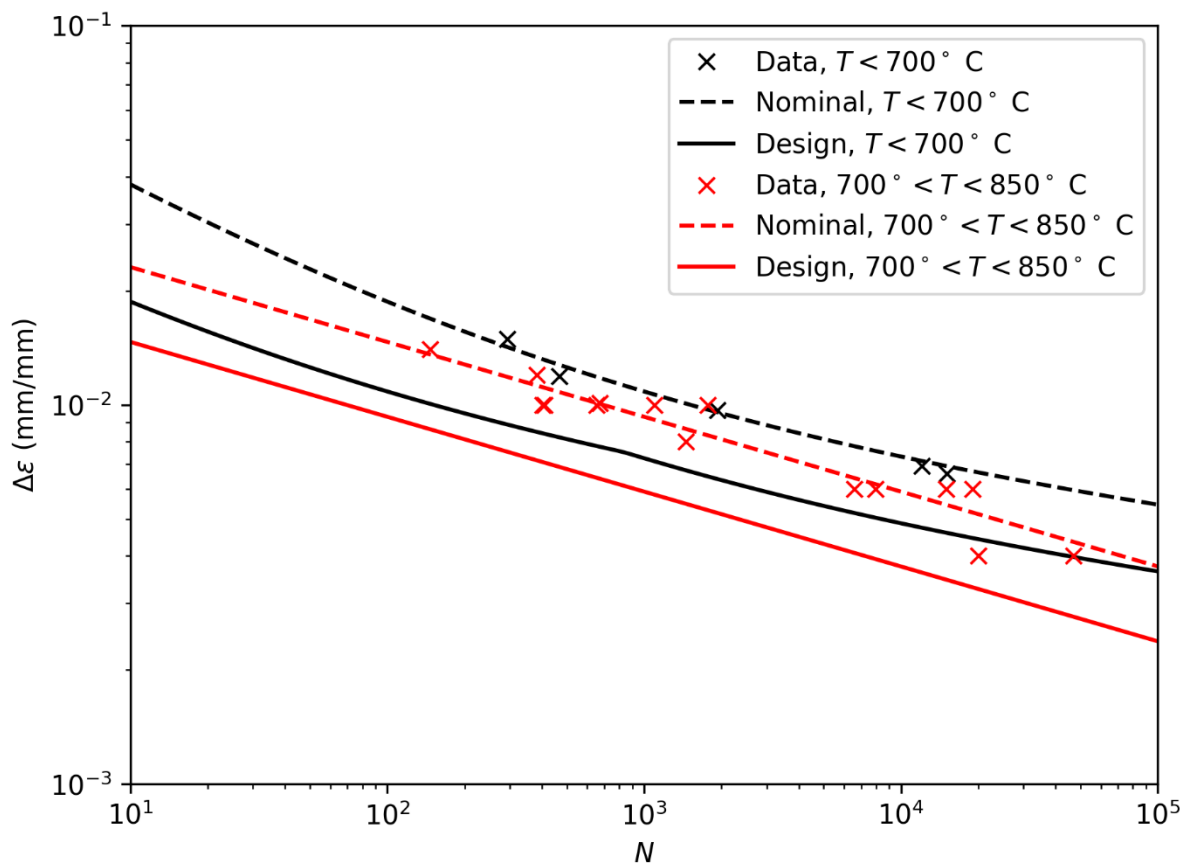


Figure 3-3.11.2.1. Chart comparing the experimental fatigue data, the mean property fatigue correlations, and the design fatigue correlations.

### 3-3.12. Creep-fatigue damage envelope

#### 3-3.12.1. Experimental database

The use of a creep-fatigue interaction diagram is explained in detail above in 3-1 and 3-2.2.3. These plots are an allowable damage envelope plotting fatigue damage on one axis and creep damage on the other axis. Typically, they are generated from a set of creep-fatigue tests. Creep-fatigue tests are strain-controlled cyclic experiments at fixed temperature and fixed fully-reversed strain range. They are different from fatigue tests in that a hold period at fixed strain is included in the cycle either at the maximum tensile, maximum compression, or both ends of the cycle.

Table 3-3.12.1.1 lists the test used to generate the Alloy 740H creep-fatigue interaction diagram. All the tests but one were run at INL as part of this project. The single test sourced from the literature<sup>21</sup> is marked with an asterisk. Early in the experimental program two tests with the same conditions but holds on the opposite ends of the cycle were used to establish that tensile holds are more damaging for Alloy 740H. This is in agreement with similar results on other high temperature nickel alloys. As such, tensile holds were used for the remainder of the tests.

Temperature (°C)	Strain range (%)	Hold time (min)	Hold type	Cycles to failure
700*	0.7	60	T	671
750	0.6	10	T	1958
750	0.6	60	T	1143
750	1	60	T	204
750	1	600	T	142
750	1	60	T	122
750	1	60	C	187
850	0.4	10	T	2488
850	0.4	10	T	2246
850	0.4	10	T	4147
850	1	10	T	342
850	1	600	T	231

Table 3-3.12.1.1. Summary of the creep-fatigue test results used to establish the design creep-fatigue damage envelope. A “T” in the Hold type column means tensile hold; a “C” means compressive hold. The single test collected from the literature is marked with an asterisk.

### 3-3.12.2. Damage envelope

The results of a creep-fatigue test are a stress/strain/time history and a number of cycles to failure. These results can be converted to a fatigue damage fraction by calculating the number of cycles to failure for a pure fatigue test at the experimental strain range and temperature using the mean property fatigue curve and dividing the actual number of cycles to failure by this number. Similarly, a creep damage fraction can be calculated using the time fraction approach via the integral equation

$$D_c = \int \frac{dt}{t_R}$$

where  $t_R$  is the time-to-rupture at a given value of uniaxial stress calculated using the mean property time to rupture correlation developed above. Notionally this integral would span the full time test data. In practice the relaxation curve at  $N/2$ , i.e. half the experimentally-observed number of cycles to failure, is used to represent the whole test.

<sup>21</sup> Zhang, Shengde, and Yukio Takahashi. "Creep and Creep-Fatigue Deformation and Life Assessment of Ni-Based Alloy 740H and Alloy 617." In ASME 2018 Pressure Vessels and Piping Conference, pp. V06AT06A060-V06AT06A060. American Society of Mechanical Engineers, 2018.

Figure 3-3.12.2.1 shows the experimental data, converted to creep and fatigue damage fractions and plotted on an interaction diagram. The figure also shows the interaction point selected for the design rules: (0.05,0.05). The processes of converting the results of a creep-fatigue test to a point on the diagram is automatic and requires no judgement beyond selecting the fatigue and creep damage models. However, going from the collection of experimental data points to the interaction envelope is a somewhat subjective process. The creep and fatigue damage calculation procedures contain the design margin in the creep-fatigue design process and so creep-fatigue diagrams are selected based on average material properties. As such, the final interaction point does not need to bound the data – it can allow for some outliers falling underneath the curve. However, the final diagram should not pass through the mean of the data as the points on the diagram represent many different experimental conditions. That is, the scatter in the plot is not entirely due to variation in material properties.

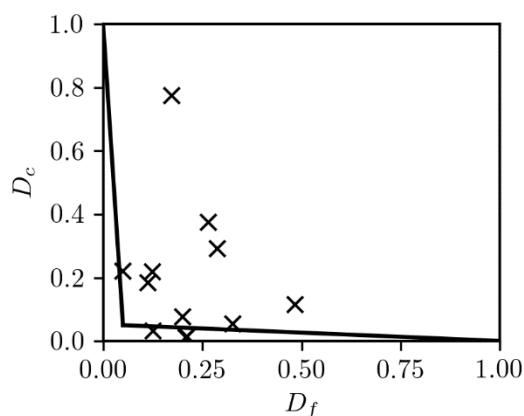


Figure 3-3.12.2.1. The creep-fatigue experiments plotted on an interaction diagram along with the final recommended damage envelope.

### 3-3.13. Weld strength reduction factors

Near weldments the creep-fatigue criteria apply a reduction factor on the minimum stress to rupture in the creep damage calculation. These reduction factors are typically based on cross-weldment rupture tests and may be temperature and time dependent.

The factor of 0.7 is drawn from ASME Code Case 2702, where it is specified for use in seam welded construction. The weld rupture factor is based on very limited data – additional weld creep data would be required to determine a more accurate value.

Note that for seam-welded tube or pipe reduced allowable stress values  $S_o$  would be required, in addition to the reduction factor applied to the rupture strength in the creep-fatigue damage calculation procedure. As noted above in 3-3.7 the elevated temperature values of these reduced allowable stresses could be calculated in Code Case 2702 is modified in the future to allow for seam-welded tube or pipe product forms.

### 3-3.14. Isochronous stress-strain relations

#### 3-3.14.1. Experimental database

ASME Section III, Division 5 design rules use hot tensile and isochronous stress strain curves to represent creep deformation, both for evaluation of the ratcheting strain limits and in assessing stress relaxation caused by creep. The isochronous curves can be read as the average stress to accumulate some amount of total strain over some period of time. The procedure used to create current Code curves for the Section III, Division 5 materials is to first fit a material model to the available tensile and creep data and then use that model to generate the hot tensile and isochronous curves. The difficulty in this analysis stems from the need for strain data during the creep test rather than just tabulated rupture times. We adopted the same procedure to develop isochronous stress strain curves for alloy 740H. The tensile test data used to determine the isochronous stress-strain relations were collected at INL while most of the creep test data were gathered from literature, except for four creep tests conducted at INL. The tensile test data consist of four elevated temperature tensile tests spanning from 700°C to 850°C in 50°C increments. Table 3-3.14.1 lists all the creep tests used. The table lists the temperature, applied constant stress, and the source of the creep test data.

Temperature (°C)	Stress (MPa)	Source
650	420	Purgert and Shingledecker <sup>17</sup>
700	265	Purgert and Shingledecker
700	395	Zhang and Takahashi <sup>19</sup>
700	420	Purgert and Shingledecker
700	430	Zhang and Takahashi
700	520	Zhang and Takahashi
750	150	Purgert and Shingledecker
750*	180	Purgert and Shingledecker
750	220	Purgert and Shingledecker
750*	265	Purgert and Shingledecker
750	265	INL
750	320	INL
750	320	Purgert and Shingledecker
750	370	Purgert and Shingledecker
800	180	Purgert and Shingledecker
800	200	INL
850	100	INL

Table 3-3.14.1. List of creep data used to construct the isochronous stress-strain relations for alloy 740H. Two sets of experimental data were collected for the test conditions marked with an asterisk.

#### 3-3.14.2. Strain equations

The isochronous stress-strain curves are based on an additive, history-independent decomposition of the total strain,  $\varepsilon$  into elastic strain,  $\varepsilon_e$ , time-independent plastic strain,  $\varepsilon_p$ , and time-dependent creep strain,  $\varepsilon_c$ .

$$\varepsilon = \varepsilon_e + \varepsilon_p + \varepsilon_c$$

The hot tensile curves are the outcome of this model when  $\varepsilon_c = 0$ , i.e. when  $t = 0$ , whereas the isochronous curves are the output of the model for some fixed, non-zero time. The elastic strain is calculated using the temperature dependent values of Young's modulus,  $E$  for Alloy 740H.

$$\varepsilon_e = \frac{\sigma}{E}$$

The plastic response of Alloy 740H was divided into two regions based on temperature. At temperatures below and equal to 800° C the composite model uses a Ramberg-Osgood model for the plastic strain to capture the experimentally-observed smooth transition from elastic to work hardening plastic behavior. Above this temperature the model uses a Voce hardening model to capture a quick transition to a nearly perfectly-plastic response. The composite model for the plastic strain is then

$$\varepsilon_p = \begin{cases} \begin{cases} 0 & \sigma \leq \sigma_0 \\ K \left( \frac{\sigma - \sigma_0}{\sigma_0} \right)^n & \sigma > \sigma_0 \end{cases} & 600^\circ\text{C} \leq T \leq 800^\circ\text{C} \\ \begin{cases} 0 & \sigma \leq \sigma_1 \\ -\frac{1}{\delta} \ln \left( 1 - \frac{\sigma - \sigma_1}{\sigma_p - \sigma_1} \right) & \sigma > \sigma_1 \end{cases} & T > 800^\circ\text{C} \end{cases}$$

All the model parameters were calibrated based on single hot tensile test data at four different temperatures – 700°C, 750°C, 800°C, and 850°C. We first fit the experimental data with the plasticity model (Ramberg-Osgood or Voce hardening) considering experimental elastic modulus which is then modified to match with the Young's modulus and the average yield strength. The values of the average yield strength for Alloy 740 were collected from the background document of ASME Code Case 2702. These modifications are done only in the elastic regime of the hot tensile curve and do not affect the shape of the curve in the plastic regime. Figure 3-3.14.2.1 plots the experimental (red curve) and model (black curve) hot tensile curves. Due to the unavailability of hot tensile data below 700°C, we considered the same plasticity model constants for all the temperatures between 600°C and 700°C.

To model the time-dependent strain,  $\varepsilon_c$  we adopted a simple creep model for alloy 740H.

$$\varepsilon_c = \dot{\varepsilon}_c(T, \sigma)t$$

where  $\dot{\varepsilon}_c$  is some constant, average creep rate, which is a function of temperature and stress. ASME Section III, Division 5 design isochronous curves only provide data out to 2.2% total strain which at most represents about 2% creep strain. The model also assumes that this average rate over the first 2% of creep strain is approximately equal to the average rate over the first 1% of creep strain. This allows the model to use the time-to-1% data for calibration. To determine the average creep rate over the first 1% of creep strain two different methods were used – (1) divide the 1% creep strain by the time and (2) convert the creep curve data to a plot of creep strain rate versus creep

strain and then average over the first 1% to produce a similar mean rate. These two rates were then averaged again to determine the average creep rate over the first 1% of creep strain to the applied stress and temperature. A model must be developed for this average creep rate in order to interpolate the data to all the conditions required to generate the design isochronous curves.

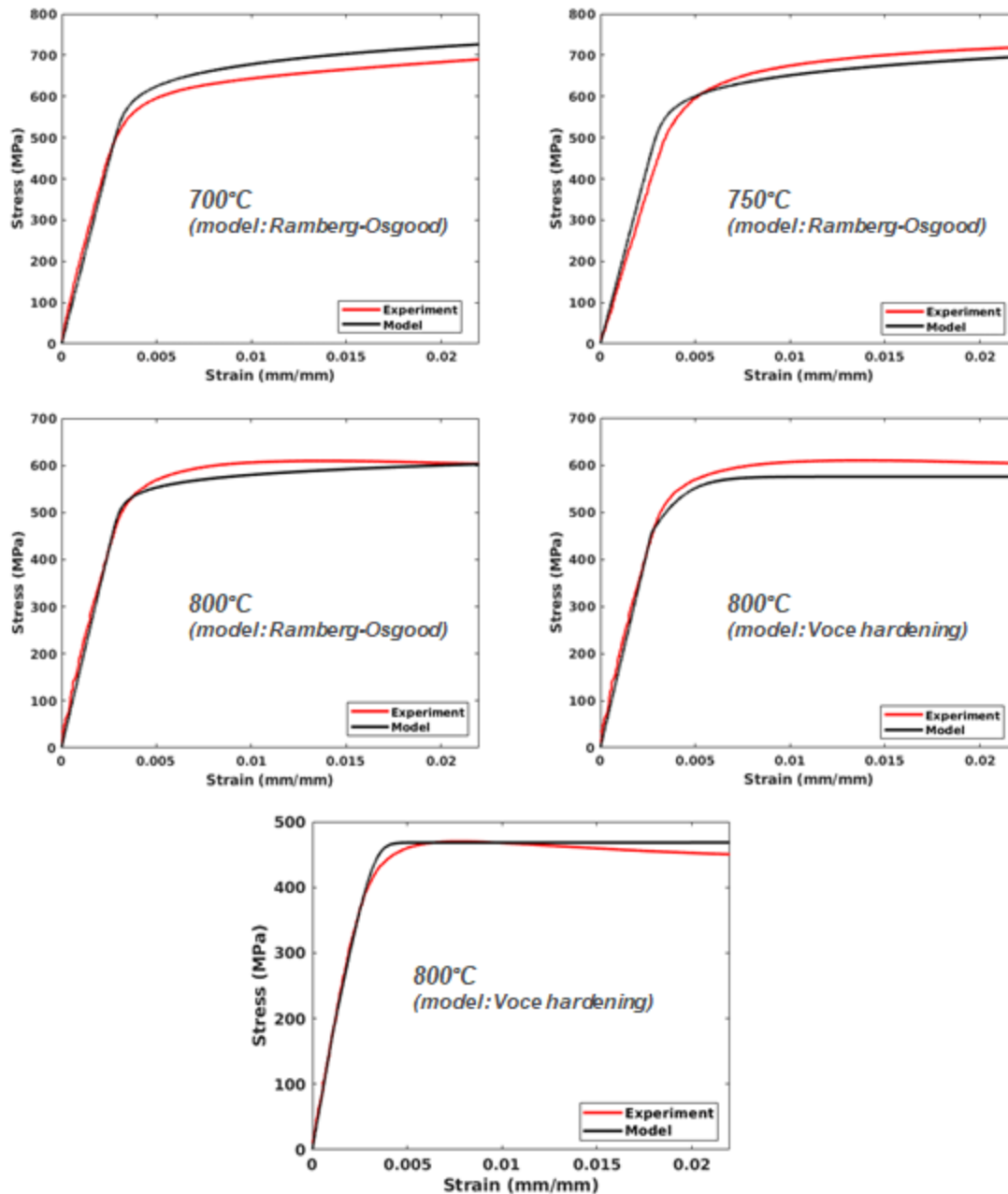


Figure 3-3.14.2.1. Experimental and hot tensile model curves for Alloy 740H at different temperatures. Hot tensile model curves were determined by fitting the experimental data with the plasticity model (Ramberg-Osgood or Voce hardening) and then modified to match with the Young's modulus and average yield strength. The average yield strength data were collected from the background document of ASME Code Case 2702.

We adopt a form developed by Kocks<sup>22</sup> and Mecking<sup>23</sup> for creep model of alloy 740H. Their model posits a linear relation between the log-normalized material flow stress  $\log \frac{\sigma}{\mu}$  and the normalized activation energy  $\frac{kT}{\mu b^3} \ln \frac{\dot{\epsilon}_0}{\dot{\epsilon}}$ . If this log-linear relation exists, the Kocks-Mecking model can be converted into a model for the deformation strain rate as a function of the linear fit slope  $A$  and intercept  $B$ .

$$\dot{\epsilon} = \dot{\epsilon}_0 e^{B\mu b^3/(AkT)} \left( \frac{\sigma}{\mu} \right)^{-\mu b^3/(AkT)}$$

Here  $\mu$  is the material shear stress given as  $\mu = \frac{E}{2(1+\nu)}$ ,  $k$  is the Boltzmann constant,  $T$  is the absolute temperature,  $b$  is a characteristic Burgers vector, and  $\dot{\epsilon}_0$  is some reference strain rate. This method was successfully implemented by Messner and Sham<sup>24</sup> for modeling the creep deformation in developing the isochronous stress-strain relationships for a similar nickel based Alloy 617. Figure 3-3.14.2.2 plots the available Alloy 740H creep data using the average rate to 1% creep strain as the deformation strain rate and the applied values of stress and temperature. As the Figure 3-3.14.2.2 shows, the Alloy 740 creep data nearly obeys the Kocks-Mecking form. Based on this diagram, the model for the creep strain adopted for Alloy 740H is

$$\epsilon_c = \dot{\epsilon}_0 e^{\frac{B\mu b^3}{AkT}} \left( \frac{\sigma}{\mu} \right)^{\frac{-\mu b^3}{AkT}} t$$

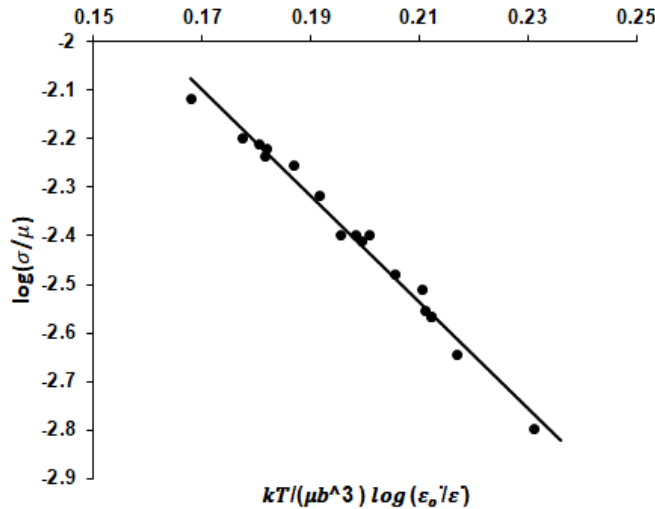


Figure 3-3.14.2.2. Kocks-Mecking diagram used to construct the model for  $\epsilon_c$ .

<sup>22</sup> U. F. Kocks, "Realistic constitutive relations for metal plasticity" *Materials Science and Engineering: A*, 317, pp. 181-187, 2001.

<sup>23</sup> Y. Estrin, and H. Mecking, "A unified phenomenological description of work hardening and creep based on one-parameter models" *Acta Metallurgica*, 32, pp 57-70, 1984.

<sup>24</sup> M. C. Messner, and T-L. Sham, "Isochronous Stress-Strain Curves for Alloy 617" In the *Proceedings of the ASME 2019 Pressure Vessels and Piping Conference*, PVP2019-93642, 2019.

### 3-3.15. Inelastic constitutive model

As noted above in the commentary on the design methods, assembling a complete inelastic constitutive model capable of accurately capturing details of elevated temperature cyclic plasticity/creep interactions is a very complicated task that has not been completed for the vast majority of high temperature materials<sup>25,26,27</sup>.

However, Design Method C detailed above purposely uses a simplified description of the material response in order to take advantage of the steady cyclic response of the system. In the general case, the material description could be elastic, perfectly-plastic, with power law creep. However, as described in 3-2.4, for Alloy 740H plasticity can be neglected, leaving an elastic-creep constitutive response.

The specific inelastic model was then formulated by taking the elastic and creep strain equations from 3-3.14 and supplementing them with the standard equation for the thermal strains, using the coefficients of thermal expansion supplied in Part 2.

This constitutive model is only suitable for use with the simplified inelastic design method detailed above. It is not suitable for a full inelastic analysis capturing all the details of elevated temperature plasticity and creep-plasticity interaction. Such a model, for example using the Chaboche form<sup>28</sup>, would be much more difficult to develop and require an extensive experimental database of creep, creep-fatigue, and other cyclic tests including full stress/strain/time hysteresis information.

### 3-3.16. Temperature limits

#### 3-3.16.1. Minimal creep

This temperature limit is the temperature at which the material accumulates 0.1% strain at the allowable stress  $S_o$  over 100,000 hours. It can be determined using the information in 3-3.7 and 3-3.14 above. This particular cutoff was invented for these rules. The rationale is that the allowable stress is a reasonable typical long-term stress level in components design using these rules. The 0.1% over 100,000 hour criteria is a typical ASME negligible creep threshold.

#### 3-3.16.2. ASME Section III, Division 5 limit on the O'Donnell-Porowski method

This temperature limit is used in the O'Donnell-Porowski design-by-elastic-analysis strain limits rules. Its purpose is to ensure that one end of the load cycle is anchored at a temperature in the

---

<sup>25</sup> M. Yaguchi, and Y. Takahashi, "Unified Inelastic Constitutive Model for Modified 9Cr-1Mo Steel Incorporating Dynamic Strain Aging Effect" *JSME International Journal Series A*, 42(1), pp. 1–10, 1999.

<sup>26</sup> M. C. Messner, V.-T. Phan, T.-L. Sham, "A Unified Inelastic Constitutive Model for the Average Engineering Response of Grade 91 Steel" In the *Proceedings of the ASME 2018 Pressure Vessels and Piping Conference* PVP2018-84104, 2018.

<sup>27</sup> Phan, V.-T., Messner, M. C. and Sham, T.-L. "A Unified Engineering Inelastic Model for 316H Stainless Steel." In the *Proceedings of the ASME 2019 Pressure Vessels and Piping Conference*, PVP2019-93641, 2019.

<sup>28</sup> J. L. Chaboche. "Constitutive equations for cyclic plasticity and cyclic viscoplasticity" *International Journal of Plasticity*, 5, pp. 247–302, 1989.



negligible creep regime – a necessary requirement for applying the O'Donnell-Porowski theorem. The specific temperature limit is the temperature at which  $S_m = S_t$  at 100,000 hours. Section 3-3.8 describes the Section III, Division 5 allowable stress  $S_m$ .  $S_t$  is a time-dependent allowable stress used in Section III, Division 5. The details of how it is calculated from creep-data are not important, as the design document provides the temperature value for Alloy 740H.

## Part 4: Sample problems

This chapter walks through two sample design problems, applying all three design methods to each problem. The structural material used in all calculations is Alloy 740H, with design properties from Part 2 above.

### 4-1. Sample problem 1

#### 4-1.1. Problem description

Figure 4-1.1 illustrates the first problem considered for evaluating design methods developed for CSP systems. This problem is an axisymmetric representation of a tube in a cavity receiver. The tube is 500 mm long and 2 mm thick. The outer diameter is 40 mm. For simplicity, we assumed uniform heat flux on the outer surface of the tube and that the heat conduction analysis is done in the steady state, even for the design criteria which require a transient analysis. This results in linear temperature gradient along the length and thickness of the tube and therefore this problem can be treated as an axisymmetric problem. This linear temperature distribution can be fully described by providing the inner and outer tube metal temperatures as a function of time and axial position. Only two points are required to define the axial gradient. Figure 4-1.1 shows the temperature and pressure loading considered for this problem. The loading cycle includes warming up of the system in the morning, steady state operation, five cloud events each with 8 minutes hold, cooling down in the evening, and no operation during night. The design life of the tube is 30 years.

The purpose of this problem is to provide designers a simple reference problem to check their understanding of the design methods.

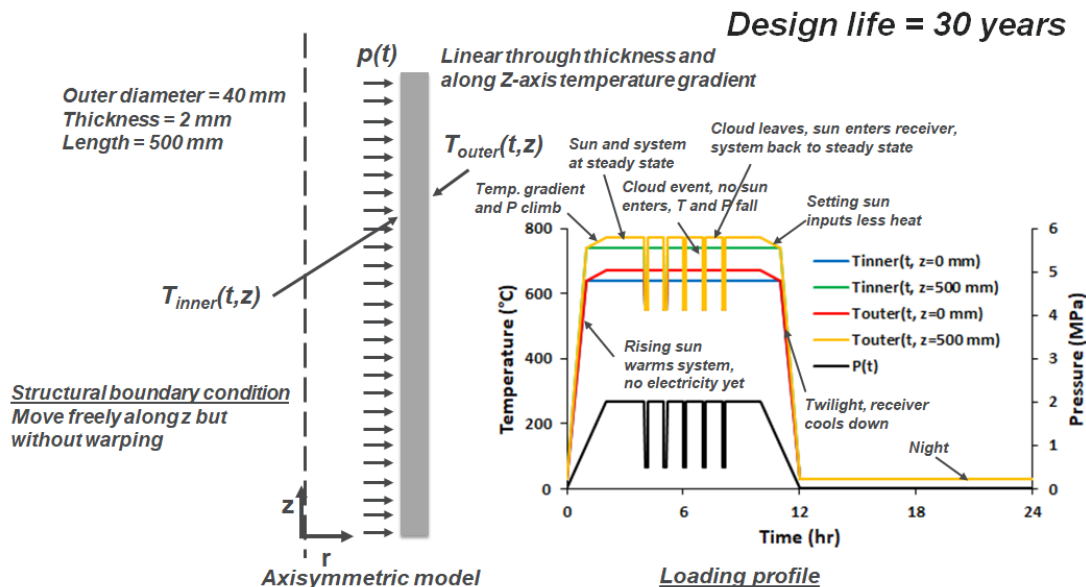


Figure 4-1.1. (Sample problem 1) An axisymmetric representation of a single tube in a cavity receiver. Loading profile shows the inner and outer wall temperature at the bottom ( $z = 0 \text{ mm}$ ) and top ( $z = 500 \text{ mm}$ ) ends of the tube, respectively, and pressure exerted on the inner wall by the salt flowing inside the tube.

## 4-1.2. Design calculations based on Method 1

### 4-1.2.1. Step-1: Defining the Design Cycle

Figure 4-1.2.1 shows the Design Cycle. The daily load cycle can be divided into two service load types – start-up/shut-down cycle and cloud events. Table provides the details of each event considered in the composite cycle.

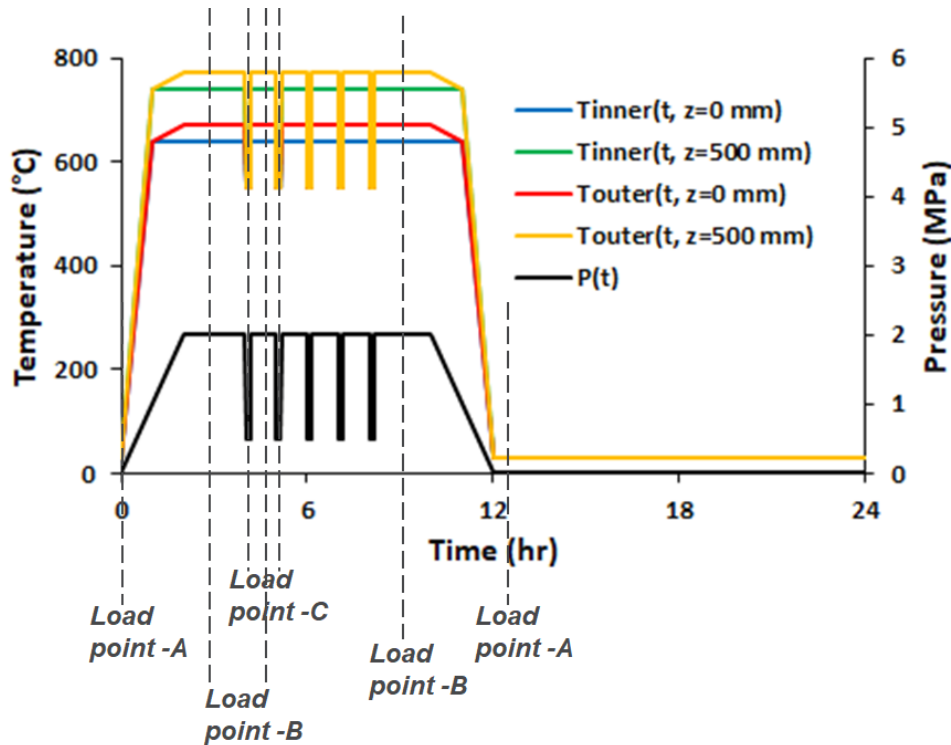


Figure 4-1.2.1 (Sample problem 1) Different load points during the loading cycle considered.

Service load types	Associated load points and cycle period	Frequency per design cycle
start-up/shut-down cycle	A and B ; 12 hours	1
cloud events	B and C ; 0.133 hours	5

Table 4-1.2.1 (Sample problem 1) Service load cycles and associated load points (illustrated in Figure 4-1.2.1) in the daily load cycle and corresponding hold times.

### 4-1.2.2. Step-2: Transient elastic thermo-mechanical analysis for each service load case and stress classification

We used MOOSE (Multiphysics Object Oriented Simulation Environment), an open source finite element solver to perform the elastic thermo-mechanical analyses. We classify stresses due to pressure as primary load and thermal stresses caused by the temperature gradient as secondary load. There is no peak load.

#### 4-1.2.3. Step-3: Primary load design check

Maximum primary load occurs at load point-B. Figure 4-1.2.3 shows the temperature distribution in the tube and stress components along the thickness of the tube at maximum wall averaged temperature location. Table 4-1.2.3 reports details of the primary load checks. First, all the stress components were linearized to divide into membrane and bending components along the stress classification line. The membrane and bending stress tensors were then used to determine the stress intensities in Table 4-1.2.3 As indicated in the table the design passes both the criteria in primary load checks.

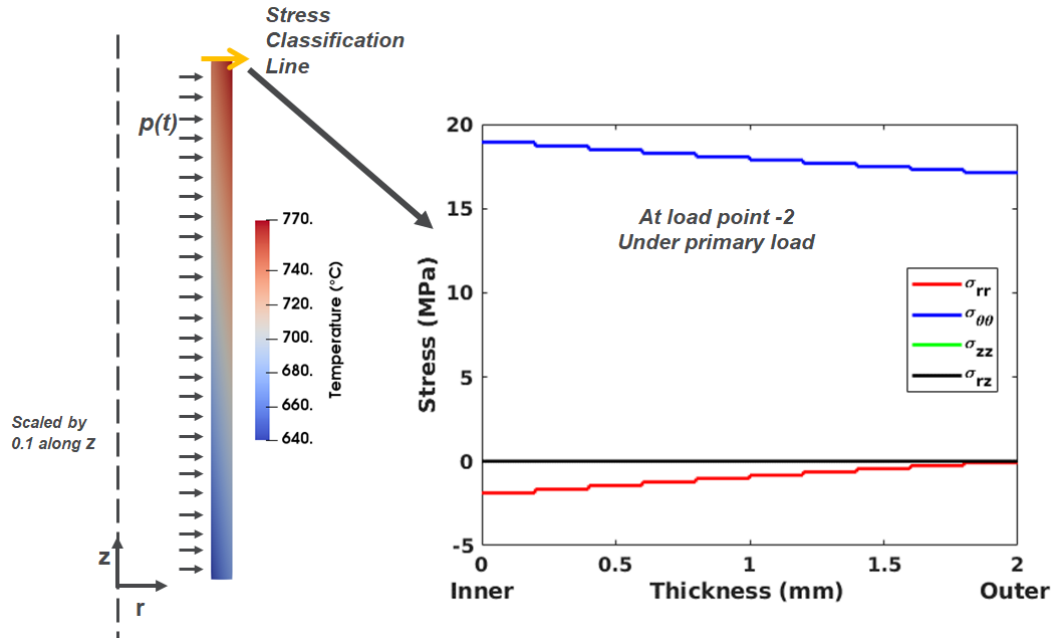


Figure 4-1.2.3. (Sample problem 1) Temperature distribution in the tube and through thickness elastic stress components at maximum wall averaged temperature location under primary load at load point -B.

Max. General primary membrane stress intensity, $P_m$	18.95 MPa
Max. Combined primary membrane plus bending stress intensity, $P_L + P_b$	20.92 MPa
Maximum metal temperature, $T_{max}$	770 °C
Allowable stress, $S_o$ at $T_{max}$	64.26 MPa
Design criteria -1: $P_m \leq S_o$	<b>PASS !</b>
Design criteria -2: $P_L + P_b \leq 1.5 S_o$	<b>PASS !</b>

Table 4-1.2.3 (Sample problem 1) Primary load design checks.

#### 4-1.2.4. Step-4: Ratcheting check

Design Method 1 uses the O'Donnell-Porowski approach, described in Section III, Division 5, HBB-1332 Test No. B-1 for ratcheting checks. In this approach, an effective creep stress parameter, Z is determined from a primary stress parameter, X and a secondary stress parameter, Y as shown in Figure 4-1.2.4.1 The effective creep stress parameter is used to calculate the effective creep stress which is then used to determine the ratcheting creep strain using isochronous stress-strain curves. The definition of X and Y are

$$X = (P_L + \frac{P_b}{K_t})_{max} / S_{yL}$$

$$Y = (Q_R)_{max} / S_{yL}$$

where,

$(P_L + \frac{P_b}{K_t})_{max}$  = the maximum value of the primary stress intensity, adjusted for bending via  $K_t$ , during the cycle being evaluated.

$(Q_R)_{max}$  = the maximum range of the secondary stress intensity during the cycle being considered  
 $S_{yL}$  = is the  $S_y$  value corresponds to the lower of the wall averaged temperature for the stress extremes defining secondary stress range,  $Q_R$ .

$$K_t = (K + 1)/2$$

$K$  is 1.5 for across-the-wall bending of shell structures or rectangular sections, see HBB-3223 (c) (6) in Section III Division 5.

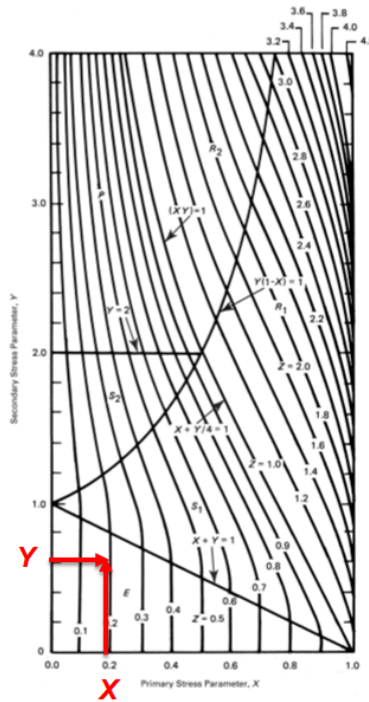


Figure 4-1.2.4.1. Illustration of determining the effective creep stress parameters from Section III, Division 5, Figure HBB-T-1332-1.

Once  $Z$  is found, effective core,  $\sigma_c$  stress is determined from

$$Z = \frac{\sigma_c}{S_{yL}}$$

It should be noted that, the average wall temperature at one of the stress extremes defining the secondary stress intensity range must be below the temperature listed in Section III, Division 5, HBB-T-1323, given as 600°C for 740H in the description of the design method above.

The creep ratcheting strain increment for a load cycle is evaluated by entering the isochronous stress strain curves at the maximum wall temperature and effective core,  $\sigma_c$  stress during the load cycle with the stress held constant for the entire service life. An example of creep ratcheting strain determination is shown in Figure 4-1.2.4.2.

Since the start-up/shut-down service load includes the extreme temperature profile and the total time of the day, considering only the start-up/shut-down load should provide conservative estimation for ratcheting design. Table 4-1.2.4 provides all the calculation details of the ratcheting design check. Figure 4-1.2.4.3 shows the stress components under secondary loading at load point B. Stress components are shown at two different locations – maximum wall averaged temperature and maximum von Mises stress. As indicated in the Table 4-1.2.4, the maximum ratcheting strain in the structure is less than 2% and therefore the design passes the ratcheting check. Note that, a design must pass the ratcheting design check before it is checked for creep-fatigue damage.

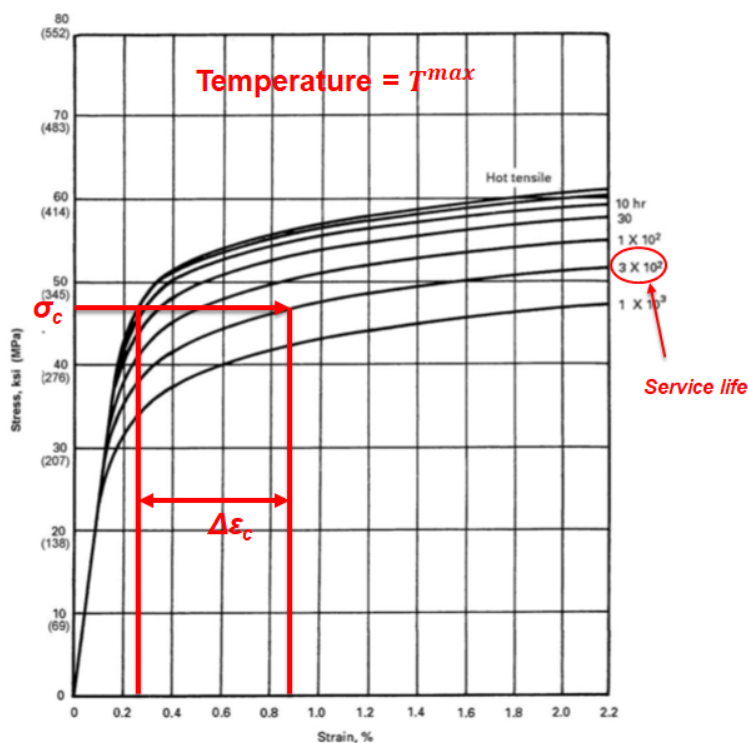


Figure 4-1.2.4.2. Illustration of determining the creep ratcheting strain increment from isochronous stress strain curves.

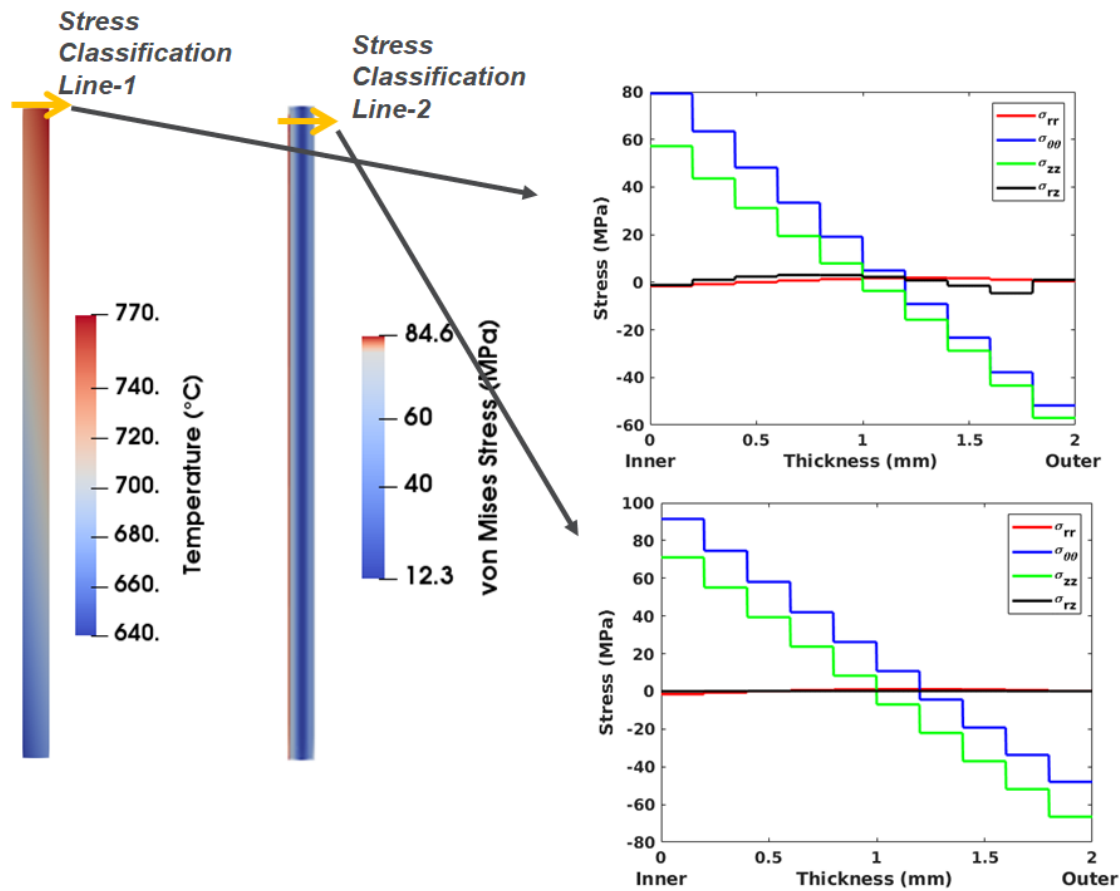


Figure 4-1.2.4.3. (Sample problem 1) Temperature and von Mises stress distribution in the tube and through thickness stress components at maximum wall averaged temperature and maximum von Mises stress locations under secondary load at load point B.

	<i>Stress classification line-1 shown in Figure 4-1.2.4.3</i>	<i>Stress classification line-2 shown in Figure 4-1.2.4.3</i>
$T_{wall\ averaged}^{max}$	755.2 °C	752.6 °C
$T_{wall\ averaged}^{min}$	30 °C	30 °C
$T^{max}$	770 °C	767.3 °C
$S_{yL}$ (at $T_{wall\ averaged}^{min}$ )	621.0 MPa	621.0 MPa
$K$	1.5	1.5
$K_t = (K + 1)/2$	1.25	1.25
$(P_L + \frac{P_b}{K_t})_{max}$	20.53	20.53
$(Q_R)_{max}$	85.06	96.81
$X = (P_L + \frac{P_b}{K_t})_{max}/S_{yL}$	0.033	0.033
$Y = (Q_R)_{max}/S_{yL}$	0.137	0.156
Z using Section III, Division 5, Figure HBB-T-1332-1	0.033	0.033
$\sigma_c$ from $Z = \frac{\sigma_c}{S_{yL}}$	20.53	20.53
Service life	30 years = 131400 hours	30 years = 131400 hours
Ratcheting strain at the end of service life	1.723e-5 %	1.393e-5 %
Ratcheting design criteria: 2% for base metal	<b>PASS!</b>	<b>PASS!</b>

Table 4-1.2.4 (Sample problem 1) Ratcheting design check according to Method 1.

#### 4-1.2.5. Step-5: Creep-fatigue damage check

According to Section III, Division 5, a design is acceptable if the creep and fatigue damage satisfy the following relation:

$$\sum_j \left( \frac{n}{N_d} \right)_j + \sum_k \left( \frac{\Delta t}{T_d} \right)_k \leq D$$

where D is the total creep-fatigue damage and the first and second terms on the left side are fatigue damage,  $D_f$  and creep damage,  $D_c$ , respectively. In the fatigue damage term,  $(n)_j$  is the number of repetitions of cycle type j and  $(N_d)_j$  is the number of design allowable cycles for respective cycle type; while in the creep damage term,  $(T_d)_k$  is the allowable time duration for a given stress at the maximum temperature occurring in the time interval k and  $(\Delta t)_k$  is the duration of the time interval k.

The design allowable cycles for fatigue damage is determined by entering fatigue curves at total strain range,  $\epsilon_t$ . Total strain range,  $\epsilon_t$  is calculated using equation HBB-T-1432-16:

$$\epsilon_t = K_v \Delta \epsilon_{mod} + K \Delta \epsilon_c$$

where K is the local geometric concentration or equivalent stress concentration factor determined by dividing effective primary plus secondary plus peak stress divided by the effective primary plus secondary stress,  $K_v$  is the multiaxial plasticity and Poisson ratio adjustment factor,  $\Delta \epsilon_c$  is the creep strain increment, and  $\Delta \epsilon_{mod}$  is the modified maximum equivalent strain range.



$\Delta\epsilon_{mod}$  is calculated using equation Section III, Division 5, HBB-T-1432-12:

$$\Delta\epsilon_{mod} = \left(\frac{S^*}{\bar{S}}\right) K^2 \Delta\epsilon_{max}$$

where  $\Delta\epsilon_{max}$  is the maximum equivalent strain range calculated from the elastic analysis of under primary and secondary loading together.  $\Delta\epsilon_{max}$  is calculated according to Section III, Division 5, HBB-T-1413 with  $\nu^* = 0.3$  for elastic analysis.  $S^*$  and  $\bar{S}$  are stresses determined by entering the isochronous stress-strain curves at  $\Delta\epsilon_{max}$  and  $K\Delta\epsilon_{max}$ , respectively.

$K_v$  is determined using equation Section III, Division 5, HBB-T-1432-15:

$$K_v = 1.0 + f(K'_v - 1.0)$$

where  $f$  is the inelastic multiaxial adjustment factor determined using Section III, Division 5, Figure HBB-T-1432-2 and triaxiality factor, T.F.

$$T.F. = \frac{|\sigma_1 + \sigma_2 + \sigma_3|}{\frac{1}{\sqrt{2}}[(\sigma_1 - \sigma_2)^2 + (\sigma_2 - \sigma_3)^2 + (\sigma_3 - \sigma_1)^2]}$$

where  $\sigma$ 's are principals stresses at the extreme of the stress cycle.

$K'_v$  is the adjustment for inelastic biaxial Poisson's ratio determined from Section III, Division 5, Figure HBB-T-1432-3 using  $K_e$ .

$$K_e = \begin{cases} 1 & ; K\Delta\epsilon_{max} \leq 3\bar{S}_m/E \\ \frac{K\Delta\epsilon_{max}E}{3\bar{S}_m} & ; K\Delta\epsilon_{max} > 3\bar{S}_m/E \end{cases}$$

where

$$3\bar{S}_m = \begin{cases} 1.5 S_m + S_{rH}; & \text{when only one of the extreme of the stress difference occurs at a} \\ & \text{temperature above those covered by Division 1, Subsection NB rules} \\ S_{rH} + S_{rL}; & \text{when both of the extreme of the stress difference occur at a} \\ & \text{temperature above those covered by Division 1, Subsection NB rules} \end{cases}$$

Here  $S_{rH}$  and  $S_{rL}$  are relaxation strengths associated with the temperatures at the hot and cold extremes of the stress cycle. These values are provided above in the 740H design data. The hot temperature condition is defined as the maximum operating temperature of the stress cycle. The hot time is equal to the portion of service life when wall averaged temperatures exceed 425°C. The cold temperature is defined as the colder of the two temperatures corresponding to the two stress extremes in the stress cycle. The cold time is again equal to the portion of service life when wall averaged temperatures exceed 425°C.

The creep strain increment per stress cycle,  $\Delta\epsilon_c$  is determined by entering the isochronous stress-strain curves at  $\sigma_c$  and maximum metal temperature for the stress cycle time, including hold times between transients (instead of total service life). Alternatively, the creep accumulated during the

entire service life divided by the number of stress cycles during the entire service life can also be used for calculating creep strain increment per stress cycle,  $\Delta\epsilon_c$ . We used the latter option.

The design allowable cycles,  $N_d$  is then calculated from design fatigue curve at maximum metal temperature and using total strain range,  $\epsilon_t$ , as illustrated in Figure 4-1.2.5.1 Fatigue damage fraction,  $D_f$  is then determined from the ratio between design cycles and design allowable cycles for each cycle type and then adding them together. Figure 4-1.2.5.2 shows the equivalent strain ranges from elastic analysis between load points A and B and between load points B and C along two stress classification lines. Table 4-1.2.5.1 shows the details of all the relevant calculations to determine fatigue damage fraction.

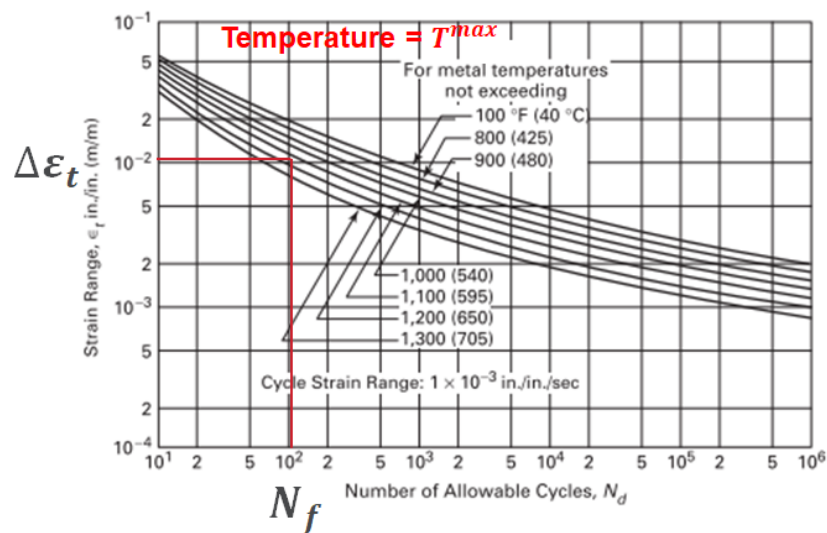


Figure 4-1.2.5.1. Illustration of determining design allowable cycles,  $N_d$ .

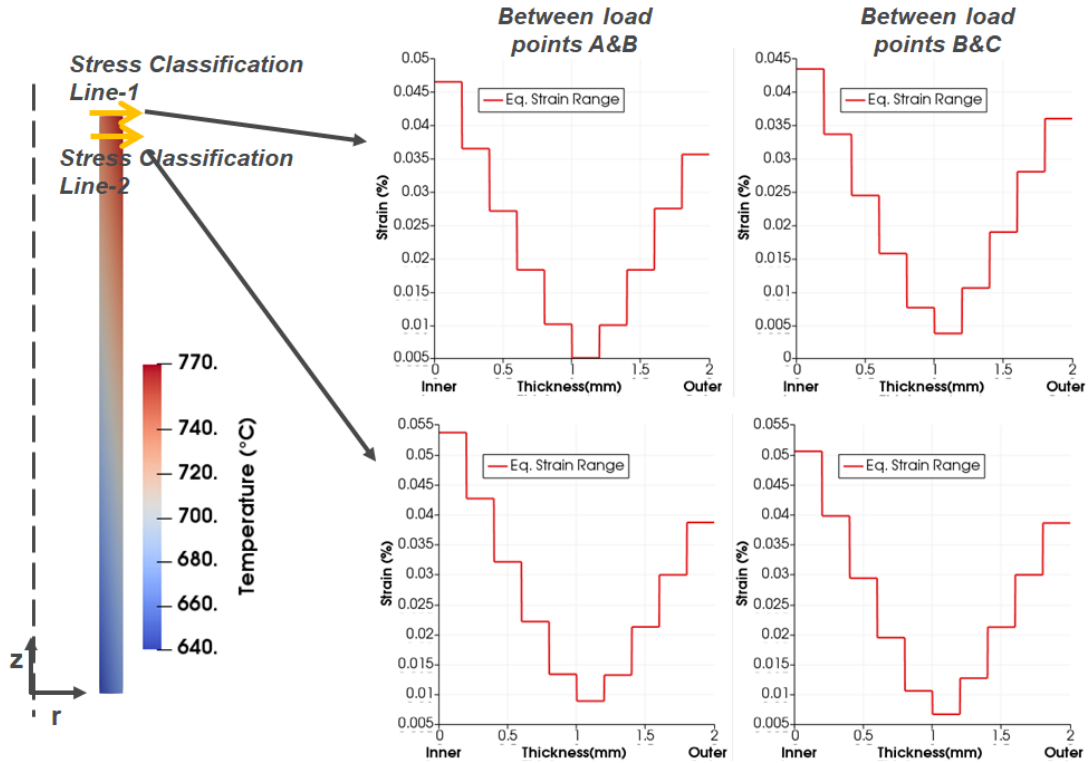


Figure 4-1.2.5.2. (Sample problem 1) Equivalent strain range from elastic analysis.

Creep damage evaluation is done in accordance to HBB-T1433(b)-option (a) but with one exception as described in the design Method 1. The lower bound stress  $S_{LB}$  is taken as  $1.0\sigma_c$ , rather than the  $1.25\sigma_c$  specified in the Code. First, stress relaxation profile is determined by entering the isochronous stress-strain curves at a strain level equal to  $\epsilon_t$  and at hold-time temperature and determining the corresponding stress levels at varying times. However, this stress relaxation process should not be permitted to a stress level less than  $S_{LB}$ . This stress relaxation procedure results in a stress-time history similar to that illustrated in Figure 4-1.2.5.3 Using the stress-time history and hold-time temperature during the cycle creep damage fraction can be calculated according to the illustration in Figure 4-1.2.5.4 For creep damage fraction calculation, we only considered the start-up/shut-down service load cycle. The time duration of the cloud events is already included in the start-up/shut-down service load cycle. Creep damage is not expected during night time. Tables 4-1.2.5.2 and 4-1.2.5.3 show the details of determining creep damage fraction,  $D_c$  from stress relaxation profile.

To determine whether the design passes the creep-fatigue damage check, the fatigue damage fraction,  $D_f$  and creep damage fraction,  $D_c$  are plotted on creep-fatigue interaction diagram as shown in Figure 4-1.2.5.5 If the  $(D_f, D_c)$  point falls inside the creep-fatigue damage envelop the design passes. As seen in Figure 4-1.2.5.5, the  $(D_f, D_c)$  points fall inside the creep-fatigue damage envelop which means the design passes for creep-fatigue damage check.

	<i>At OD on stress classification line-1 shown in Figure 4-1.2.5.2</i>		<i>At OD on Stress classification line-2 shown in Figure 4-1.2.5.2</i>	
	<i>Start-up/shut-down cycle</i>	<i>Cloud event</i>	<i>Start-up/shut-down cycle</i>	<i>Cloud event</i>
$T^{max}$	770°C	770°C	767.3°C	767.3°C
Hot temperature	770°C	770°C	767.3°C	767.3°C
Cold temperature	30°C	550°C	30°C	550°C
Hot time	12hr*(30*365) =131400 hr	0	12hr*(30*365) =131400 hr	0
Cold time	12hr*(30*365) =131400 hr	8min*(30*365) =1460 hr	12hr*(30*365) =131400 hr	8min*(30*365) =1460 hr
$S_{rH}$	107.2 MPa	354.8 MPa	110.5 MPa	358.9 MPa
$S_{rL}$	Not required	153.3 MPa	Not required	158.4 MPa
$S_m$ at $T^{max}$	241.0	Not required	243.2	Not required
$3\bar{S}_m$	468.7 MPa	508.1 MPa	475.3 MPa	517.3 MPa
$\Delta\epsilon_{max}$	0.0356 %	0.0360 %	0.0387 %	0.0376 %
$K$	1 (no peak stress)	1 (no peak stress)	1 (no peak stress)	1 (no peak stress)
$K\Delta\epsilon_{max}$	0.0356 %	0.0360 %	0.0387 %	0.0376 %
$E$	171700 MPa	171700 MPa	171943 MPa	171943 MPa
$3\bar{S}_m/E$	0.278 %	0.296 %	0.276 %	0.301 %
$K_e$	1	1	1	1
$K'_v$	1	1	1	1
$K_v$	1	1	1	1
$\frac{s^*}{\bar{s}}$	1	1	1	1
$\Delta\epsilon_{mod}$	0.0356 %	0.0360 %	0.0387 %	0.0376 %
$\Delta\epsilon_c$	1.57e-9%	0	1.27e-9%	0
$\epsilon_t$	0.0356 %	0.0360 %	0.0387 %	0.0376 %
Design allowable cycles, $N_d$	5086519	5047174	4789440	4892815
Design cycles, $n$	30*365=10950	30*365*5=54750	30*365=10950	30*365*5=54750
<b>Fatigue damage fraction, <math>D_f</math></b>	<b>0.0130</b>		<b>0.0135</b>	

Table 4-1.2.5.1. (Sample problem 1) Sample calculation of fatigue damage fraction,  $D_f$  according to Method 1.

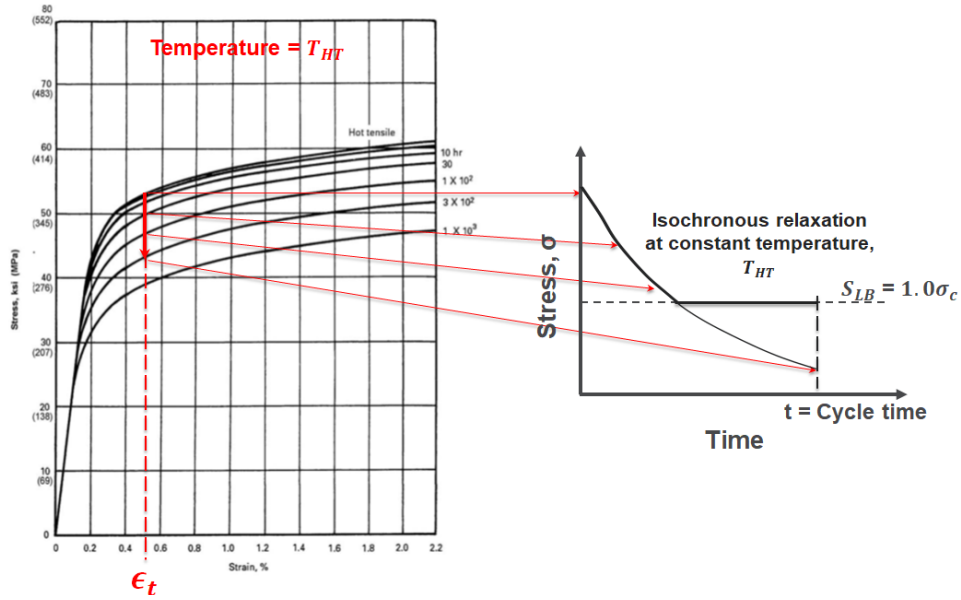


Figure 4-1.2.5.3. Illustration of determining stress relaxation profile from isochronous stress-strain curves for creep damage calculation in Method 1.

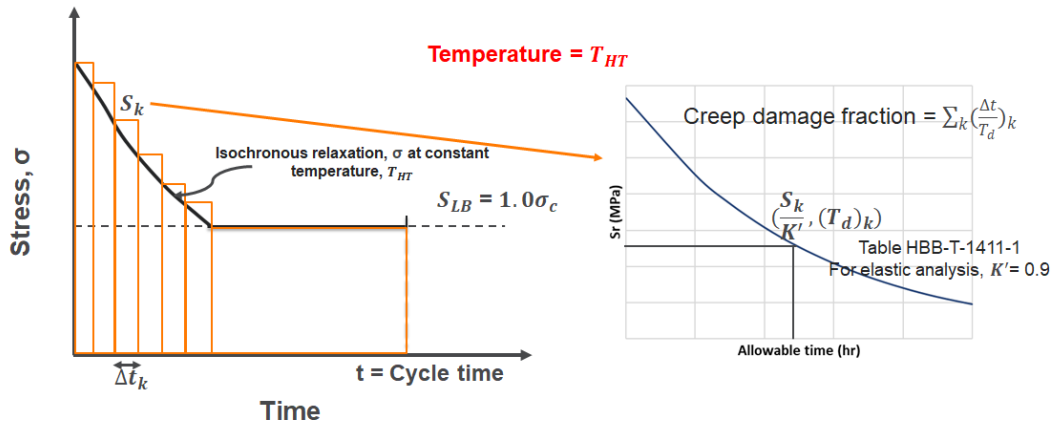


Figure 4-1.2.5.4. (Sample problem 1) Illustration of calculating creep damage fraction in Method 1.

	<i>At OD on stress classification line-1 shown in Figure 4-1.2.5.2</i>	<i>At ID on stress classification line-1 shown in Figure 4-1.2.5.2</i>	<i>At OD on stress classification line-2 shown in Figure 4-1.2.5.2</i>	<i>At ID on stress classification line-2 shown in Figure 4-1.2.5.2</i>
	<i>Start-up/shut-down cycle</i>	<i>Start-up/shut-down cycle</i>	<i>Start-up/shut-down cycle</i>	<i>Start-up/shut-down cycle</i>
$\Delta\epsilon_t$	0.0356 %	0.0465 %	0.0377 %	0.0537 %
$T_{HT}$	770°C	740°C	767.3°C	737.3°C
$S_{LB} = \sigma_c$	20.53	20.53	20.53	20.53
$K'$ (Table HBB-T-1411-1) for elastic analysis	0.9	0.9	0.9	0.9
Creep damage fraction per cycle (from Table 4-1.2.5.3)	2.02e-5	2.04e-5	2.53e-5	3.23e-5
Design cycles, $n$	30*365=10950	30*365=10950	30*365=10950	30*365=10950
<b>Creep damage fraction, <math>D_c</math></b>	<b>0.22</b>	<b>0.22</b>	<b>0.28</b>	<b>0.35</b>

Table 4-1.2.5.2. (Sample problem 1) Sample creep damage fraction,  $D_c$  calculation according to Method 1.

<i>At OD on stress classification line-1 shown in Figure 4-1.2.5.2</i>						<i>At OD on stress classification line-2 shown in Figure 4-1.2.5.2</i>					
<i>Time (hr)</i>	<i>S<sub>k</sub> (MPa)</i>	<i>S<sub>k</sub> K' (MPa)</i>	<i>(T<sub>d</sub>)<sub>k</sub> (hr)</i>	<i>Δt<sub>k</sub> (hr)</i>	<i>(<math>\frac{\Delta t}{T_d}</math>)<sub>k</sub></i>	<i>Time (hr)</i>	<i>S<sub>k</sub> (MPa)</i>	<i>S<sub>k</sub> K' (MPa)</i>	<i>(T<sub>d</sub>)<sub>k</sub> (hr)</i>	<i>Δt<sub>k</sub> (hr)</i>	<i>(<math>\frac{\Delta t}{T_d}</math>)<sub>k</sub></i>
0	6.11e1	6.79e1	5.95e5	1	1.68e-6	0	6.65e1	7.39e1	4.73e5	1	2.11e-6
1	6.11e1	6.79e1	5.95e5	1	1.68e-6	1	6.65e1	7.39e1	4.73e5	1	2.11e-6
2	6.11e1	6.79e1	5.95e5	1	1.68e-6	2	6.65e1	7.39e1	4.73e5	1	2.11e-6
3	6.11e1	6.79e1	5.95e5	1	1.68e-6	3	6.65e1	7.39e1	4.73e5	1	2.11e-6
4	6.11e1	6.79e1	5.95e5	1	1.68e-6	4	6.65e1	7.39e1	4.73e5	1	2.11e-6
5	6.11e1	6.79e1	5.95e5	1	1.68e-6	5	6.65e1	7.39e1	4.73e5	1	2.11e-6
6	6.11e1	6.79e1	5.95e5	1	1.68e-6	6	6.65e1	7.39e1	4.73e5	1	2.11e-6
7	6.11e1	6.79e1	5.95e5	1	1.68e-6	7	6.65e1	7.39e1	4.73e5	1	2.11e-6
8	6.11e1	6.79e1	5.95e5	1	1.68e-6	8	6.65e1	7.39e1	4.73e5	1	2.11e-6
9	6.11e1	6.79e1	5.95e5	1	1.68e-6	9	6.65e1	7.39e1	4.73e5	1	2.11e-6
10	6.11e1	6.79e1	5.95e5	1	1.68e-6	10	6.65e1	7.39e1	4.73e5	1	2.11e-6
11	6.11e1	6.79e1	5.95e5	1	1.68e-6	11	6.65e1	7.39e1	4.73e5	1	2.11e-6
12	6.11e1	6.79e1	5.95e5			12	6.65e1	7.39e1	4.73e5		
<b>Creep damage fraction per cycle</b>					<b>2.02e-5</b>	<b>Creep damage fraction per cycle</b>					<b>2.53e-5</b>
<i>At ID on stress classification line-1 shown in Figure 4-1.2.5.2</i>						<i>At ID on stress classification line-2 shown in Figure 4-1.2.5.2</i>					
<i>Time (hr)</i>	<i>S<sub>k</sub> (MPa)</i>	<i>S<sub>k</sub> K' (MPa)</i>	<i>(T<sub>d</sub>)<sub>k</sub> (hr)</i>	<i>Δt<sub>k</sub> (hr)</i>	<i>(<math>\frac{\Delta t}{T_d}</math>)<sub>k</sub></i>	<i>Time (hr)</i>	<i>S<sub>k</sub> (MPa)</i>	<i>S<sub>k</sub> K' (MPa)</i>	<i>(T<sub>d</sub>)<sub>k</sub> (hr)</i>	<i>Δt<sub>k</sub> (hr)</i>	<i>(<math>\frac{\Delta t}{T_d}</math>)<sub>k</sub></i>
0	8.11e1	9.01e1	5.88e5	1	1.70e-6	0	9.37e1	1.04e2	3.72e5	1	2.69e-6
1	8.11e1	9.01e1	5.88e5	1	1.70e-6	1	9.37e1	1.04e2	3.72e5	1	2.69e-6
2	8.11e1	9.01e1	5.88e5	1	1.70e-6	2	9.37e1	1.04e2	3.72e5	1	2.69e-6
3	8.11e1	9.01e1	5.88e5	1	1.70e-6	3	9.37e1	1.04e2	3.72e5	1	2.69e-6
4	8.11e1	9.01e1	5.88e5	1	1.70e-6	4	9.37e1	1.04e2	3.72e5	1	2.69e-6
5	8.11e1	9.01e1	5.88e5	1	1.70e-6	5	9.37e1	1.04e2	3.72e5	1	2.69e-6
6	8.11e1	9.01e1	5.88e5	1	1.70e-6	6	9.36e1	1.04e2	3.72e5	1	2.69e-6
7	8.11e1	9.01e1	5.88e5	1	1.70e-6	7	9.36e1	1.04e2	3.72e5	1	2.69e-6
8	8.11e1	9.01e1	5.88e5	1	1.70e-6	8	9.36e1	1.04e2	3.72e5	1	2.69e-6
9	8.11e1	9.01e1	5.88e5	1	1.70e-6	9	9.36e1	1.04e2	3.72e5	1	2.69e-6
10	8.11e1	9.01e1	5.88e5	1	1.70e-6	10	9.36e1	1.04e2	3.72e5	1	2.69e-6
11	8.11e1	9.01e1	5.88e5	1	1.70e-6	11	9.36e1	1.04e2	3.72e5	1	2.69e-6
12	8.11e1	9.01e1	5.88e5			12	9.36e1	1.04e2	3.72e5		
<b>Creep damage fraction per cycle</b>					<b>2.04e-5</b>	<b>Creep damage fraction per cycle</b>					<b>3.23e-5</b>

Table 4-1.2.5.3. (Sample problem 1) Sample calculation to determine creep damage fraction,  $D_c$  per cycle from stress-time history according to Method 1.

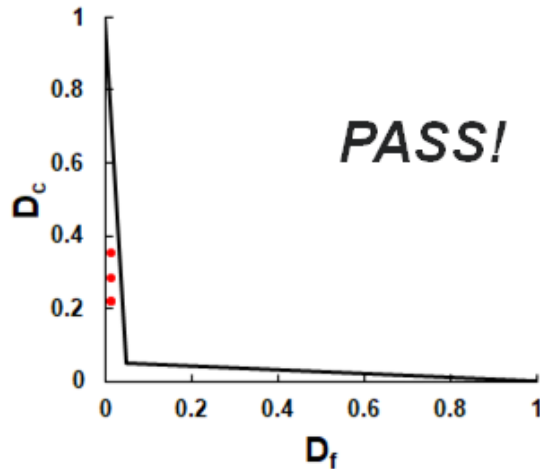


Figure 4-1.2.5.5. (Sample problem 1) Illustration of creep-fatigue design check. Plotted data are results from analysis according to Method 1.

#### **4-1.2.6. Step-6: Time-independent buckling check**

As buckling is not expected under the salt pressure and thermal loading considered in this problem and because wind load is not considered, this design check was not performed.

#### **4-1.2.7. Step-7: Time-dependent buckling check**

As buckling is not expected under the salt pressure and thermal loading considered in this problem, this design check was not performed.

### **4-1.3. Design calculations based on Method 2**

#### **4-1.3.1. Step-1: Defining the Design Cycle**

Same as in Method 1 Step 1.

#### **4-1.3.2. Step-2: Transient elastic thermo-mechanical analysis for each service load case and stress classification**

Same as in Method 1 Step 2.

#### **4-1.3.3. Step-3: Primary load design check**

Same as in Method 1 Step 3.

#### **4-1.3.4. Step-4: Ratcheting check**

Same as in Method 1 Step 4.



#### 4-1.3.5. Step-5: Creep-fatigue damage check

Method 2 is applicable only if the total stress intensity ( $P + Q + F$ ) remains less than  $S_y$  for all service loading and if peak stresses are minimal.

For a design to be acceptable, the following relation must be satisfied:

$$\sum_j \left( \frac{n}{N_d} \right)_j + \sum_k \left( \frac{\Delta t}{T_d} \right)_k \leq D$$

where  $D$  is the total creep-fatigue damage and the first and second terms on the left side are fatigue damage,  $D_f$  and creep damage,  $D_c$ , respectively. In the fatigue damage term,  $(n)_j$  is the number of repetitions of cycle type  $j$  and  $(N_d)_j$  is the number of design allowable cycles for respective cycle type; while in the creep damage term,  $(T_d)_k$  is the allowable time duration for a given stress at the maximum temperature occurring in the time interval  $k$  and  $(\Delta t)_k$  is the duration of the time interval  $k$ .

The design allowable cycles for fatigue damage is determined by entering fatigue curves at total strain range,  $\epsilon_t$ . Total strain range,  $\epsilon_t$  is calculated using equation HBB-T-1432-16:

$$\Delta \epsilon = \Delta \epsilon_1 + \Delta \epsilon_2$$

where  $\Delta \epsilon_1$  is the maximum equivalent strain range calculated from the elastic analysis of under primary and secondary loading together, according to Section III, Division 5, HBB-T-1413.  $\Delta \epsilon_2$  is the creep strain increment per stress cycle.  $\Delta \epsilon_2$  can be determined by entering the isochronous stress-strain curves at the O'Donnell-Porowski core stress,  $\sigma_c$  (determined in Method 1, Step 4) and maximum metal temperature for the stress cycle time, including hold times between transient (instead of total service life). Alternatively,  $\Delta \epsilon_2$  can be calculated by dividing the creep strain accumulated during the entire service life by the number of stress cycles during the entire service life. We used the latter option.

Creep damage for each service load cycle is evaluated from the von Mises stress profile, determined from elastically calculated stresses, versus time profile for this load cycle. Using the stress-time profile and the hold time temperature,  $T_{HT}$  during the cycle, creep damage fraction can be calculated according to the illustration in Figure 4-1.3.5.1 As mentioned before, we only considered the start-up/shut-down service load cycle for creep damage fraction calculation.

Tables 4-1.3.5.1 and 4-1.3.5.2 show few sample calculations of determining creep damage fraction,  $D_c$  and fatigue damage fraction,  $D_f$ , respectively, according to Method 2. Similar to Method 1, Method 2 also uses creep-fatigue interaction diagram to determine whether a design passes creep-fatigue damage check. Comparing  $(D_f, D_c)$  with the damage envelop in creep-fatigue interaction diagram, as shown in Figure 4-1.3.5.2, the design is found to be passed according to Method 2.

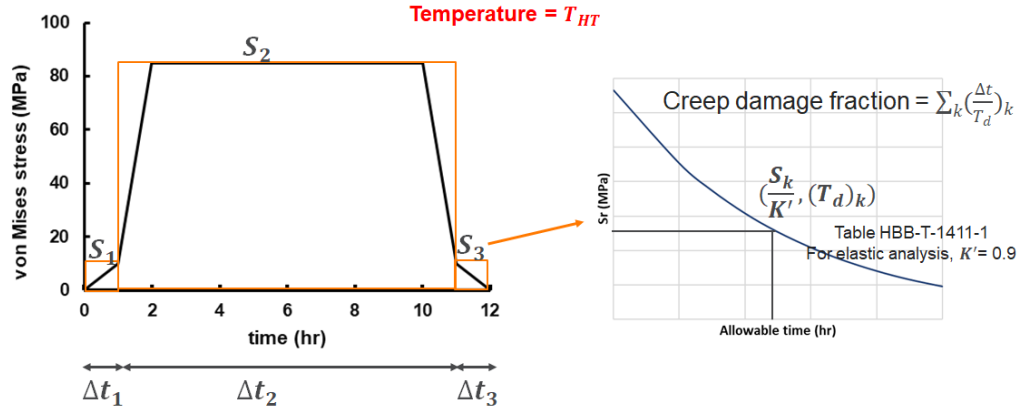


Figure 4-1.3.5.1. (Sample problem 1) Illustration of calculating creep damage fraction in Method 2.

At OD on stress classification line-1 shown in Figure 4-1.2.5.2						At OD on stress classification line-2 shown in Figure 4-1.2.5.2					
$T_{HT} = 770^{\circ}\text{C}$ $S_y$ at $T_{HT} = 490 \text{ MPa}$ (Method 2 is applicable!)						$T_{HT} = 767.3^{\circ}\text{C}$ $S_y$ at $T_{HT} = 492.3 \text{ MPa}$ (Method 2 is applicable!)					
Time (hr)	$S_k$ (MPa)	$\frac{S_k}{K' (= 0.9)}$ (MPa)	$(T_d)_k$ (hr)	$\Delta t_k$ (hr)	$(\frac{\Delta t}{T_d})_k$	Time (hr)	$S_k$ (MPa)	$\frac{S_k}{K' (= 0.9)}$ (MPa)	$(T_d)_k$ (hr)	$\Delta t_k$ (hr)	$(\frac{\Delta t}{T_d})_k$
0	0	-	-	-	-	0	0	-	-	-	-
1	7.88	8.76	1.47e7	1	6.80e-8	1	9.05	10.06	1.37e7	1	7.23e-8
2	57.17	63.52	7.55e5	10	1.32e-5	2	59.93	66.59	6.95e5	10	1.44e-5
10	57.17	-	-	-	-	10	59.93	-	-	-	-
11	7.88	8.76	1.47e7	1	6.80e-8	11	9.05	10.06	1.37e7	1	7.23e-8
12	0	-	-	-	-	12	0	-	-	-	-
Creep damage fraction per cycle					1.33e-5	Creep damage fraction per cycle					1.45e-5
Creep damage fraction, $D_c$					0.15	Creep damage fraction, $D_c$					0.16
At ID on stress classification line-1 shown in Figure 4-1.2.5.2						At ID on stress classification line-2 shown in Figure 4-1.2.5.2					
$T_{HT} = 740^{\circ}\text{C}$ $S_y$ at $T_{HT} = 512 \text{ MPa}$ (Method 2 is applicable!)						$T_{HT} = 737.3^{\circ}\text{C}$ $S_y$ at $T_{HT} = 513 \text{ MPa}$ (Method 2 is applicable!)					
Time (hr)	$S_k$ (MPa)	$\frac{S_k}{K' (= 0.9)}$ (MPa)	$(T_d)_k$ (hr)	$\Delta t_k$ (hr)	$(\frac{\Delta t}{T_d})_k$	Time (hr)	$S_k$ (MPa)	$\frac{S_k}{K' (= 0.9)}$ (MPa)	$(T_d)_k$ (hr)	$\Delta t_k$ (hr)	$(\frac{\Delta t}{T_d})_k$
0	0	-	-	-	-	0	0	-	-	-	-
1	9.72	10.80	1.58e7	1	6.33e-8	1	10.55	11.7	1.60e7	1	6.25e-8
2	74.01	82.23	8.16e5	10	1.23e-5	2	86.03	95.59	5.25e5	10	1.90e-5
10	74.01	-	-	-	-	10	86.03	-	-	-	-
11	9.72	10.8	1.58e7	1	6.33e-8	11	10.55	11.7	1.60e7	1	6.25e-7
12	0	-	-	-	-	12	0	-	-	-	-
Creep damage fraction per cycle					1.36e-5	Creep damage fraction per cycle					1.91e-5
Creep damage fraction, $D_c$					0.15	Creep damage fraction, $D_c$					0.21

Table 4-1.3.5.1. (Sample problem 1) Sample calculation to determine creep damage fraction,  $D_c$  per cycle from stress-time history according to Method 2.

	<i>At OD on stress classification line-1 shown in Figure 4-1.2.5.2</i>		<i>At OD on Stress classification line-2 shown in Figure 4-1.2.5.2</i>	
	<i>Start-up/shut-down cycle</i>	<i>Cloud event</i>	<i>Start-up/shut-down cycle</i>	<i>Cloud event</i>
$T^{max}$	770°C	770°C	767.3°C	767.3°C
$\Delta\epsilon_1$	0.0356 %	0.0360 %	0.0377 %	0.0376 %
$\Delta\epsilon_2$	1.10e-6%	0	1.10e-6%	0
$\Delta\epsilon$	0.0356 %	0.0360 %	0.0377 %	0.0376 %
Design allowable cycles, $N_d$	5086519	5047174	4883326	4892815
Design cycles, $n$	30*365=10950	30*365*5=54750	30*365=10950	30*365*5=54750
<b>Fatigue damage fraction, <math>D_f</math></b>	<b>0.0130</b>		<b>0.0134</b>	

Table 4-1.3.5.2. (Sample problem 1) Sample calculations of determining fatigue damage fraction,  $D_f$  according to Method 2.

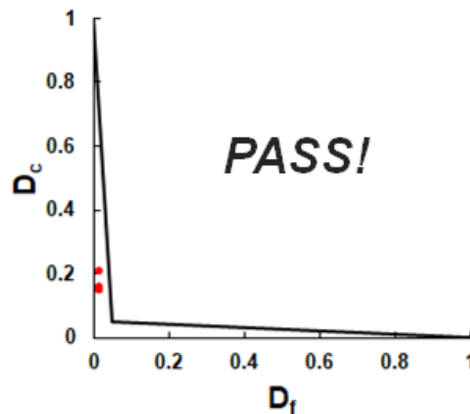


Figure 4-1.3.5.2. (Sample problem 1) Illustration of creep-fatigue design check. Plotted data are results from analysis according to Method 2.

#### 4-1.3.6. Step-6: Time-independent buckling check

Same as in Method 1 Step 6.

#### 4-1.3.7. Step-7: Time-dependent buckling check

Same as in Method 1 Step 7.

#### 4-1.4. Design calculations based on Method 3

This method is applicable only if the elastically-calculated stresses remain below the material yield stress,  $S_y$ . In the discussion of design calculation based on Method 2, it is shown that the elastically-calculated stress for this sample problem is always less than  $S_y$  and therefore Method 3 is applicable.

For primary load design, Method 3 uses the same procedures in Method 1 which is based on elastic analysis. For ratcheting and creep-fatigue design checks, however, this method uses inelastic analysis where material's constitutive response is described by an elastic-creep model. The description of the elastic-creep material model is provided above. Design calculations related to ratcheting and creep-fatigue damage are discussed for Method 3.

#### **4-1.4.1. Step-1: Defining the Design Cycle**

Same as in Method 1 Step 1.

#### **4-1.4.2.**

##### **Step-2a: Transient elastic thermo-mechanical analysis for each service load case and stress classification (for primary load design check)**

Same as in Method 1 Step 2.

##### **Step-2b: Transient elastic-creep thermo-mechanical analysis for each service load case (for ratcheting and creep-fatigue evaluation)**

We used MOOSE (Multiphysics Object Oriented Simulation Environment), an open source finite element solver to perform the transient elastic-creep thermo-mechanical analyses under the loading conditions mentioned in Step 1. The analysis was repeated until a steady state cyclic response was achieved.

#### **4-1.4.3. Step-3: Primary load design check**

Same as in Method 1 Step 3.

#### **4-1.4.4. Step-4: Ratcheting check**

To determine ratcheting strain Method 3 requires to run the analysis using elastic-creep material model, described above, and monitor the maximum effective strain,  $\sqrt{\frac{2}{3}} \varepsilon: \varepsilon$  at the beginning and end of the cycle. The criterion is that the ratcheting strain does not exceed 10% at any point of the structure for base metal. Figure 4-1.4.4 plots the maximum effective strain at the critical tube location as a function of cycle count. Extrapolating the maximum effective strain out to design life of the tube, i.e. 30 years (=30\*365 cycles), gives the ratcheting strain of 0.00565% which is less than 10%.

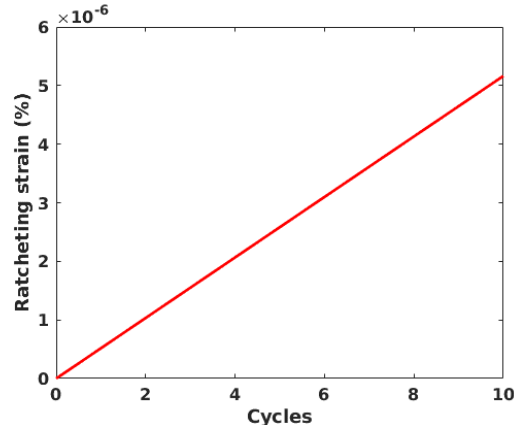


Figure 4-1.4.4. (Sample problem 1) Maximum ratcheting strain in the structure versus number of cycles determined from elastic-creep thermo-mechanical analysis.

#### 4-1.4.5. Step-5: Creep-fatigue damage check

Once steady cyclic response was achieved in the analysis, the temperature, stress, strain, time history for a single cycle of the periodic loading were extracted. To determine fatigue damage fraction, the effective strain range,  $\Delta\epsilon$  was first computed from the strain history according to Section III, Division 5, HBB-T-1413 with  $\nu^* = 0.5$  for inelastic analysis. Fatigue damage fraction,  $D_f$  was then calculated from  $\Delta\epsilon$  using rainflow counting and Miner's rule. Figure 4-1.4.5.1 plots temperature, von Mises stress, and effective strain range profiles at four critical locations of the tube after a steady cyclic response was achieved. Table 4-1.4.5.1 shows details of the fatigue damage fraction calculation according to Method 3. The von Mises effective stress,  $\sigma_{eff}(t)$  was used to determine the creep damage fraction. Figure 4-1.4.5.2 illustrates the method of creep damage fraction,  $D_c$  calculation and Table 4-1.4.5.2 reports details of the calculation for four critical locations in the structure. All four sets of  $(D_f, D_c)$  fall inside the damage envelop in the creep-fatigue interaction diagram, as shown in Figure 4-1.4.5.3, which means according to Method 3 the design passes creep-fatigue damage check.

Note, according to Table HBB-1411-1 in Section III, Division 5 of ASME Code, a design margin (i.e.,  $K'$ ) is applied to the effective stress while determining the allowable rupture time from the design rupture table. ASME Code recommends to use  $K' = 0.9$  for elastic analysis and  $K' = 0.67$  for inelastic analysis. However, the history behind the ASME stress factors is somewhat murky and given the lower consequences of failure for CSP systems, the design method developed here uses  $K' = 0.9$  for all analysis methods, including the inelastic analysis.

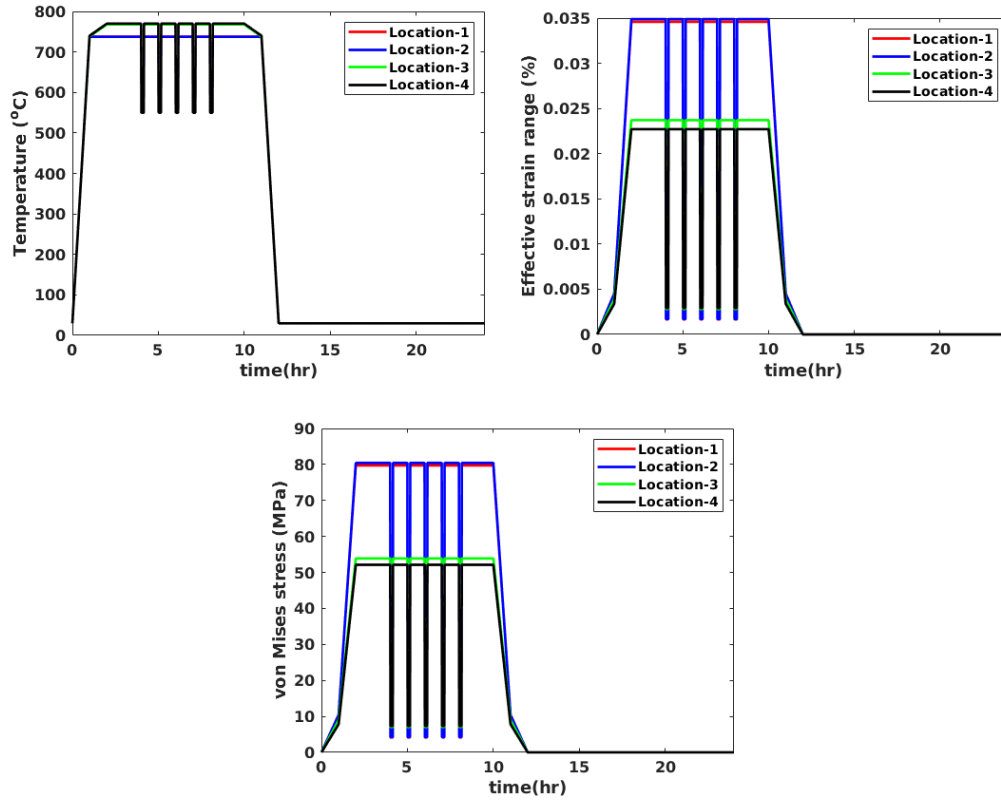


Figure 4-1.4.5.1. (Sample problem 1) Temperature, effective strain range, and von Mises stress profiles at four critical location of the tube after a steady cyclic response is achieved in the elastic-creep thermo-mechanical analysis.

	Location-1		Location-2		Location-3		Location-4	
$T^{max}$	738.0°C		737.4°C		768.0°C		770.0°C	
Strain range and corresponding cycle frequency according to rainflow counting of effective strain range, $\Delta\epsilon$	0.0346%	0.0329%	0.0349%	0.0332%	0.0237%	0.0209%	0.0302%	0.0273%
	1	5	1	5	1	5	1	5
Design allowable cycles, $N_d$	5186228	5360239	5156112	5329113	6408388	6766364	5648690	5975819
Fatigue damage fraction per cycle	1.126e-6		1.132e-6		8.950e-7		1.014e-6	
Design cycles, $n$	30*365=10950		30*365=10950		30*365=10950		30*365=10950	
<b>Fatigue damage fraction, <math>D_f</math></b>	<b>0.0123</b>		<b>0.0124</b>		<b>0.0098</b>		<b>0.0110</b>	

Table 4-1.4.5.1. (Sample problem 1) Sample calculation of determining fatigue damage fraction,  $D_f$  according to Method 3.

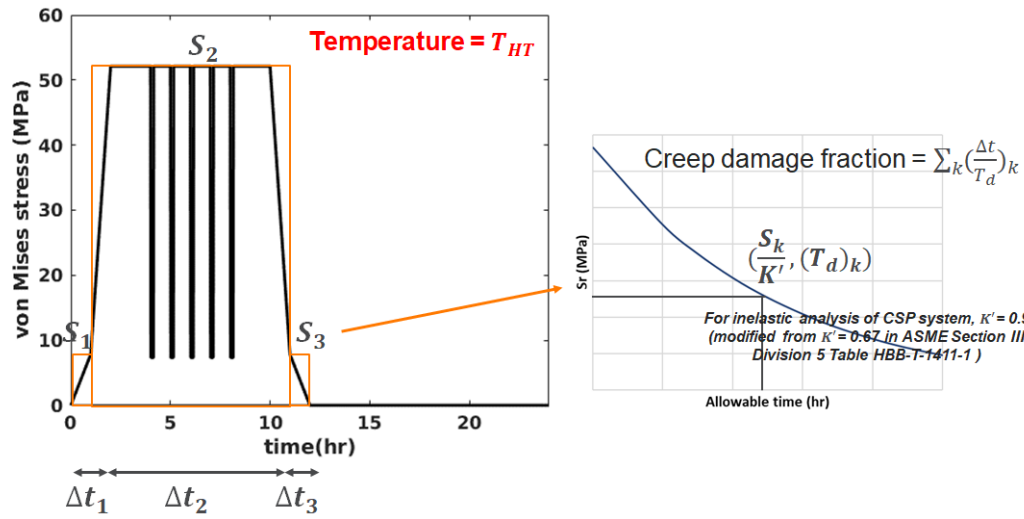


Figure 4-1.4.5.2. Illustration of calculating creep damage fraction in Method 3.

	Location-1			Location-2			Location-3			Location-4		
Temperature during hold, $T_{HT}$	738.0°C			737.4°C			768.0°C			770.0°C		
von Mises effective stress, $\sigma_{eff}$ (MPa) and corresponding time interval, $\Delta t_k$ (hr)	10.5	79.7	10.5	10.4	80.4	10.4	8.9	53.9	8.9	7.8	52.1	7.8
$\frac{S_k (= \sigma_{eff})}{K' (=0.9)}$	11.7	88.6	11.7	11.6	89.3	11.6	9.9	59.9	9.9	8.7	57.9	8.7
Allowable time, $(T_d)_k$ (hr)	1.58e7	6.78e5	1.58e7	1.61e7	6.75e5	1.61e7	1.38e7	9.71e5	1.38e7	1.47e7	1.02e6	1.47e7
$(\frac{\Delta t}{T_d})_k$	6.33e-8	1.47e-5	6.33e-8	6.21e-8	1.48e-5	6.21e-8	7.25e-8	1.03e-5	7.25e-8	6.80e-8	9.80e-6	6.80e-8
Creep damage fraction per cycle	1.49e-5			1.49e-5			1.04e-5			9.94e-6		
Design cycles, $n$	30*365=10950			30*365=10950			30*365=10950			30*365=10950		
Creep damage fraction, $D_c$	0.16			0.16			0.11			0.11		

Table 4-1.4.5.2. (Sample problem 1) Sample calculation of determining creep damage fraction,  $D_c$  according to Method 3.

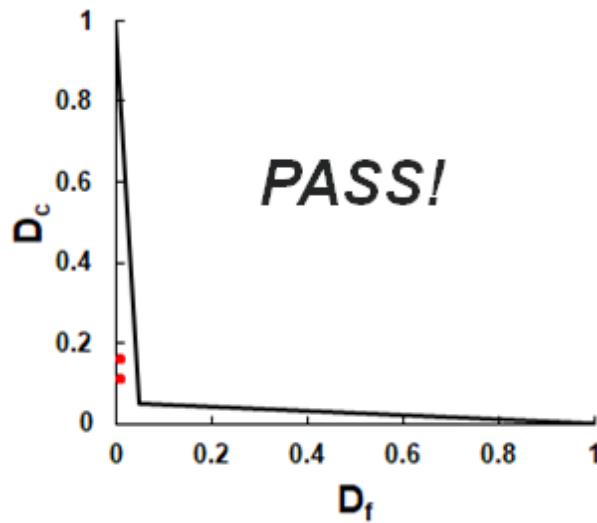


Figure 4-1.4.5.3. (Sample problem 1) Illustration of creep-fatigue design check. Plotted data are results from analysis according to Method 3.

#### 4-1.4.6. Step-6: Time-independent buckling check

Same as in Method 1 Step 6.

#### 4-1.4.7. Step-7: Time-dependent buckling check

Same as in Method 1 Step 7.

### 4-2. Sample problem 2

#### 4-2.1. Problem description

For sample problem 2 we considered a tube in an external tubular receiver. The receiver has parabolic reflectors at the back of the tubes which help reduce the variation in the circumferential heat flux distribution on the tube. Figure 4-2.1.1 shows the schematic of the tubular receiver. The tube is 10.5 m long, 42.2 mm diameter, and 1 mm thick. Heat flux on the tube is non uniform along both the length and circumference. We considered only one type of cycle for this problem which represent heat flux on the day of spring equinox. Figure 4-2.1.2 plots the loading profiles of maximum flux incident, salt inlet and outlet temperature, and salt pressure during day (10 hrs). Table 4-2.1.1 lists values of flux incident loading at noon (i.e. time = 5hr in Figure 4-2.1.2) for different locations on the tube outer surface. To determine the wind load on the receiver for time-independent buckling check, we considered the external receiver located in an open terrain in the U.S. and 100 m above the ground.

The salt considered for this problem is  $\text{MgCl}_2/\text{KCl}$  (mole: 32/68%) binary molten salt. The mass flow rate of the salt is 44.5 kg/s. Salt inlet and outlet temperatures are 700°C and 720°C,



respectively. To determine the convective heat transfer coefficient between salt and metal Gnielinski correlation<sup>29</sup> for turbulent flow (forced convection) in tubes was used.

$$Nu_D = \frac{\left(\frac{f}{8}\right)(Re_D - 1000)Pr}{1 + 12.7 \left(\frac{f}{8}\right)^{\frac{1}{2}} (Pr^{\frac{2}{3}} - 1)} \quad ; \text{ for } 3000 < Re_D < 5 \times 10^6 \text{ and } 0.5 < Pr < 2000$$

where  $Nu_D$  is the Nusselt number,  $Re_D$  is the Reynolds number,  $Pr$  is the Prandtl number, and  $f$  is the Darcy friction factor which can be obtained from the following equation.

$$f = (0.79 \ln(Re_D) - 1.64)^{-2}$$

All the required properties of salt, as listed in Table 4-2.1.2, to determine convective heat transfer coefficient were taken from<sup>30</sup>. Note the pressure loading profile shown in Figure 4-2.1.2 was selected based on the pressure loss due to friction and elevation. We assumed a surface roughness of 0.049 mm to determine the frictional pressure loss. In the heat transfer calculation for this sample problem, we also considered heat loss due to radiation and natural convection of air. The convective heat transfer coefficient of air is assumed to be  $14 \frac{W}{m^2 K}$ . For structural boundary condition, we considered the tube can freely expand both in radial and axial direction but no warping in the axial direction. The design life of the tube is considered to be 4.4 years. Design calculations according all three methods are provided below.

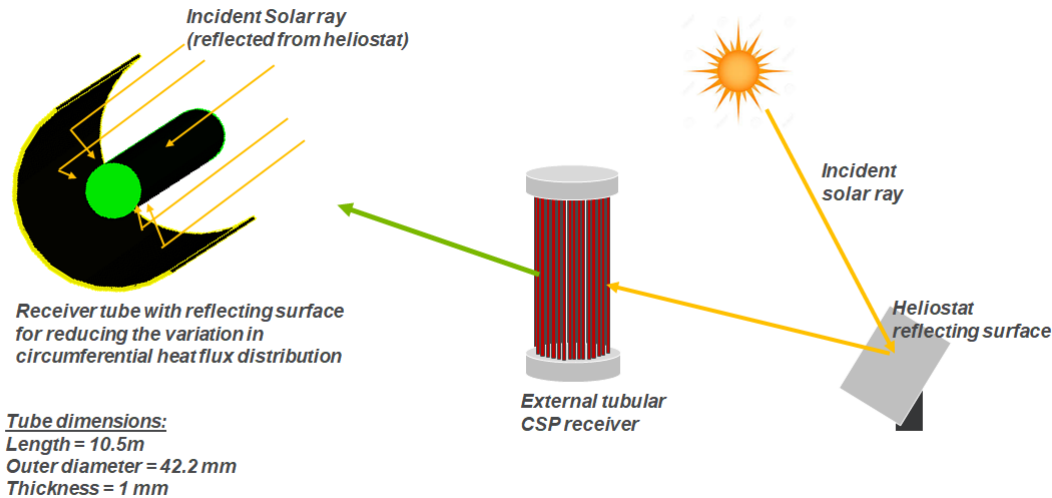


Figure 4-2.1.1. (Sample problem 2) Schematic of an external tubular receiver.

<sup>29</sup> V. Gnielinski, "Neue Gleichungen für den Wärme- und den Stoffübergang in turbulent durchströmten Rohren und Kanälen" *Forschung im Ingenieurwesen A*, 41(1), pp. 8-16, 1975.

<sup>30</sup> Xu, X. X. Wang, P. Li, Y. Li, Q. Hao, B. Xiao, H. Elsentriecy, and D. Gervasio, "Experimental Test of Properties of KCl-MgCl<sub>2</sub> Eutectic Molten Salt for Heat Transfer and Thermal Storage Fluid in Concentrated Solar Power Systems" *Journal of Solar Energy Engineering*, 140(5), pp. 051011, 2018.

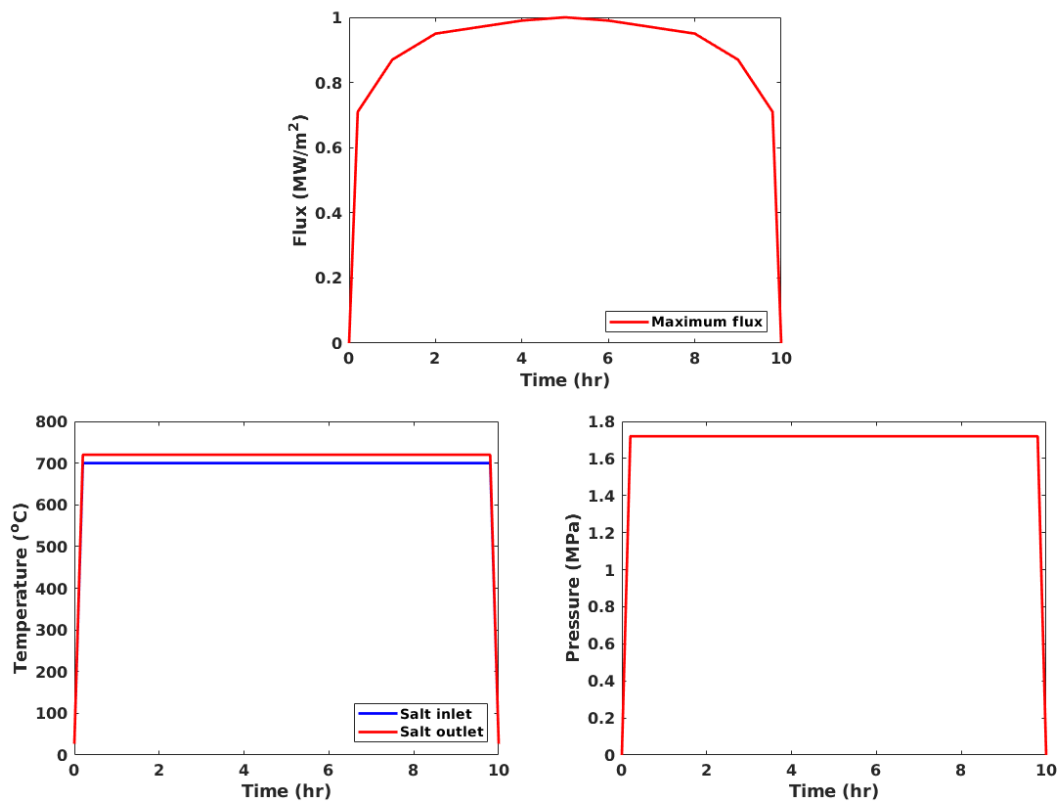


Figure 4-2.1.2. (Sample problem 2) Loading profiles of maximum flux incident, salt inlet and outlet temperature, and salt pressure during day. Only one type of cycle is considered. Receiver operation time per day is 10 hours. Loading profiles shown are only for the tube considered for design study.

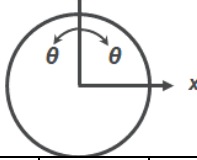
Flux on the tube outer surface (MW/m <sup>2</sup> )		Angular location, $\theta$ <i>y</i> (radially outward from the receiver cylindrical axis) 						
		0	30	60	90	120	150	180
Location along the axis of the tube, <i>m</i>	-5.250	0.195	0.189	0.182	0.176	0.169	0.163	0.156
	-4.812	0.314	0.304	0.293	0.283	0.272	0.262	0.251
	-4.375	0.454	0.439	0.424	0.409	0.393	0.378	0.363
	-3.938	0.597	0.577	0.557	0.537	0.517	0.498	0.478
	-3.500	0.728	0.704	0.679	0.655	0.631	0.607	0.582
	-3.062	0.835	0.807	0.779	0.752	0.724	0.696	0.668
	-2.625	0.915	0.885	0.854	0.824	0.793	0.763	0.732
	-2.188	0.971	0.939	0.906	0.874	0.842	0.809	0.777
	-1.750	1.000	0.967	0.933	0.900	0.867	0.833	0.800
	-1.313	1.010	0.976	0.943	0.909	0.875	0.842	0.808
	-0.875	1.000	0.967	0.933	0.900	0.867	0.833	0.800
	-0.438	0.988	0.955	0.922	0.889	0.856	0.823	0.790
	0.000	0.976	0.943	0.911	0.878	0.846	0.813	0.781
	0.437	0.972	0.940	0.907	0.875	0.842	0.810	0.778
	0.875	0.980	0.947	0.915	0.882	0.849	0.817	0.784
	1.312	0.993	0.960	0.927	0.894	0.861	0.828	0.794
	1.750	1.000	0.967	0.933	0.900	0.867	0.833	0.800
	2.188	0.994	0.961	0.928	0.895	0.861	0.828	0.795
	2.625	0.969	0.937	0.904	0.872	0.840	0.808	0.775
	3.062	0.918	0.887	0.857	0.826	0.796	0.765	0.734
	3.500	0.834	0.806	0.778	0.751	0.723	0.695	0.667
	3.937	0.714	0.690	0.666	0.643	0.619	0.595	0.571
	4.375	0.568	0.549	0.530	0.511	0.492	0.473	0.454
	4.812	0.414	0.400	0.386	0.373	0.359	0.345	0.331
	5.250	0.272	0.263	0.254	0.245	0.236	0.227	0.218

Table 4-2.1.1. (Sample problem 2) Flux incident loading at noon.

Properties	Values as function of temperature, $T$ (°C)
Heat capacity, $C_p$ ( $\frac{J}{kg K}$ )	$989.6 + 0.1046 \times (T - 430)$
Density, $\rho$ ( $\frac{kg}{m^3}$ )	$1903.7 - 0.552 \times T$
Viscosity, $\mu$ (Pa s)	$1.4965 \times 10^{-2} - 2.91 \times 10^{-5} \times T + 1.784 \times 10^{-8} \times T^2$
Thermal conductivity, $K$ ( $\frac{W}{m K}$ )	$0.5047 - 0.0001 \times T$

Table 4-2.1.2. (Sample problem 2) Temperature dependent properties of MgCl<sub>2</sub>/KCl (mole: 32/68%) binary molten salt taken from<sup>30</sup>.

## 4-2.2. Design calculations based on Method 1

### 4-2.2.1. Step-1: Defining the Design Cycle

The loading profile is shown in Figure 4-2.1.2.

### 4-2.2.2. Step-2: Transient elastic thermo-mechanical analysis for each service load case and stress classification

We used MOOSE (Multiphysics Object Oriented Simulation Environment), an open source finite element solver to perform the elastic thermo-mechanical analyses. We classify pressure as primary load and temperature gradient as secondary load. There is no peak load.

### 4-2.2.3. Step-3: Primary load design check

Figure 4-2.2.3.1 shows the heat flux and tube outer wall temperature distribution at noon. Figure 4-2.2.3.2 shows through thickness elastic stress components at noon at a critical location of the tube.

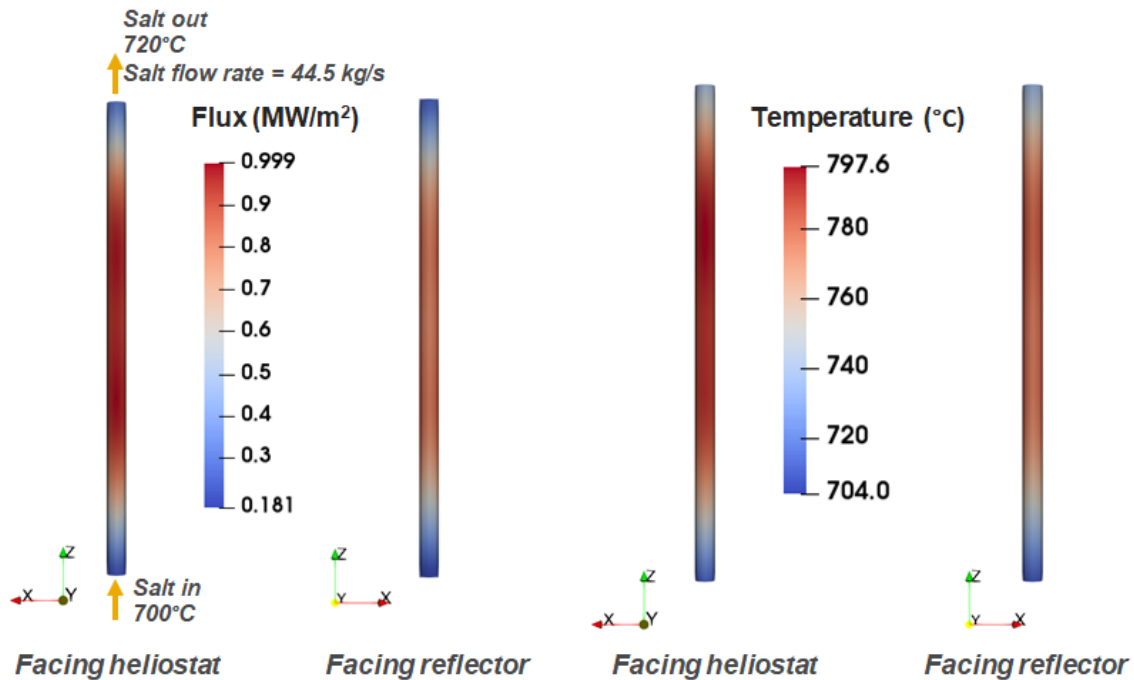


Figure 4-2.2.3.1. (Sample problem-2) Contour plot of flux incident on tube and tube outer wall temperature at noon.

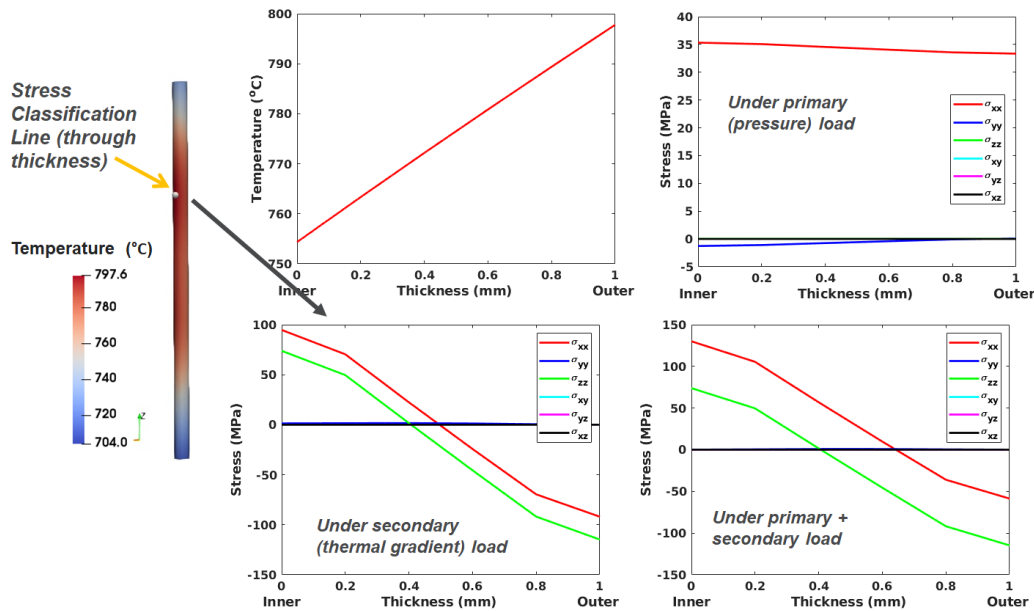


Figure 4-2.2.3.2. (Sample problem-2) Through thickness temperature and elastic stresses at a critical location of the tube at noon.

Maximum primary load occurs at noon. Table 4-2.2.3 reports details of the primary load checks. First, all the stress components were linearized to divide into membrane and bending components along the stress classification line. The membrane and bending stress components were then used to determine the stress intensities in Table 4-2.2.3 As indicated in the table the design passes both the criteria in primary load checks.

Max. General primary membrane stress intensity, $P_m$	34.90 MPa
Max. Combined primary membrane plus bending stress intensity, $P_L + P_b$	36.76 MPa
Maximum metal temperature, $T_{max}$	797.6 °C
Allowable stress, $S_o$ at $T_{max}$	36.89 MPa
Design criteria -1: $P_m \leq S_o$	<b>PASS !</b>
Design criteria -2: $P_L + P_b \leq 1.5 S_o$	<b>PASS !</b>

Table 4-2.2.3. (Sample problem-2) Primary load design checks along the stress classification line shown in Figure 4-2.2.3.2.

#### 4-2.2.4. Step-4: Ratcheting check

Design method 1 uses the O'Donnell-Porowski approach, described in Section III, Division 5, HBB-1332 for ratcheting checks. In this approach, an effective creep stress parameter, Z is determined from a primary stress parameter, X and a secondary stress parameter, Y as shown in Figure 4-1.2.4.1 The effective creep stress parameter is used to calculate the effective creep stress which is then used to determine the ratcheting creep strain using isochronous stress-strain curves. The definition of X and Y are

$$X = (P_L + \frac{P_b}{K_t})_{max} / S_{yL}$$

$$Y = (Q_R)_{max} / S_{yL}$$

where,

$(P_L + \frac{P_b}{K_t})_{max}$  = the maximum value of the primary stress intensity, adjusted for bending via  $K_t$ , during the cycle being evaluated.

$(Q_R)_{max}$  = the maximum range of the secondary stress intensity during the cycle being considered  
 $S_{yL}$  = is the  $S_y$  value corresponds to the lower of the wall averaged temperature for the stress extremes defining secondary stress range,  $Q_R$ .

$$K_t = (K + 1)/2$$

$K$  is 1.5 for across-the-wall bending of shell structures or rectangular sections, see HBB-3223 (c) (6) in Section III Division 5. Once  $Z$  is found, effective core,  $\sigma_c$  stress is determined from

$$Z = \frac{\sigma_c}{S_{yL}}$$

It should be noted that, the average wall temperature at one of the stress extremes defining the secondary stress intensity range must be below the temperature listed in Section III, Division 5, HBB-T-1323, given as 600°C for 740H in the description of the design Method 1. The creep ratcheting strain increment for a load cycle is evaluated by entering the isochronous stress strain curves at the maximum wall temperature and effective core,  $\sigma_c$  stress during the load cycle with the stress held constant for the entire service life. An example of creep ratcheting strain determination is shown in Figure 4-1.2.4.2 Table 4-2.2.4 provides all the calculation details of the ratcheting design check. As indicated in the table, the design passes the ratcheting check.

	<i>Stress classification line shown in Figure 4-2.2.3.2</i>
$T_{wall\ averaged}^{max}$	776.4 °C
$T_{wall\ averaged}^{min}$	30 °C
$T^{max}$	797.6 °C
$S_{yL}$ (at $T_{wall\ averaged}^{min}$ )	621.0 MPa
$K$	1.5
$K_t = (K + 1)/2$	1.25
$(P_L + \frac{P_b}{K_t})_{max}$	36.39 MPa
$(Q_R)_{max}$	114.76 MPa
$X = (P_L + \frac{P_b}{K_t})_{max}/S_{yL}$	0.0586
$Y = (Q_R)_{max}/S_{yL}$	0.184
$Z$ using Section III, Division 5, Figure HBB-T-1332-1	0.0586
$\sigma_c$ from $Z = \frac{\sigma_c}{S_{yL}}$	36.39
Service life	4.4 years = 16060 hours
Ratcheting strain at the end of service life	6.93e-4%
Ratcheting design criteria: 2% for base metal	<b>PASS!</b>

Table 4-2.2.4. (Sample problem-2) Ratcheting design checks according to Method 1.

#### 4-2.2.5. Step-5: Creep-fatigue damage check

According to Section III, Division 5, a design is acceptable if the creep and fatigue damage satisfy the following relation:

$$\sum_j \left(\frac{n}{N_d}\right)_j + \sum_k \left(\frac{\Delta t}{T_d}\right)_k \leq D$$

where D is the total creep-fatigue damage and the first and second terms on the left side are fatigue damage,  $D_f$  and creep damage,  $D_c$ , respectively. In the fatigue damage term,  $(n)_j$  is the number of repetitions of cycle type j and  $(N_d)_j$  is the number of design allowable cycles for respective cycle type; while in the creep damage term,  $(T_d)_k$  is the allowable time duration for a given stress at the maximum temperature occurring in the time interval k and  $(\Delta t)_k$  is the duration of the time interval k.

The design allowable cycles for fatigue damage is determined by entering fatigue curves at total strain range,  $\epsilon_t$ . Total strain range,  $\epsilon_t$  is calculated using equation HBB-T-1432-16:

$$\epsilon_t = K_v \Delta \epsilon_{mod} + K \Delta \epsilon_c$$

where K is the local geometric concentration or equivalent stress concentration factor determined by dividing effective primary plus secondary plus peak stress divided by the effective primary plus secondary stress,  $K_v$  is the multiaxial plasticity and Poisson ratio adjustment factor,  $\Delta \epsilon_c$  is the creep strain increment, and  $\Delta \epsilon_{mod}$  is the modified maximum equivalent strain range.

$\Delta \epsilon_{mod}$  is calculated using equation Section III, Division 5, HBB-T-1432-12:

$$\Delta \epsilon_{mod} = \left(\frac{S^*}{\bar{S}}\right) K^2 \Delta \epsilon_{max}$$

where  $\Delta \epsilon_{max}$  is the maximum equivalent strain range calculated from the elastic analysis of under primary and secondary loading together.  $\Delta \epsilon_{max}$  is calculated according to Section III, Division 5, HBB-T-1413 with  $\nu^* = 0.3$  for elastic analysis.  $S^*$  and  $\bar{S}$  are stresses determined by entering the isochronous stress-strain curves at  $\Delta \epsilon_{max}$  and  $K \Delta \epsilon_{max}$ , respectively.

$K_v$  is determined using equation Section III, Division 5, HBB-T-1432-15:

$$K_v = 1.0 + f(K'_v - 1.0)$$

where f is the inelastic multiaxial adjustment factor determined using Section III, Division 5, Figure HBB-T-1432-2 and triaxiality factor, T.F.

$$T.F. = \frac{|\sigma_1 + \sigma_2 + \sigma_3|}{\frac{1}{\sqrt{2}} [(\sigma_1 - \sigma_2)^2 + (\sigma_2 - \sigma_3)^2 + (\sigma_3 - \sigma_1)^2]}$$

where  $\sigma$ 's are principals stresses at the extreme of the stress cycle.

$K'_v$  is the adjustment for inelastic biaxial Poisson's ratio determined from Section III, Division 5, Figure HBB-T-1432-3 using  $K_e$ .

$$K_e = \begin{cases} 1 & ; K\Delta\epsilon_{max} \leq 3\bar{S}_m/E \\ \frac{K\Delta\epsilon_{max}E}{3\bar{S}_m} & ; K\Delta\epsilon_{max} > 3\bar{S}_m/E \end{cases}$$

where

$$3\bar{S}_m = \begin{cases} 1.5 S_m + S_{rH}; & \text{when only one of the extreme of the stress difference occurs at a} \\ & \text{temperature above those covered by Division 1, Subsection NB rules} \\ S_{rH} + S_{rL}; & \text{when both of the extreme of the stress difference occur at a} \\ & \text{temperature above those covered by Division 1, Subsection NB rules} \end{cases}$$

Here  $S_{rH}$  and  $S_{rL}$  are relaxation strengths associated with the temperatures at the hot and cold extremes of the stress cycle. These values are provided above in the 740H design data. The hot temperature condition is defined as the maximum operating temperature of the stress cycle. The hot time is equal to the portion of service life when wall averaged temperatures exceed 425°C. The cold temperature is defined as the colder of the two temperatures corresponding to the two stress extremes in the stress cycle. The cold time is again equal to the portion of service life when wall averaged temperatures exceed 425°C.

The creep strain increment per stress cycle,  $\Delta\epsilon_c$  is determined by entering the isochronous stress-strain curves at  $\sigma_c$  and maximum metal temperature for the stress cycle time, including hold times between transients (instead of total service life). Alternatively, the creep accumulated during the entire service life divided by the number of stress cycles during the entire service life can also be used for calculating creep strain increment per stress cycle,  $\Delta\epsilon_c$ . We used the latter option.

The design allowable cycles,  $N_d$  is then calculated from design fatigue curve at maximum metal temperature and using total strain range,  $\epsilon_t$ . Fatigue damage fraction,  $D_f$  is then determined from the ratio between design cycles and design allowable cycles for each cycle type and then adding them together. Note, we considered only one type of cycle in the sample problem 2. Table 4-2.3.5.1 shows the details of all the relevant calculations to determine fatigue damage fraction.

Creep damage evaluation is done in accordance to HBB-T1433(b)-option (a) but with one exception as described in the design Method 1. The lower bound stress  $S_{LB}$  is taken as  $1.0\sigma_c$ , rather than the  $1.25\sigma_c$  specified in the Code. First, stress relaxation profile is determined by entering the isochronous stress-strain curves at a strain level equal to  $\epsilon_t$  and at hold-time temperature and determining the corresponding stress levels at varying times. However, this stress relaxation process should not be permitted to a stress level less than  $S_{LB}$ . This stress relaxation procedure results in a stress-time history. Using the stress-time history and hold-time temperature during the cycle creep damage fraction can be calculated according to the illustration in Figure 4-1.2.5.4. Tables 4-2.3.5.2 and 4-2.3.5.3 show the details of determining creep damage fraction,  $D_c$  from stress relaxation profile.



To determine whether the design passes the creep-fatigue damage check, the fatigue damage fraction,  $D_f$  and creep damage fraction,  $D_c$  are plotted on creep-fatigue interaction diagram as shown in Figure 4-2.3.5.1. As indicated in the figure, the  $(D_f, D_c)$  points fall inside the creep-fatigue damage envelop which means the design passes for creep-fatigue damage check.

	<i>At OD on stress classification line shown in Figure 4-2.2.3.2</i>	<i>At ID on stress classification line shown in Figure 4-2.2.3.2</i>
$T^{max}$	797.6°C	754.4°C
Hot temperature	797.6°C	754.4°C
Cold temperature	30°C	30°C
Hot time	10hr*(4.4*365) = 16060 hr	10hr*(4.4*365) = 16060 hr
Cold time	14hr*(30*365) = 22484 hr	14hr*(30*365) = 22484 hr
$S_{rH}$	78.4 MPa	126.4 MPa
$S_{rL}$	Not required	Not required
$S_m$ at $T^{max}$	218.9 MPa	253.5 MPa
$3\bar{S}_m$	406.8 MPa	506.7 MPa
$\Delta\epsilon_{max}$	0.0569 %	0.0644 %
$K$	1 (no peak stress)	1 (no peak stress)
$K\Delta\epsilon_{max}$	0.0569 %	0.0644 %
$E$	169216 MPa	173104 MPa
$3\bar{S}_m/E$	0.240%	0.293%
$K_e$	1	1
$K'_v$	1	1
$K_v$	1	1
$\frac{s^*}{\bar{s}}$	1	1
$\Delta\epsilon_{mod}$	0.0569 %	0.0644 %
$\Delta\epsilon_c$	4.315e-7%	1.925e-8%
$\epsilon_t$	0.0569 %	0.0644 %
Design allowable cycles, $N_d$	3363890	2908103
Design cycles, $n$	4.4*365=1602	4.4*365=1606
<b>Fatigue damage fraction, <math>D_f</math></b>	<b>4.774e-4</b>	<b>5.522e-4</b>

Table 4-2.3.5.1. (Sample problem-2) Sample calculation of determining fatigue damage fraction,  $D_f$  according to Method 1.

	<i>At OD on stress classification line shown in Figure 4-2.2.3.2</i>	<i>At ID on stress classification line shown in Figure 4-2.2.3.2</i>
$\Delta\epsilon_t$	0.0569 %	0.0644 %
$T_{HT}$	797.6°C	754.4°C
$S_{LB} = \sigma_c$	42.17 MPa	42.17 MPa
$K'$ (Table HBB-T-1411-1) for elastic analysis	0.9	0.9
Creep damage fraction per cycle (from Table 4-2.3.5.3)	6.05e-4	1.45e-4
Design cycles, $n$	4.4*365=1602	4.4*365=1602
<b>Creep damage fraction, <math>D_c</math></b>	<b>0.97</b>	<b>0.23</b>

Table 4-2.3.5.2. (Sample problem-2) Sample creep damage fraction,  $D_c$  calculation according to Method 1.

At OD on stress classification line shown in Figure 4-2.2.3.2						At ID on stress classification line shown in Figure 4-2.2.3.2					
Time (hr)	$S_k$ (MPa)	$\frac{S_k}{K'}$ (MPa)	$(T_d)_k$ (hr)	$\Delta t_k$ (hr)	$\frac{\Delta t}{(T_d)_k}$	Time (hr)	$S_k$ (MPa)	$\frac{S_k}{K'}$ (MPa)	$(T_d)_k$ (hr)	$\Delta t_k$ (hr)	$\frac{\Delta t}{(T_d)_k}$
0	96.28	106.98	16341	1	6.12e-05	0	111.48	123.87	68686	1	1.46e-05
1	96.25	106.94	16378	1	6.11e-05	1	111.47	123.86	68718	1	1.46e-05
2	96.20	106.89	16424	1	6.09e-05	2	111.46	123.84	68782	1	1.45e-05
3	96.17	106.86	16452	1	6.08e-05	3	111.46	123.84	68782	1	1.45e-05
4	96.13	106.81	16498	1	6.06e-05	4	111.45	123.83	68814	1	1.45e-05
5	96.09	106.77	16535	1	6.05e-05	5	111.44	123.82	68846	1	1.45e-05
6	96.06	106.73	16573	1	6.03e-05	6	111.43	123.81	68878	1	1.45e-05
7	96.02	106.69	16610	1	6.02e-05	7	111.43	123.81	68878	1	1.45e-05
8	95.98	106.64	16657	1	6.00e-05	8	111.42	123.80	68910	1	1.45e-05
9	95.94	106.60	16695	1	5.99e-05	9	111.41	123.79	68942	1	1.45e-05
10	95.91	106.57	16723			10	111.41	123.79	68942		
Creep damage fraction per cycle					6.05e-4	Creep damage fraction per cycle					1.45e-4

Table 4-2.3.5.3. (Sample problem-2) Sample calculation of creep damage fraction,  $D_c$  per cycle from stress-time history according to Method 1.

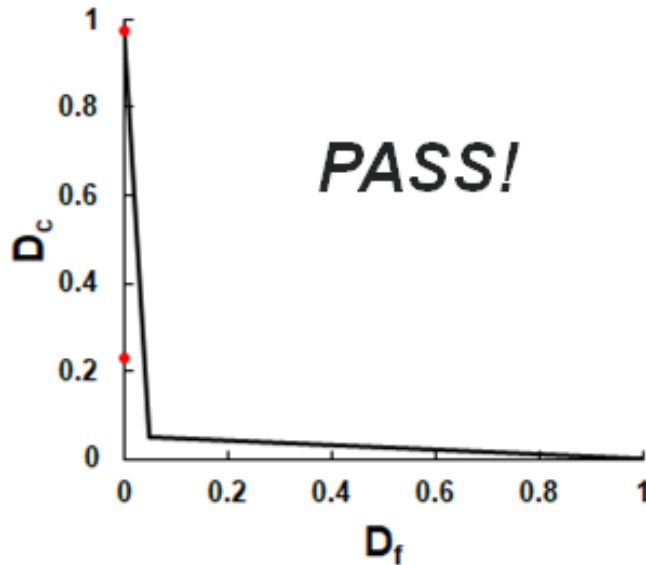


Figure 4-2.3.5.1. (Sample problem-2) Illustration of creep-fatigue design check. Plotted data are results from analysis according to Method 1.

#### 4-2.2.6. Step-6: Time-independent buckling check

Since this is a tube in an external receiver, wind load should be considered in the time-independent buckling check. To determine the design wind load on the receiver tube, we first determine the wind pressure along the wind direction. We adopted the method provided in ASME STS-1-2016 Steel Stacks<sup>31</sup> for calculating the wind pressure. According to Equation 4-4 in STS-1-2016, the design wind pressure along the wind direction is,

<sup>31</sup> American Society of Mechanical Engineers Code for Steel Stacks, ASME STS-1-2016.

$$q_z = 0.00256V^2IK_{zt}K_z \quad psf$$

$$\text{i.e. } q_z = 1.228 * 10^{-07} * V^2IK_{zt}K_z \quad \text{MPa}$$

where  $V$  is the wind speed in mph,  $I$  is the importance factor,  $K_{zt}$  is the topographic factor, and  $K_z$  is the velocity pressure exposure coefficient evaluated at height,  $z$ .

Importance factor,  $I$  can be determined according to Tables I-2 and I-3 in STS-1-2016 Mandatory Appendix I. As a part of a power generation facility, the CSP receiver falls under category IV in Table I-2. From Table I-3 for category IV structure, the importance factor is found to be 1.15. Considering the CSP tower located in an open terrain,  $K_{zt}$  is 1 according to Fig. I-2 in STS-1-2016 Mandatory Appendix I.  $K_z$  is determined from Table I-4 in STS-1-2016 Mandatory Appendix I. This table provides the values of  $K_z$  as a function of height,  $z$  and the exposure category of the structure. According to Paragraph 4.3.3.4 of STS-1-2016, the exposure category for a structure located in an open terrain is C. As mentioned in the problem definition, the CSP receiver stands on a 100 m tall tower which makes the value of  $K_z$  to vary from 1.61 at the bottom of the receiver to 1.66 at the top of the receiver.

A structure under wind load is analyzed by computing the total force exerted on the structure from the drag coefficient for the whole structure and the design wind pressure. Then, use the computed force to determine stresses on the structure. However, this method cannot be applied for analyzing individual tube of a CSP receiver. We, therefore, used a pressure coefficient,  $C_p$  to determine the distribution of wind pressure around the receiver and use the maximum positive and negative values of the distributed wind pressure as wind load on the tube. The value of  $C_p$  depends on the geometry and dimensions of the structure. The overall structure of the external receiver considered for this design problem can be considered as a cylinder. The variation in  $C_p$  around a cylindrical structure can be determined from the following equation<sup>32</sup>.

$$C_p = -0.54 + 0.16 * \frac{D}{L} + \left(0.28 + 0.04 * \frac{D}{L}\right) * \cos\theta + \left(1.04 - 0.2 * \frac{D}{L}\right) * \cos 2\theta \\ + \left(0.36 - 0.05 * \frac{D}{L}\right) * \cos 3\theta - \left(0.14 - 0.05 * \frac{D}{L}\right) \cos 4\theta$$

where  $D$  is the diameter of the whole receiver which is 8.5 m for our design problem,  $L$  is the height of the receiver which should be approximately equal to the length of the tube, and  $\theta$  is the circumferential coordinate from the direction of wind. The distribution of  $C_p$  along the circumference of the external receiver considered in this sample problem is shown in Figure 4-2.2.6.1.

---

<sup>32</sup> C. Lei, and J. M. Rotter, "Buckling of anchored cylindrical shells of uniform thickness under wind load" *Engineering Structures*, 41, pp. 199-208, 2012.

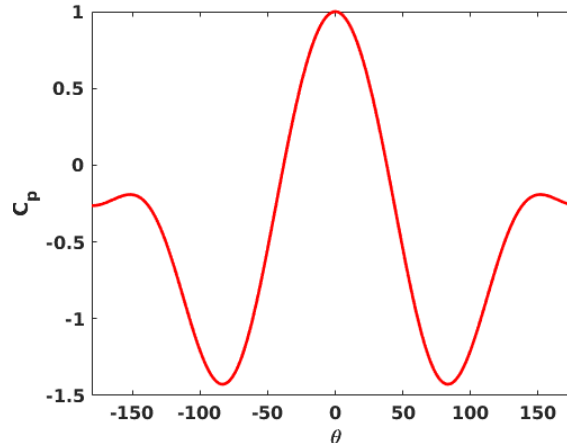


Figure 4-2.2.6.1. Distribution of wind pressure coefficient,  $C_p$  around the circumference of the external cylindrical receiver. Receiver diameter,  $D = 8.5 \text{ m}$  and height,  $L = 10.5 \text{ m}$ .  $\theta = 0$  is along the direction of wind velocity.

By multiplying  $q_z$  with  $C_p$ , the distribution of design wind pressure around the cylindrical external receiver can be found. Depending on the location of the tube with respect to the wind direction the value of  $C_p$  and the corresponding design wind pressure acting on the tube will vary. Considering wind can blow from any direction, the maximum acting positive and negative design wind pressure on the tube, according to Figure 4-2.2.6.1, are  $q_z$  and  $-1.43q_z$ , respectively. Thus, the buckling analysis is performed for two cases of design wind load – the maximum positive wind pressure which pushes the tube toward the cylindrical axis of the overall receiver and the maximum negative wind pressure which radially pulls the tube away from the overall cylindrical shape of the receiver. For structural analysis, the design wind pressure load is applied as a pressure field on the outer half (that faces heliostat) of the outer surface of the tube. The direction of the positive pressure field is toward the cylindrical axis of the overall receiver.

To determine  $q_z$ , a design wind speed is required. For time-independent buckling check, we considered the conventional 3s gust wind speed used in design codes for tall structures. According to Figure I-1 in STS-1-2016 Mandatory Appendix I, the maximum 3s gust wind speed in the U.S. open terrains (excluding the coastal area) varies between 85 mph and 90 mph. We, therefore, used 90 mph wind speed in our design calculations for time-independent buckling check. Table 4-2.2.6.1 tabulates the wind load applied on the receiver tube for buckling analysis.

	Design wind load (MPa)	$V$ mph	$C_p$	$I$	$K_{zt}$	$K_z(z)$
Case-1	$1.228 * 10^{-07} * V^2 I K_{zt} K_z C_p$	90.0	1.0	1.15	1.0	Varies linearly from 1.62 (bottom of the tube) to 1.66 (top of the tube)
Case-2			-1.43			

Table 4-2.2.6.1. Applied design wind load on the tube for time-independent buckling analysis.

According to the design methods developed for the high temperature components, time-independent buckling can be checked by analyzing the structure assuming a constitutive response given by the hot tensile curves and a load factor of 1.5. Note that, the load factor 1.5 is a slight reduction from the ASME Section III Division 5 HBB factor of 1.67, reflecting the lower consequences of failure for CSP systems. Thus, we used a load factor of 1.5 on the primary internal pressure load due to the salt pressure and on the thermal loading due to the temperature gradient.

To apply the load factor on thermal loading in finite element calculations we multiplied the coefficient of thermal expansion, CTE by 1.5. In the case of wind load, the design wind load expression, provided in Table 4-2.2.6.1, already includes several safety factors and therefore we did not use any additional load factor. Table 4-2.2.6.2 lists all the factors used for different types of loads.

	Load factors	Notes
Design primary salt pressure	1.5	
Design thermal load	1.5	Applied through multiplying the CTE with the load factor
Design wind load	1.0	Several safety factors are already included in the design load

Table 4-2.2.6.2. Factors applied on different types of loads for buckling checks.

The constitutive response of alloy 740H described by the hot tensile or isochronous stress strain curves can be implemented in commercial finite element software such as Abaqus by providing the tabulated values of flow stress and corresponding plastic strain. However, this option is not yet available in the open source finite element package we used for this project. We, therefore, used an elastic perfectly-plastic material model already implemented into our finite element solver for analyzing the structure for buckling checks. Figure 4-2.2.6.2 plots in red the hot tensile curves at different temperatures for alloy 740H. Curves in black represent the elastic perfectly-plastic material models used in the finite element calculations. As seen in Figure 4-2.2.6.2, the curves for elastic perfectly-plastic material models are the original stress-strain curves without the hardening portion which means use of these models would be a more conservative estimation of the buckling.

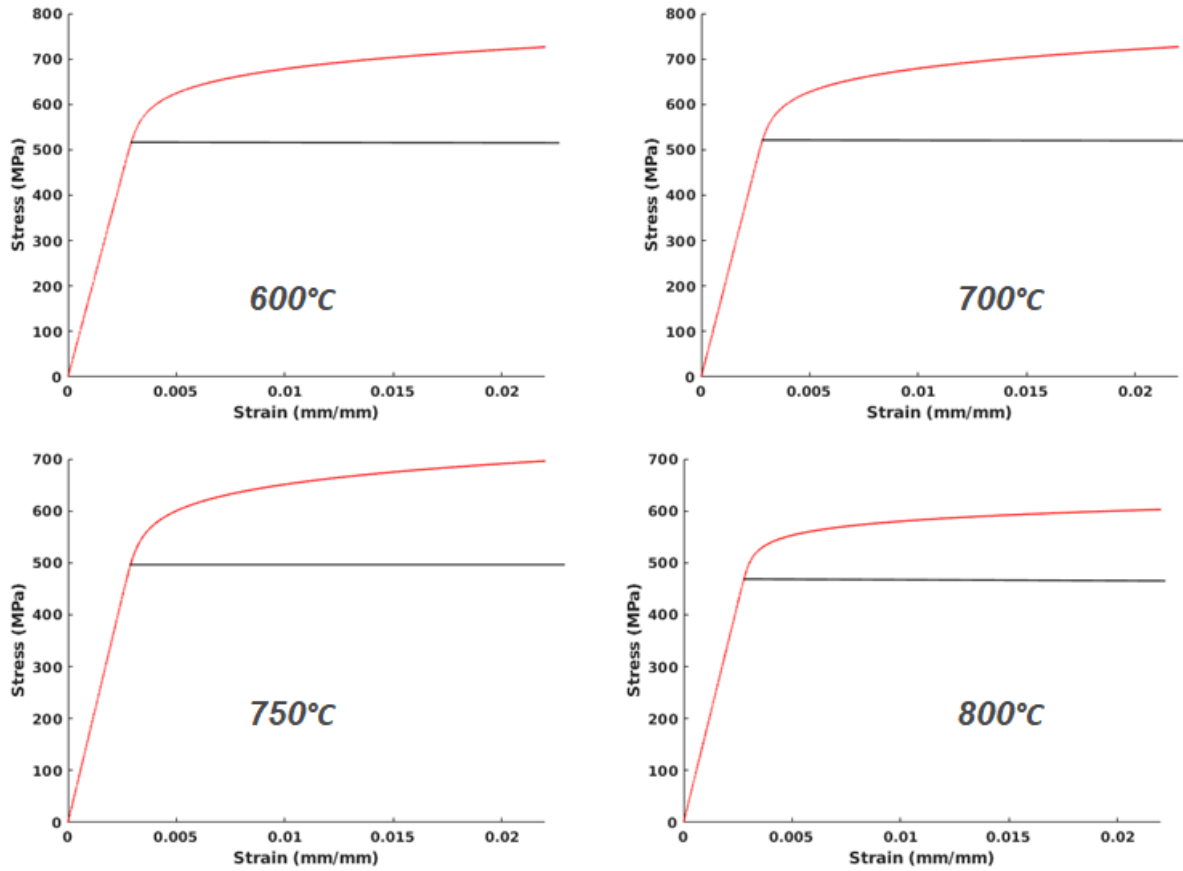


Figure 4-2.2.6.2. Plots in red are hot tensile curves and plots in black represent the elastic perfectly-plastic material models used in finite element simulation for buckling analysis.

We performed two separate thermo-mechanical analyses of the receiver for time-independent buckling checks. The flux, salt inlet and outlet temperatures, and salt pressure are the same for both cases. While the wind load varies between the two cases by the value of  $C_p$  provided in Table 4-2.2.6.1. In both loading cases the finite element solver reaches to a solution implying that the tube passes the time-independent buckling check. Figure 4-2.2.6.3 illustrates the temperature, von Mises stress, and radial (with respect to the cylindrical axis of the overall receiver) displacement distribution of the tube under the applied for time-independent buckling check.

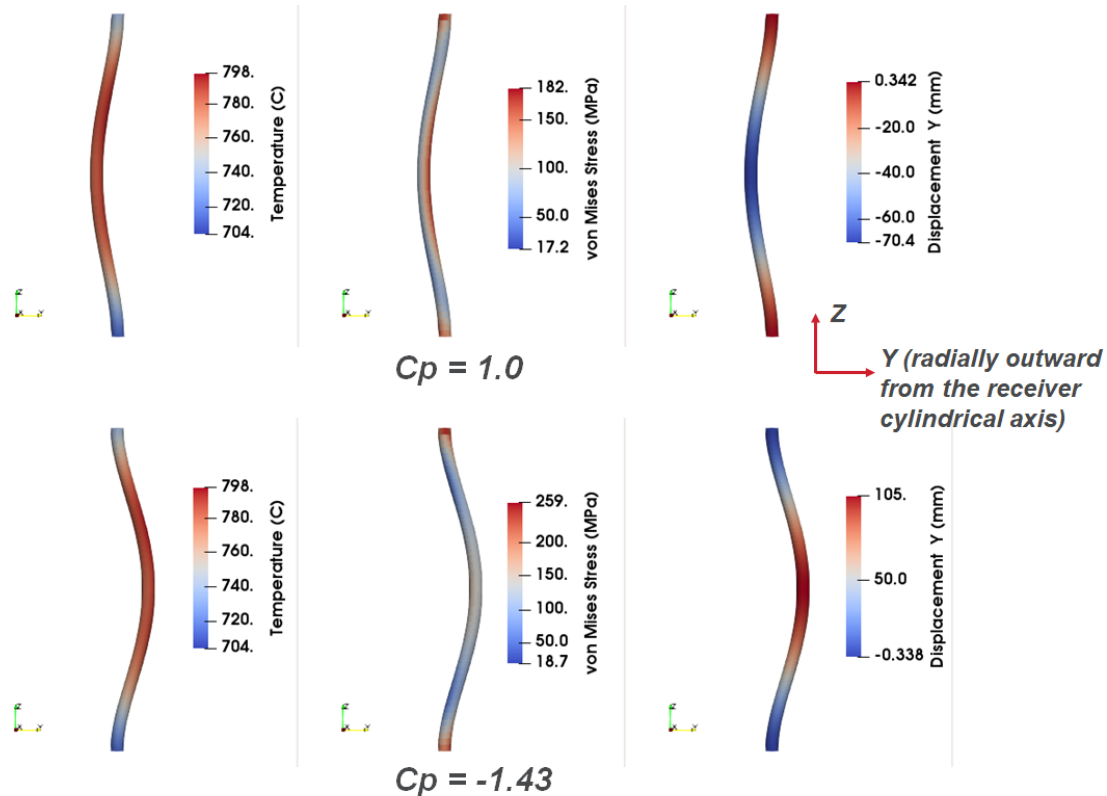


Figure 4-2.2.6.3. Distribution of temperature, von Mises stress, and radial (with respect to the cylindrical axis of the whole receiver) displacement at noon under the load applied for time-independent buckling check.

#### 4-2.2.7. Step-7: Time-dependent buckling check

As time-dependent buckling is not expected under the salt pressure and thermal loading considered in this problem, this design check was not performed.

### 4-2.3. Design calculations based on Method 2

#### 4-2.3.1. Step-1: Defining the Design Cycle

Same as in Method 1 Step 1.

#### 4-2.3.2. Step-2: Transient elastic thermo-mechanical analysis for each service load case and stress classification

Same as in Method 1 Step 2.

#### 4-2.3.3. Step-3: Primary load design check

Same as in Method 1 Step 3.

#### 4-2.3.4. Step-4: Ratcheting check

Same as in Method 1 Step 4.

#### 4-2.3.5. Step-5: Creep-fatigue damage check

Method 2 is applicable only if the primary plus secondary stress intensity ( $P + Q$ ) remains less than  $S_y$  for all service loading and if peak stresses are minimal.

For a design to be acceptable, the following relation must be satisfied:

$$\sum_j \left( \frac{n}{N_d} \right)_j + \sum_k \left( \frac{\Delta t}{T_d} \right)_k \leq D$$

where  $D$  is the total creep-fatigue damage and the first and second terms on the left side are fatigue damage,  $D_f$  and creep damage,  $D_c$ , respectively. In the fatigue damage term,  $(n)_j$  is the number of repetitions of cycle type  $j$  and  $(N_d)_j$  is the number of design allowable cycles for respective cycle type; while in the creep damage term,  $(T_d)_k$  is the allowable time duration for a given stress at the maximum temperature occurring in the time interval  $k$  and  $(\Delta t)_k$  is the duration of the time interval  $k$ .

The design allowable cycles for fatigue damage is determined by entering fatigue curves at total strain range,  $\epsilon_t$ . Total strain range,  $\epsilon_t$  is calculated using equation HBB-T-1432-16:

$$\Delta \epsilon = \Delta \epsilon_1 + \Delta \epsilon_2$$

where  $\Delta \epsilon_1$  is the maximum equivalent strain range calculated from the elastic analysis of under primary and secondary loading together, according to Section III, Division 5, HBB-T-1413.  $\Delta \epsilon_2$  is the creep strain increment per stress cycle.  $\Delta \epsilon_2$  can be determined by entering the isochronous stress-strain curves at the O'Donnell-Porowski core stress,  $\sigma_c$  (determined in Method 1, Step 4) and maximum metal temperature for the stress cycle time, including hold times between transient (instead of total service life). Alternatively,  $\Delta \epsilon_2$  can be calculated by dividing the creep strain accumulated during the entire service life by the number of stress cycles during the entire service life. We used the latter option.

Creep damage for each service load cycle is evaluated from the von Mises stress profile, determined from elastically calculated stresses, versus time profile for this load cycle. Using the stress-time profile and the hold time temperature,  $T_{HT}$  during the cycle, creep damage fraction can be calculated according to the illustration in Figure 4-2.3.5.1.

Tables 4-2.3.5.1 and 4-2.3.5.2 show example calculations of determining creep damage fraction,  $D_c$  and fatigue damage fraction,  $D_f$ , respectively, according to Method 2. Comparing  $(D_f, D_c)$  with the damage envelop in creep-fatigue interaction diagram, as shown in Figure 4-2.3.5.2, the design is found to be passed according to Method 2.



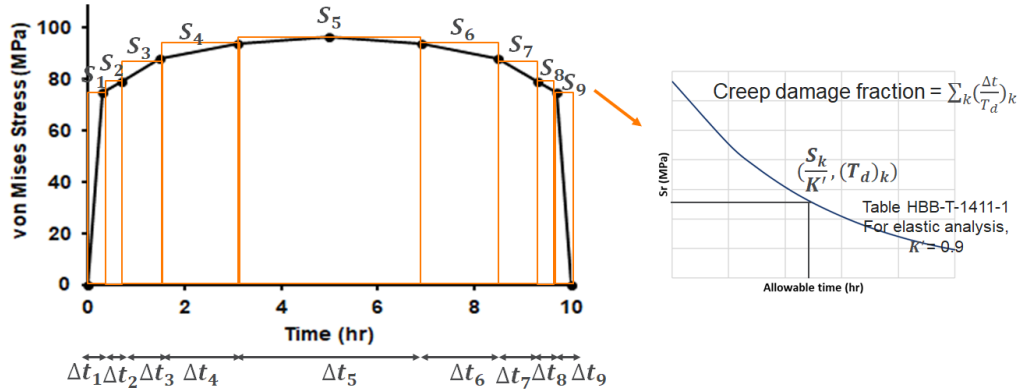


Figure 4-2.3.5.1. (Sample problem-2) Illustration of calculating creep damage fraction in Method 2.

<i>At OD on stress classification line shown in Figure 4-2.2.3.2</i>					
$T_{HT} = 797.6^{\circ}\text{C}$					
$S_y \text{ at } T_{HT} = 465.2 \text{ MPa (Method 2 is applicable!)}$					
Time (hr)	$S_k \text{ (MPa)}$	$\frac{S_k}{K' (=0.9)} \text{ (MPa)}$	$(T_d)_k \text{ (hr)}$	$\Delta t_k \text{ (hr)}$	$\left(\frac{\Delta t}{T_d}\right)_k$
0.3	74.40	82.66	73194	0.3	4.10e-06
0.7	78.79	87.55	53047	0.4	7.54e-06
1.5	87.99	97.77	27470	0.8	2.91e-05
3.1	93.71	104.13	19190	1.6	8.34e-05
5	96.30	107.00	16322	3.8	2.33e-04
6.9	93.71	104.13	19190	1.6	8.34e-05
8.5	87.99	97.77	27470	0.8	2.91e-05
9.3	78.79	87.55	53047	0.4	7.54e-06
9.7	74.40	82.66	73194	0.3	4.10e-06
10	0	0			
<i>Creep damage fraction per cycle</i>					<b>4.81e-4</b>
<i>Creep damage fraction, <math>D_c</math></i>					<b>0.77</b>

Table 4-2.3.5.1. (Sample problem-2) Sample calculation of creep damage fraction,  $D_c$  per cycle from stress-time history according to Method 2.

	<i>At OD on stress classification line shown in Figure 4-2.2.3.2</i>
$T^{max}$	797.6°C
$\Delta\epsilon_1$	0.0569 %
$\Delta\epsilon_2$	4.315e-7%
$\Delta\epsilon$	0.0569 %
Design allowable cycles, $N_d$	3363890
Design cycles, $n$	4.4*365=1602
<i>Fatigue damage fraction, <math>D_f</math></i>	<b>4.774e-4</b>

Table 4-2.3.5.2. (Sample problem-2) Sample calculation of fatigue damage fraction,  $D_f$  according to Method 2.

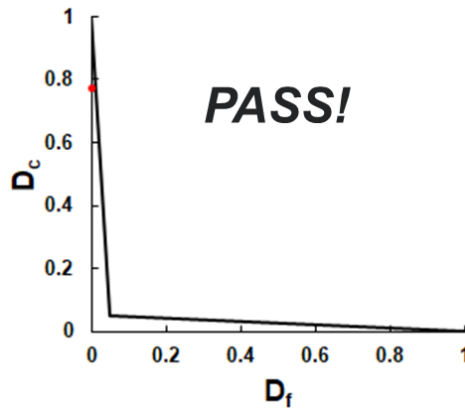


Figure 4-2.3.5.2. (Sample problem-2) Illustration of creep-fatigue design check. Plotted data are results from analysis according to Method 2.

#### 4-2.3.6. Step-6: Time-independent buckling check

Same as in Method 1 Step 6.

#### 4-2.3.7. Step-7: Time-dependent buckling check

Same as in Method 1 Step 7.

### 4-2.4. Design calculations based on Method 3

#### 4-2.4.1. Step-1: Defining the Design Cycle

Same as in Method 1 Step 1.

#### 4-2.4.2.

##### Step-2a: Transient elastic thermo-mechanical analysis for each service load case and stress classification (for primary load design check)

Same as in Method 1 Step 2.

##### Step-2b: Transient elastic-creep thermo-mechanical analysis for each service load case (for ratcheting and creep-fatigue evaluation)

We used MOOSE (Multiphysics Object Oriented Simulation Environment), an open source finite element solver to perform the transient elastic-creep thermo-mechanical analyses under the loading conditions mentioned in Step 1. The analysis was repeated until a steady state cyclic response was achieved.

#### 4-2.4.3. Step-3: Primary load design check

Same as in Method 1 Step 3.

#### 4-2.4.4. Step-4: Ratcheting check

To determine ratcheting strain Method 3 requires to run the analysis using elastic-creep material model, described above, and monitor the maximum effective strain,  $\sqrt{\frac{2}{3}} \varepsilon: \varepsilon$  at the beginning and end of the cycle. The criterion is that the ratcheting strain does not exceed 10% at any point of the structure for base metal. Figure 4-2.4.4 plots the maximum effective strain at the critical tube location as a function of cycle count. Extrapolating the maximum effective strain out to design life of the tube, i.e. 4.4 years ( $=4.4*365$  cycles), gives the ratcheting strain of 0.745% which is less than 10%.

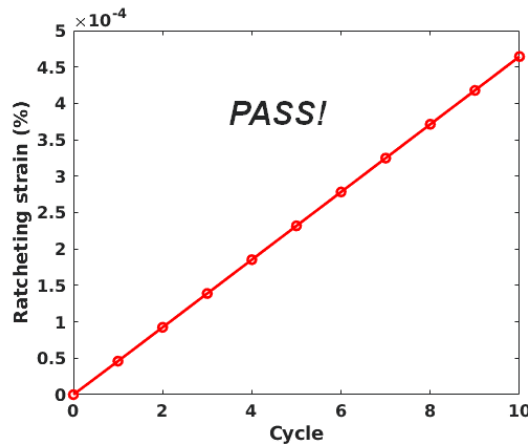


Figure 4-2.4.4. (Sample problem-2) Maximum ratcheting strain in the structure versus number of cycles determined from elastic-creep thermo-mechanical analysis.

#### 4-2.4.5. Step-5: Creep-fatigue damage check

Once steady cyclic response was achieved in the analysis, the temperature, stress, and strain-time history for a single cycle of the periodic loading were extracted. Figure 4-2.4.5.1 plots the temperature, and the steady cyclic effective strain range and von Mises effective stress at the critical location of the tube. Details of the fatigue damage fraction calculation is provided in Table 4-2.4.5.1. The tube experiences negligible fatigue damage. Figure 4-2.4.5.2 illustrates creep damage fraction evaluation from the steady cyclic von Mises effective stress profile. Detailed calculation of creep damage fraction is provided in Table 4-2.4.5.2. Comparing ( $D_f, D_c$ ) with the damage envelop in creep-fatigue interaction diagram, as shown in Figure 4-2.4.5.3, the design is found to be passed according to Method 3.

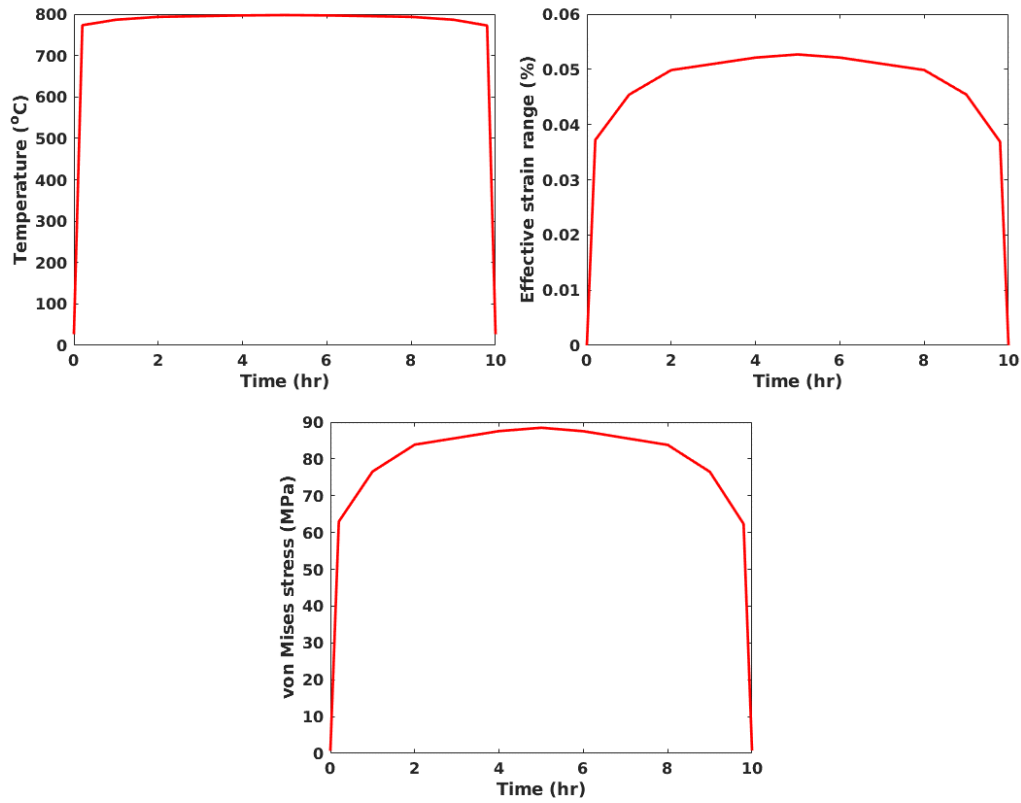


Figure 4-2.4.5.1. (Sample problem-2) Temperature, effective strain range, and von Mises stress profiles at the critical location of the tube after a steady cyclic response is achieved in the elastic-creep thermo-mechanical analysis.

	<i>At the critical location</i>
$T^{max}$	797.6°C
Strain range and corresponding cycle frequency according to rainflow counting of effective strain range, $\Delta\epsilon$	0.0527%
	1
Design allowable cycles, $N_d$	3649654
Design cycles, $n$	4.4*365=1606
<b><i>Fatigue damage fraction, <math>D_f</math></i></b>	<b><i>4.40e-4</i></b>

Table 4-2.4.5.1. (Sample problem-2) Sample calculation of fatigue damage fraction,  $D_f$  according to Method 3.

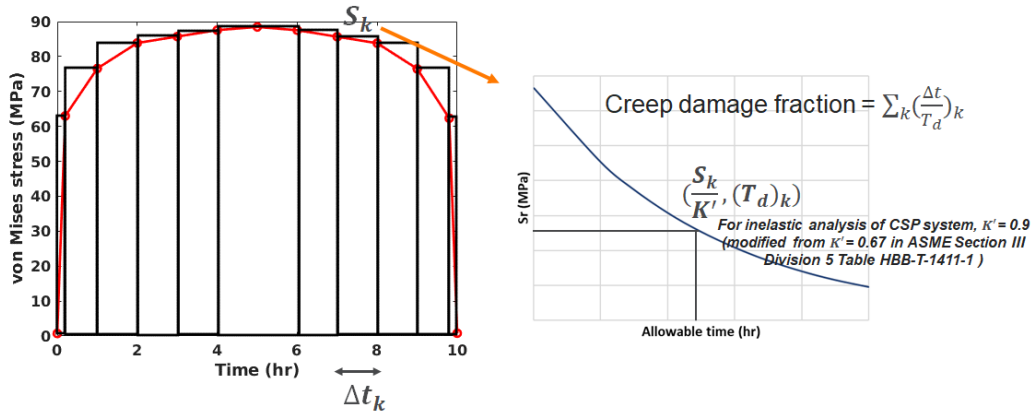


Figure 4-2.4.5.2. (Sample problem-2) Illustration of calculating creep damage fraction in Method 3.

At the critical location					
$T_{HT} = 797.6^{\circ}C$					
$S_y$ at $T_{HT} = 465.2$ MPa (Method 3 is applicable!)					
Time (hr)	$S_k$ (MPa)	$\frac{S_k}{K' (=0.9)}$ (MPa)	$(T_d)_k$ (hr)	$\Delta t_k$ (hr)	$(\frac{\Delta t}{T_d})_k$
0.2	62.98	69.98	168661	0.2	1.19e-06
1.0	76.57	85.08	62412	0.8	1.28e-05
2.0	83.87	93.19	36594	1	2.73e-05
3.0	85.71	95.23	31995	1	3.13e-05
4.0	87.55	97.28	28240	1	3.54e-05
5.0	88.47	98.30	26661	2	7.50e-05
6.0	87.53	97.26	28271	1	3.54e-05
7.0	85.66	95.18	32100	1	3.12e-05
8.0	83.81	93.12	36763	1	2.72e-05
9.0	76.49	84.99	62785	0.8	1.27e-05
9.8	62.34	69.27	176732	0.2	1.13e-06
10	0				
Creep damage fraction per cycle					2.91e-4
Creep damage fraction, $D_c$					0.47

Table 4-2.4.5.2. (Sample problem-2) Sample calculation of creep damage fraction,  $D_c$  according to Method 3.

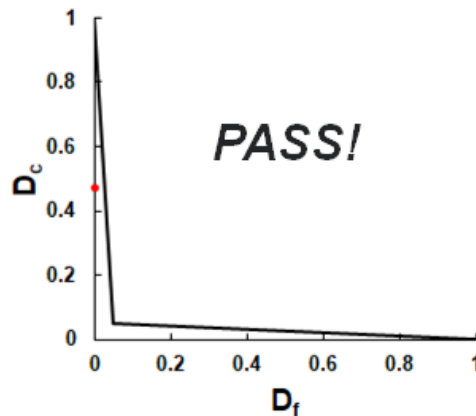


Figure 4-2.4.5.3. (Sample problem-2) Illustration of creep-fatigue design check. Plotted data are results from analysis according to Method 3.

#### **4-2.4.6. Step-6: Time-independent buckling check**

Same as in Method 1 Step 6.

#### **4-2.4.7. Step-7: Time-dependent buckling check**

Same as in Method 1 Step 7.

## **Acknowledgements**

This work was funded by the U.S. Department of Energy through the Office of Energy Efficiency and Renewable Energy, Solar Energy Technologies Office, CSP Program. We gratefully acknowledge the guidance of Mark Lausten, the DOE project manager for this project as well as the contributions of Robert Jetter who served as a high temperature design consultant in the development of the design rules and corresponding material data.



## **Applied Materials Division**

Argonne National Laboratory  
9700 South Cass Avenue, Bldg. 362  
Argonne, IL 60439

[www.anl.gov](http://www.anl.gov)



U.S. DEPARTMENT OF  
**ENERGY**

Argonne National Laboratory is a U.S. Department of Energy  
laboratory managed by UChicago Argonne, LLC